Doctorate Program in Molecular Oncology and Endocrinology
Doctorate School in Molecular Medicine

XXV cycle - 2009–2012
Coordinator: Prof. Massimo Santoro

"Identification of genes regulated by CBX7 protein and characterization of the transcriptional regulation mechanism of the *SPP1* gene"

Romina Sepe

Università degli Studi di Napoli "Federico II"
Dipartimento di Medicina Molecolare e Biotecnologie Mediche

Administrative Location

Università degli Studi di Napoli Federico II
Dipartimento di Medicina Molecolare e Biotecnologie Mediche

Partner Institutions

Italian Institutions
Università degli Studi di Napoli "Federico II", Naples, Italy
Istituto di Endocrinologia ed Oncologia Sperimentale "G. Salvatore", CNR, Naples, Italy
Seconda Università di Napoli, Naples, Italy
Università degli Studi di Napoli "Parthenope", Naples, Italy
Università degli Studi del Sannio, Benevento, Italy
Università degli Studi di Genova, Genova, Italy
Università degli Studi di Padova, Padova, Italy
Università degli Studi "Magna Graecia", Catanzaro, Italy
Università degli Studi di Udine, Udine, Italy

Foreign Institutions
Université Libre de Bruxelles, Bruxelles, Belgium
Universidade Federal de Sao Paulo, Brazil
University of Turku, Turku, Finland
Université Paris Sud XI, Paris, France
University of Madras, Chennai, India
University Pavol Jozef Šafàrik, Kosice, Slovakia
Universidad Autonoma de Madrid, Centro de Investigaciones Oncologicas (CNIO), Spain
Johns Hopkins School of Medicine, Baltimore, MD, USA
Johns Hopkins Krieger School of Arts and Sciences, Baltimore, MD, USA
National Institutes of Health, Bethesda, MD, USA
Ohio State University, Columbus, OH, USA
Albert Einstein College of Medicine of Yeshiwa University, N.Y., USA

Supporting Institutions
Dipartimento di Biologia e Patologia Cellulare e Molecolare "L. Califano", Università degli Studi di Napoli "Federico II", Naples, Italy
Istituto di Endocrinologia ed Oncologia Sperimentale "G. Salvatore", CNR, Naples, Italy
Istituto Superiore di Oncologia, Italy

Italian Faculty

Salvatore Maria Aloj
Francesco Saverio Ambesi
Impiombato
Francesco Beguinot
Maria Teresa Berlingieri
Bernadette Biondi
Francesca Carlomagno
Gabriella Castoria
Maria Domenica Castellone
Angela Celetti
Lorenzo Chiariotti
Annamaria Cirafici
Annamaria Colao
Sabino De Placido
Gabriella De Vita
Monica Fedele
Pietro Formisano
Alfredo Fusco
Domenico Grieco
Michele Grieco
Maddalena Illario
Paolo Laccetti
Antonio Leonardi
Paolo Emidio Macchia
Barbara Majello
Rosa Marina Melillo
Claudia Miele
Nunzia Montuori
Roberto Pacelli
Giuseppe Palumbo
Maria Giovanna Pierantoni
Rosario Pivonello
Giuseppe Portella
Maria Fiammetta Romano
Giuliana Salvatore
Massimo Santoro
Giampaolo Tortora
Donatella Tramontano
Giancarlo Troncone
Giancarlo Vecchio,
Giuseppe Viglietto
Mario Vitale

“Identification of genes regulated by CBX7 protein and characterization of the transcriptional regulation mechanism of the *SPP1* gene”

TABLE OF CONTENTS

LIST OF PUBLICATIONS

This dissertation is based upon the following publications:

1. Pallante P, **Sepe R**, Federico A, Forzati F, Bianco M, Fusco A. **CBX7 modulates the expression of genes critical for cancer progression.** Manuscript in preparation. (Main body of dissertation).

2. **Sepe R**, Pallante P, Federico A, Forzati F, Fusco A. **CBX7 and HMGA1 proteins act in opposite way on the regulation of the *SPP1* gene expression.** Manuscript in preparation. (Main body of dissertation).

3. Piscuoglio S, Zlobec I, Pallante P, **Sepe R**, Esposito F, Zimmermann A, Diamantis I, Terracciano L, Fusco A, Karamitopoulou E. **HMGA1 and HMGA2 protein expression correlates with advanced tumour grade and lymph node metastasis in pancreatic adenocarcinoma.** Histopathology 2012;60(3):397-404. (Attached at the end).

4. Pallante P, Malapelle U, Berlingieri MT, Bellevicine C, **Sepe R**, Federico A, Rocco D, Galgani M, Chiariotti L, Sanchez-Cespedes M, Fusco A, Troncone G. **UbcH10 overexpression in human lung carcinomas and its correlation with EGFR and p53 mutational status.** Eur J Cancer 2013;49(5):1117-26. (Attached at the end).

LIST OF ABBREVIATIONS

PcG = Polycomb group
PRC1/PRC2 = Polycomb repressive complex 1/ Polycomb repressive complex 2
CBX7 = Chromobox homolog 7
HMGA = High mobility group A
SPP1 = Secreted Phosphoprotein 1
qRT-PCR = quantitative RT-PCR
ChIP = Chromatin immunoprecipitation
TSS = Transcriptional start site
TF = Transcriptional factor
MEF = Mouse embryonic fibroblast
WT = Wild type
PTC = Papillary thyroid carcinoma
ATC = Anaplastic thyroid carcinoma
FVPTC = Follicular-variant papillary thyroid carcinoma

ABSTRACT

CBX7 is a member of the Polycomb Repressive Complex 1 (PRC1) involved in the process of human and mouse tumorigenesis. Recently, we have demonstrated that CBX7 is drastically decreased in several human carcinomas and that CBX7 protein levels progressively decreased in relation with the malignant grade and the neoplastic stage. To characterize the mechanisms by which the loss of CBX7 contributes to the process of carcinogenesis, we analyzed the gene expression profiling of an anaplastic thyroid carcinoma cell line in which the expression of *CBX7* was restored and found that CBX7 was able to negatively or positively regulate the expression of several genes (such as *SPP1, SPINK1, STEAP1*, and *FOS, FOSB, EGR1*, respectively) associated with cancer progression. By quantitative (q)RT-PCR, we confirmed these data in mouse and rat system in which the expression of *Cbx7* was silenced. Then, we showed that CBX7 was able to physically interact with the promoter region of these genes, thus regulating their activity. qRT-PCR analysis performed on thyroid and lung carcinoma samples with different degree of malignancy, showed a negative correlation between CBX7 and its down-regulated genes, while a positive correlation was observed between CBX7 and its up-regulated genes. Recently, we have demonstrated that CBX7 protein is able to interact with the High Mobility Group A 1 (HMGA1) protein. Therefore, we asked whether this interaction could be involved in the transcriptional regulation of the *SPP1* gene.qRT-PCR analysis demonstrated that HMGA1 protein is able to increase the *SPP1* expression in several cellular systems. Moreover, by chromatin immunoprecipitation assays, we found that HMGA1 binds together with CBX7 protein to the *SPP1* promoter and that the two proteins compete for the binding. Finally, functional assays showed that CBX7 is able to negatively regulate cellular migration by repressing transcriptional activation of the *SPP1*promoter.
In conclusion, the loss of CBX7 expression might play a critical role in cancer progression by deregulating the expression of specific effector genes.

1. BACKGROUND

1.1 Polycomb Group proteins (PcG)

Polycomb Group (PcG) proteins are transcriptional repressors that bind to histone modifications, thus maintaining gene expression in a silenced state (Otte et al. 2003,Lund and van Lohuizen 2004). PcG proteins are part of two complexes with high molecular weight named Polycomb Repressive Complex 1 and 2 (PRC1 and PRC2) (Sparmann and Van Lohuizen 2006, Schwartz and Pirrotta 2007). The PRC2 has associated histone deacetylase and histone methyl transferase activities (specific for the lysine 27 on the histone H3, K27H3me3) (Kuzmichev et al. 2002, Kirmizis et al. 2007) while the PRC1 recognizes and binds to the K27H3me3 through the chromodomain of the Polycomb (Pc) proteins thus catalyzing the mono-ubiquitilation of the histone H2A on lysine 119 and shutting down gene transcription (Wang et al. 2004, Cao et al. 2005, Sparmann and van Lohuizen 2006). However, a recent study has demonstrated that PRC1 is also able to mono-ubiquitilate the histone H2A in a H3K27me3-independent pathwayin PRC2-deficient mouse embryonic stem cells (mESCs) (Tavares et al. 2012).
The components of the PRC1 in mammals are the homologs of *Drosophila melanogaster* Polycomb (Pc), Posterior sex combs (Psc), Sex combs extra (Sce) and Polyhomeiotic (Ph) proteins (Shao et al 1999, Saurin et al 2001). Because of the presence in mammalian cells of five Pc proteins (Chromobox homolog proteins, CBX2, CBX4, CBX6, CBX7 and CBX8), six Psc proteins (BMI1, MEL18, MBLR, NSPC1, RNF159, and RNF3), three Ph proteins (HPH1, HPH2 and HPH3) and two Sce ubiquitin ligase activity proteins (RING1a and RING1b), there is an enormous diversity for combinatorial association between these proteins (Gil and Peters 2006, Whitcomb et al. 2007). The histone lysine methyl-transferase enhancer of zeste homolog 2 (EZH2), embryonic ectoderm development (EED) and suppressor of zeste homolog 12 (SUZ12) are the known mammalian components of the PRC2 (Figure 1.1). Mammalian PRC1 may exhibit additional contextual specifity by selecting one of the multiple Pc/CBX proteins. Each of every chromobox protein confers distinct sub-chromosomic distribution and dynamic patterns to the complex (Bernstein et al. 2006).

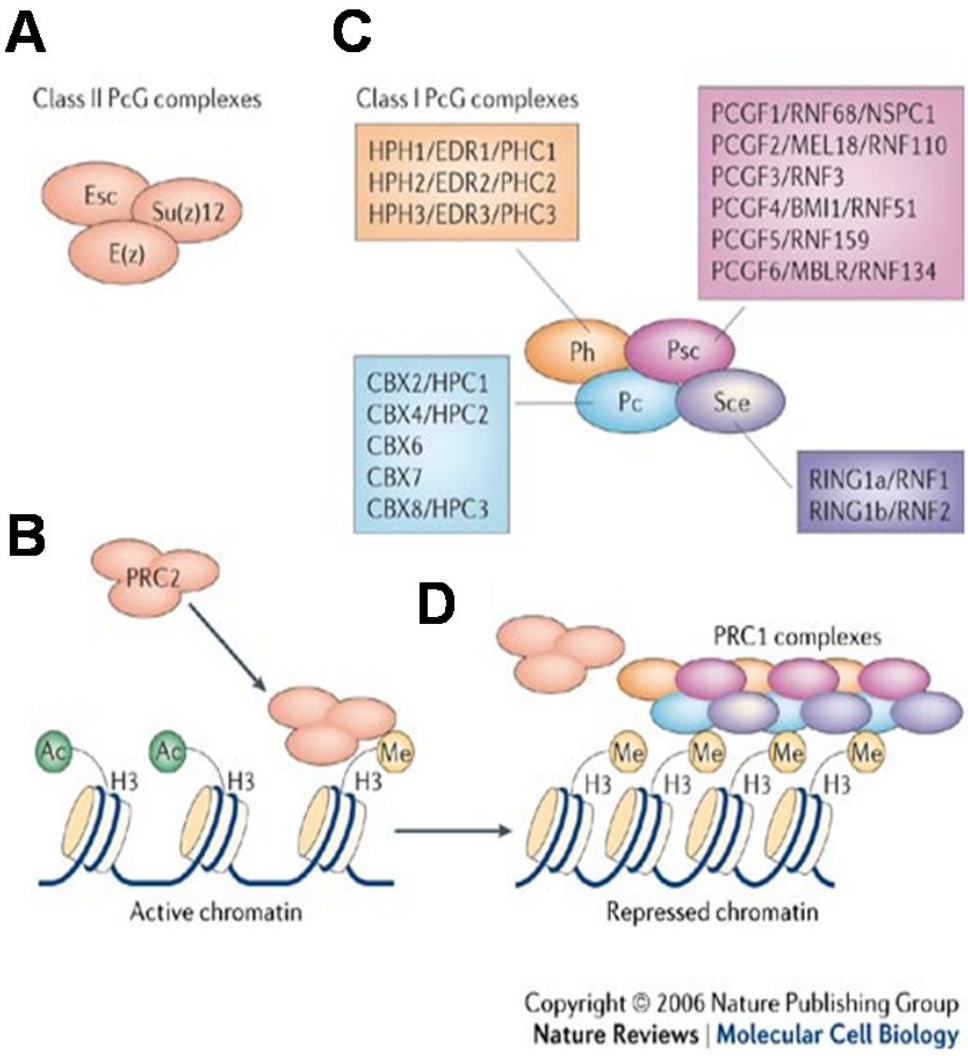

Figure 1.1 Polycomb Group proteins and the mechanism of transcriptional repression
(A) EED, SUZ12 and EZH2 are the mammals homolog of the *Drosophila melanogaster* components of the PRC2 reported in the red box.(B) The binding of the PRC2 to the Polycomb responsive elements (PREs) promotes methylation of the histone H3 on the lysine 27 (H3K27), mediated by EZH2, around the PREs in the promoter of the silenced genes. (C) In mammals there is enormous diversity for combinatorial association of PRC1 members due to the presence of many homolog of these *Drosophila melanogaster* proteins. (D) The PRC1 recognizes and binds to the H3K27 through the chromodomain of its Pc proteins thus silencing gene transcription.

Several studies have shown that PcG proteins deregulation contributes to tumorigenesis in different tissues (Piunti and Pasini 2011). For example, an overexpression of Bmi1 and EZH2 was found overexpressed in hematological diseases (Raaphorst et al. 2000), SUZ12 is up-regulated in colon tumors (Kirmizis et al. 2004), while Mel18 has been suggested to act as a tumor-suppressor (Kanno et al. 1995). Moreover, genetic ablation of specific PcG genes in mice has confirmed their role in embryonic patterning and *Hox* gene regulation. In fact, *Bmi-1* null mice display hematological and neurological defects, depending on a failure in the self-renewal of the relevant stem cells (Lessard and Sauvageau 2003, Park et al. 2003).
Recently, genome-wide chromatin immunoprecipitation (ChIP) analysis have identified over 1000 genes that are potential targets of PcG-mediated repression, many of which are implicated in the maintenance of pluripotency (Bracken et al. 2006, Tolhuis et al. 2006). Some evidences are rapidly increasing the idea that PcG genes represent a novel class of oncogenes and anti-oncogenes, which, in future years, may become central to the development of novel cancer therapies based on epigenetic gene silencing (Nakao et al. 2004, Egger et al. 2004). In addition, the correlation between PcG expression and biological behavior of clinically defined cancer subtypes suggests that these genes may also be used as novel diagnostic markers (Raaphorst et al. 2004).

1.2 Characteristics of the CBX7 protein

CBX7 gene is located on the chromosome 22q13.1 and encodes a novel Pc protein of 28.4 kDa and 251 amino acids that contains a characteristic domain called "chromodomain" (**chr**omatin **o**rganization **mo**difier domain, CD) at the N-terminal between the amino acids 10 and 46. The CD is an highly conserved domain and represents a 37 amino acids region of homology shared by Heterochromatin protein 1 (HP1) and Pc proteins (Paro and Hogness 1991). Phylogenetic and sequence analysis of the CD show that CBX7 has a great similarity to other known or putative Pc proteins like CBX2 (Pc1), CBX4 (Pc2), CBX6 and CBX8 (Pc3) (Figure 1.2). This similarity is more pronounced respect to the similarity that CBX7 shares with HP1 proteins, such as CBX1 (HP1β), CBX3 (HP1γ), CBX5 (HP1α), in fact, CBX7 does not contain the "chromo-shadow domain", a hallmark of HP1 proteins. Despite of a high degree of conservation, the CD displays significant differences for the binding to the histone H3 modifications. Unlike *Drosophila* Pc, not all mammalian Pc-like CDs bind preferentially to tri-methylated Lys 27 on histone H3 (H3K27me3). In fact, mouse Cbx2 and Cbx7 bind to K9me3 as well as K27me3,

Cbx4 has high affinity for K9me3 and Cbx6 and Cbx8 do not significantly bind to either modifications, but their CD may bind to another methylation site not yet identified or tested (Bernstein et al. 2006). Therefore, CBX7 is able to associate with repressive histone modifications, including dimethylated and trimethylated H3K9, as well as trimethylated H3K27 (Bernstein et al. 2006) suggesting that a CBX7-containing complex may be able to read histone modifications found in promoters of key genes, including those susceptible to cancer-specific DNA methylation.

CBX7 chromodomain contains also specific conserved residues necessary for both Pc dimerization and recognition of H3K27me3 (Min et al. 2003). In addition to the high homology within the CD, CBX7 displays also homology to Pc proteins in a C-terminal region (amino acids 231-243) previously defined as Pc box or C-box. Both Pc box and CD are necessary for CBX7 function (Jones et al. 2000).

It has been demonstrated that a fusion protein between CBX7 and the DNA-binding domain of Gal4 represses the transcription of a 4xGal4-tk-luc reporter in a dose-dependent manner, suggesting CBX7 as a transcriptional repressor. Moreover, mouse Cbx7 is able to associate with facultative heterochromatin and with the inactive X chromosome, indicating the involvement of Cbx7 in the repression of gene transcription (Bernstein et al. 2006). It has also been found that the CD of CBX7 is able to bind to RNA molecules *in vitro* and *in vivo,* and this ability elucidates, at least in part, the association of CBX7 and the inactive X chromosome. These reports suggest that the capacity of CBX7 to associate with the inactive X chromosome and any other region of chromatin depends not only on its CD, but also on the combination of histone modifications and RNA molecules present on its target sites (Bernstein et al. 2006).

Similarly to other Pc proteins, CBX7 is able to interact with different Pc group members and, in particular, is able to inter-functions with itself and with the ring-finger protein Ring1, while there is no association with Bmi1, EED or EZH2, suggesting that CBX7 is part of different complexes (Gil et al. 2004). In particular, CBX7 co-localizes with Ring1 in nuclear distinct foci-like structure (Pc-bodies), as demonstrated in several cell lines by immunofluorescence microscopy studies (Saurin et al. 1998).

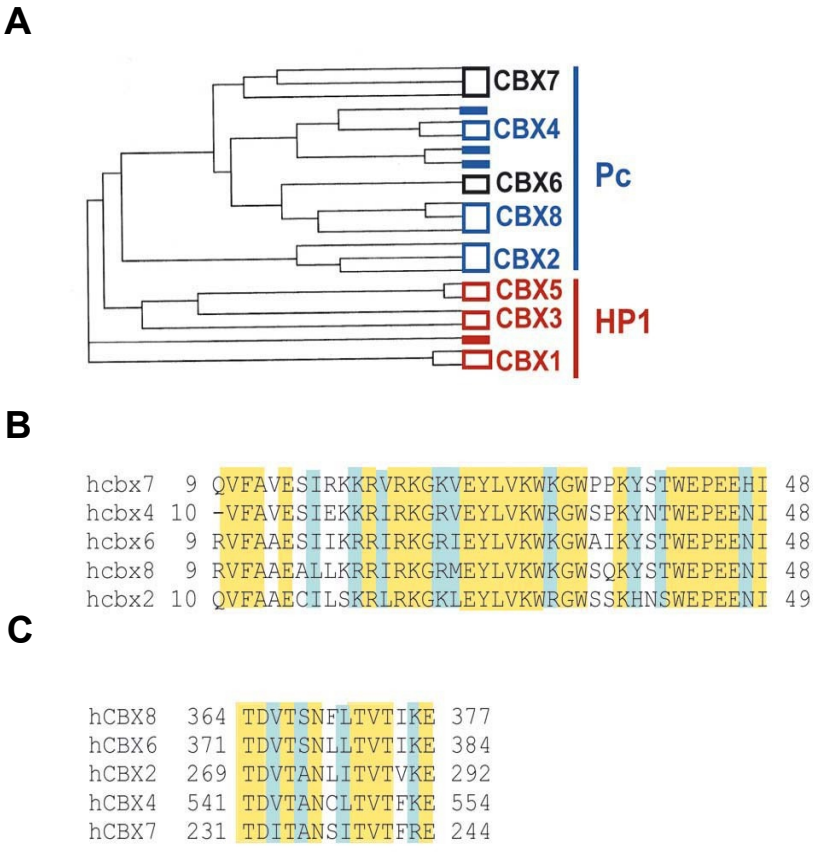

Figure 1.2 Phylogenetic analysis of CBX7 and its chromodomain
(A) Lines grouped by open rectangles represent orthologs of a same CBX7 protein (name in the right). Full rectangles indicate proteins that cannot be considered orthologs of any of the CBX proteins. Pc proteins are shown in blue, while HP1 proteins in red. (B) Alignment of the CBX7 chromodomain with that of the other known human Polycomb proteins. Similar residues are shown in cyan while identical residues are shown in yellow background. (C) Alignment of CBX7 Pc box with that of the other known Polycomb proteins. Colors are the same reported in (B).

1.3 Role of CBX7 protein in cancer

CBX7 is highly expressed in different normal tissues, including brain, kidney, heart and skeletal muscle (Gil et al. 2004), while a decreased expression of CBX7

seems to be a general event in human tumors. However, its role in carcinogenesis is still not clear. Recent studies have characterized CBX7 as a tumor-suppressor protein. In fact, the expression of *CBX7* gene is strongly decreased in thyroid (Pallante et al., 2008), colon (Pallante et al. 2010), bladder (Hinz et al. 2008), pancreatic (Karamitopoulou et al. 2010), breast (Mansueto et al. 2010, Hannafon et al. 2011) and lung carcinomas (Forzati et al. 2012). Interestingly, its expression progressively decreases with the appearance of a highly malignant phenotype. However, in several papers CBX7 has been shown to play like an oncogene. In fact, CBX7 expression is associated with expansion of cellular lifespan in human prostate primary epithelial cells (Bernard et al. 2005) and in mouse fibroblasts through the repression of the *Ink4a/Arf* locus (Gil et al. 2004) while its ablation by shRNA treatment is able to inhibit growth of normal cells through induction of the *Ink4a* locus (Gil et al. 2004). Furthermore, CBX7 resulted overexpressed in gastric cancer cell lines and gastric tumors where its silencing leads to increased cellular senescence, decreased cellular proliferation and migration ability (Zhang et al. 2010). Finally, *CBX7* expression has been reported to be high in human germinal center lymphocytes and in human germinal center-derived follicular lymphomas. In mouse systems Cbx7 has been shown to enhance T-cell lymphomagenesis and to initiate highly aggressive B cell lymphomas*in vivo* by cooperating with c-Myc (Scott et al. 2007).

1.3.1 CBX7 in thyroid carcinomas

A decreased expression of CBX7 in relation to differentiation and malignancy grade has been observed in human thyroid carcinomas. Thyroid neoplasms represent a good model for studying the events involved in epithelial cell multistep carcinogenesis. In fact, they include a wide spectrum of lesions with different degrees of malignancy. Thyroid tumours can originate from follicular cells or from C cells. Follicular cell-derived thyroid neoplasms include benign follicular adenomas (FA), which are not invasive and very well differentiated, and carcinomas. Thyroid carcinomas are divided into well-differentiated, poorly differentiated (PDCT) and undifferentiated anaplastic thyroid carcinomas (ATC). Well-differentiated thyroid carcinomas include papillary carcinomas (PTC), that represent more than 70% of thyroid tumours, and follicular carcinomas (FTC) that represent 10% of thyroid carcinomas. PTC and FTC are not aggressive tumors and have a good prognosis (Kondo et al. 2006, Saltman et al. 2006) while PDTC and ATC seem to derive from the progression of differentiated carcinomas and display a more aggressive behaviour (Van der Laan et al. 1993). Although the ATCs represent 2-5% of thyroid malignant tumours, they are one of the most lethal human

neoplasms being fast growing, very aggressive and always fatal. *CBX7* resulted strongly down-regulated in several thyroid carcinoma cell lines with different grade of malignancy compared to primary normal thyroid cells. In particular, *CBX7* expression progressively decreased in relation to malignant grade and neoplastic stage. Indeed, CBX7 protein levels decreased in an increasing percentage of cases going from benign adenomas to papillary, follicular and anaplastic thyroid carcinomas (Pallante et al. 2008) (Figure 1.3). The loss of *CBX7* expression in relation to tumor grade was supported by the analysis of tumors generating in transgenic mice expressing several oncogenes under the control of the thyroglobulin promoter (Pallante et al. 2008). Moreover, the restoration of *CBX7* expression in thyroid cancer cell lines is able to decrease the formation rate of colonies and to reduce cell growth rate with retention of cells in G1 phase. This suggesst a critical role of CBX7 in the regulation of transformed thyroid cell proliferation (Pallante et al. 2008).

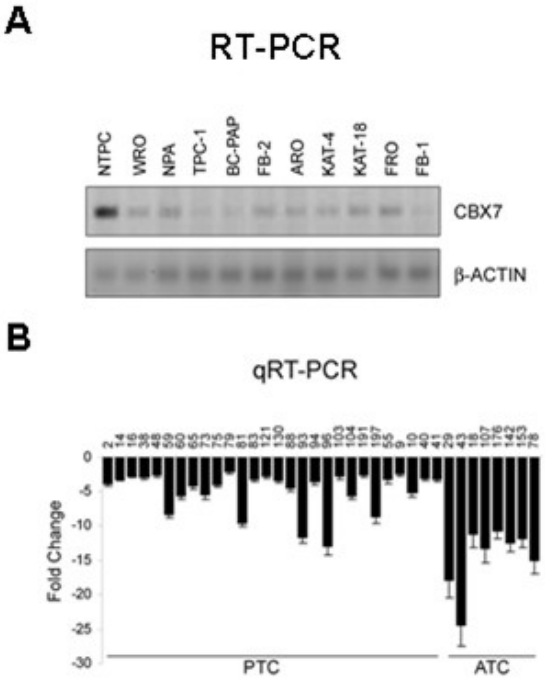

Figure 1.3 Analysis of CBX7 expression in human thyroid carcinoma samples
(A) Expression analysis of CBX7 by RT-PCR in thyroid carcinoma cell lines compared to the normal human thyroid primary culture cells (NTPC). β-actin was used as control. (B) Expression analysis of CBX7 by qRT-PCR in several human papillary (PTC) and anaplastic (ATC) thyroid carcinoma samples. Fold Change value represents the *CBX7* expression levels in samples compared to the mean expression levels of three normal thyroid samples.

1.3.2 CBX7 in colorectal carcinomas

The association between the loss of *CBX7* expression and an aggressive tumor phenotype is an event occurring also in colorectal carcinomas (CRC) (Pallante et al. 2010). The molecular mechanisms that lead to CRC, both familiar and sporadic, are well-known. About the 85% of CRC originate from chromosomal instability pathway (CIN), a multistep process leading to a loss of tumor-suppressor genes, while the 15% of CRC are characterized by microsatellite instability (MSI), this latter caused by deregulation of the DNA damage repair mechanisms (*mismatch repair, MMR* pathway) (Centelles 2012). Recent studies have demonstrated that CBX7 expression is reduced or absent in a significant number of CRC samples in comparison to the normal colonic mucosa. Interestingly, CBX7 retention is strongly associated with the benign phenotype, as observed in colonic adenomas, while its loss correlates with tumor grade and with a low survival time of CRC patients (Figure 1.4). A significant association has been found between CBX7 expression and clinic-pathological parameters in MMR-proficient patients, that do not have any alteration of the *MMR* pathway. In addition, functional studies have shown that the restoration of *CBX7* expression in CRC cell lines is able to reduce the cellular proliferation suggesting an important role in the progression step of colon carcinogenesis (Pallante et al. 2010).

1.3.3 CBX7 in pancreatic carcinomas

The correlation between the loss of CBX7 expression and the appearance of malignant phenotype seem to be a general event in tumorigenesis. This event occurs also in pancreatic carcinomas. Pancreatic tumors can originate both from the esocrine and the endocrine zone. Benign neoplasms are rare, while malignant tumors are very aggressive, invasive and always fatal. Among the latest ones, the most frequent carcinoma type is the pancreatic ductal adenocarcinoma that originates from a precursor lesions called pancreatic intraepithelial neoplasia (PanIN) and becomes an aggressive neoplasm through a multistep progression (Karamitopoulou et al. 2010). PanIN are divided in PanIN-1A, -1B, -2, -3 and only PanIN-3 neoplasms are associated with the presence of invasive carcinomas in the 30-50% of cases. By immunohistochemical analysis of a tissue microarray (TMA) comprising pancreatic normal samples and in carcinoma samples with different grade of malignancy, it has been demonstrated that CBX7 protein expression strongly and progressively decreases going from normal pancreatic tissue, to PanIN samples to invasive ductal adenocarcinomas (Karamitopoulou et al. 2010). In addition, it has been observed that the loss of *CBX7* expression is associated with

an increasing malignancy grade of pancreatic adenocarcinoma, whereas the maintenance of CBX7 expression shows a trend toward a longer survival. In fact, patients with carcinomas expressingCBX7 have a longer survival time compared with patients having carcinoma not expressing CBX7 (Karamitopoulou et al. 2010) (Figure 1.4).

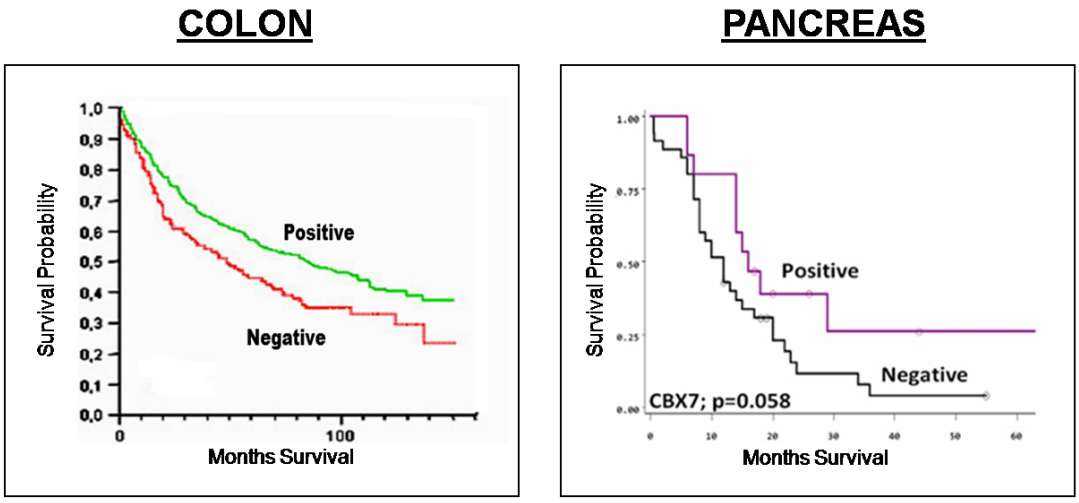

Figure 1.4 Association between CBX7 expression and survival time of cancer patient Kaplan-Meier survival curves showing differences in survival time between patients with colon or pancreas tumors positive or negative for CBX7 expression. The expression of the CBX7 protein positively correlates with a long survival time. On the contrary, loss of CBX7 expression is a marker of poor prognosis.

1.3.4 CBX7 in lung carcinomas

Lung neoplasms represent one of the principal cause of cancer mortality and its incidence is in constant increasing (Christiani 2006, Walker 2008). The *World Health Organization* classification of 2004, actually the standard system used to classify lung carcinomas on the basis of their morphological characteristics, classifies lung carcinomas in *small cell lung cancer* (SCLC) and *non-small cell lung cancer* (NSCLC). NSCLC represent the 80% of lung carcinomas and include the *adenocarcinoma* (AD), the *squamous cell carcinoma* (SCC) and the *large cell carcinoma* (LCC). As thyroid, colon and pancreatic carcinomas, also lung tumors are characterized by the loss of CBX7 expression. Immunohistochemical analysis have shown that the expression of CBX7 protein is absent in all the AD samples

analysed, while its expression is present in the normal tissues. Decreased expression is associated with loss of heterozygosity (LOH) at *CBX7* locus in the 50% of carcinoma samples analysed. The role of CBX7 in lung carcinogenesis was supported by a lower rate of colonies formation after restoration of *CBX7* expression in lung carcinoma cell lines. The anti-oncogenic role of CBX7 in lung carcinogenesis, was also supported by the phenotypical analysis of *Cbx7*$^{-/-}$ mice. In fact, *Cbx7*$^{-/-}$ mice have an higher incidence to develop lung carcinomas than wild type mice, while *Cbx7*$^{+/-}$ preferentially develop lung adenomas (Forzati et al. 2012). This suggests that the loss of CBX7 expression is strongly associated with the acquisition of a malignant phenotype and that the maintenance of *CBX7* expression prevents the malignant transformation of lung tissues.

1.4 Mechanisms of action of CBX7 protein

CBX7 is a chromatin protein able to regulate gene transcription by contributing to the assembling of macromolecular complexes. Studies performed in our laboratory, have characterized different molecular mechanisms by which CBX7 is able to carry out its role of transcriptional regulator. In one model CBX7 prevents cancer progression through a mechanism involving the interaction with the histone deacetylase 2 (HDAC2), a protein that catalyzes the histone deacetylation, thus promoting the silencing of gene expression (Marks et al. 2001). In particular, it has been shown that CBX7 is able to positively regulate the expression of the *CDH1* gene encoding the E-cadherin, an adhesion protein whose expression decreases during the epithelial-mesenchymal transition (EMT), by interacting and inhibiting the activity of HDAC2 on the promoter of *CDH1* (Federico et al. 2009).
CBX7 is also involved in the regulation of microRNAs. In fact, we have demonstrated that CBX7 protein is able to negatively regulate the expression of miR-181b, whose expression is found to be up-regulated in breast carcinomas. Moreover, we identified CBX7 as a target of the miR-181b, thus demonstrating that the expression of *CBX7*, in turn, is negatively modulated by the miR-181b, suggesting the existence of a loop involved in breast cancer progression (Mansueto et al. 2010).
In addition, a very recent study has demonstrated that CBX7 is able to interact with the high mobility group A1 (HMGA1) protein. In particular, we have demonstrated that CBX7 protein negatively regulates the expression of the *CCNE1* gene, encoding the Cyclin-E protein, a key mediator of cell proliferation, through a mechanism involving the interaction with HMGA1. In fact, we have found that CBX7 is able to interact with and to counteract the activity of HMGA1 on promoter

of the *CCNE1* gene, thus inhibiting cell proliferation. Moreover, the presence of CBX7 on the *CCNE1* promoter recruits also the HDAC2 (Forzati et al. 2012).
It has been demonstrated that CBX7 is directly involved in gene repression and promoter DNA hypermethylation of genes that are not expressed in cancer. CBX7, in fact, is able to complex with DNA methyltransferase (DNMT) enzymes on the promoter of specific genes suggesting a role in the initiation of epigenetic changes involving abnormal DNA hypermethylation of genes frequently silenced in adult cancer (Mohammed et al. 2009). In cancer, CBX7 has contrasting roles due to the cellular context in which it is located and to the different proteins interacting with it. In fact, CBX7 silences the expression of the *INK4b-ARF-INK4a* gene cluster, thus promoting cell proliferation and inhibiting cell senescence (Gil et al. 2004). In this mechanism is involved the long non-coding RNA (lcnRNA) *ANRIL*, a mRNA transcribed in the antisense orientation of the *INK4b-ARF-INK4a* gene cluster. In particular, the nascent *ANRIL* lncRNA is transcribed by the RNA Polymerase II at the transcription start site (TSS) in the $p16^{INK4a}$ gene and associates with SUZ12 to recruit PRC2 complex that initiates H3K27me3. Subsequently, PRC1 is recuited by *ANRIL* through CBX7 chromodomain that binds to H3K27me3 and in turn in the maintenance of epigenetic respression of $p16^{INK4a}$ gene expression (Yap et al. 2010).

1.5 High Mobility Group A (HMGA) protein family

In order to understand the role of CBX7 protein in cancer, we searched for its partners of interaction involving in the formation of macro-molecular complexes that regulate gene transcription. In this context, we identified HMGA1 as an important CBX7 interacting protein. The high mobility group A (HMGA) protein family is composed of non-histone components of chromatin acting as architectural factors able to regulate gene transcription. These proteins are key elements of multiprotein complexes comprising transcriptional factors and co-factors that leads to the regulation of the expression of several genes.The HMGA proteins share an higly conserved structured during evolution. The HMGA proteins comprise HMGA1 (isoforms HMGA1a, HMGA1b, HMGA1c) and HMGA2. They are characterized by three DNA binding domains containing a specific sequence called “AT-hooks”, short basic repeats through which they bind to AT-rich sequences in the minor groove of DNA. In addition, they are characterized by an acid C-terminal tail that may be involved in protein-protein interaction and in the recruitment of specific proteins to the enhanceosome (Reeves et al. 2001).The HMGA proteins are encoded by two different genes. The human *HMGA1* gene is located on the chromosome 6p21 and consists of 8 exons among which only exons from 5 to 8 are

transcribed in mRNA: it encodes the HMGA1 protein with a molecular weight of 19-20 kDa (Friedmann et al. 1993). Exons from 5 to 7 encodes the AT-hook domains. The *HMGA1* mRNA is subject to alternative splicing process generating two HMGA1 isoforms, HMGA1a and HMGA1b. These isoforms differ in their sequence for 11 additional amino acids between the first and the second AT-hook domains of the HMGA1a protein compared with the sequence of the HMGA1b protein (Figure 1.5 A). Both HMGA1a and HMGA1b proteins are the most abundant HMGA1 spliced variants in mammalian cells (Friedmann et al. 1993, Johnson et al. 1990). Finally, *HMGA1c* encodes a protein with a molecular weight of 26-27 kDa. This isoform is characterized by a 67 nucleotides deletion at RNA level in comparison with the other two HMGA1 proteins. This deletion results in a frameshift mutation, so the HMGA1 proteins are identical in their first 65 amino acids while they differs thereafter (Napgal et al. 1999). The HMGA1c isoform is not yet well characterized, but it appears to be the only *HMGA1* transcript present in normal human and mouse testis (Chieffi et al. 2002) and, it has been shown that HMGA1c binds to retinoid acid receptors thus promoting the activation of transcription (Napgal et al. 1999).

The human *HMGA2* gene is located on the chromosome 12q13-15 and consists of 5 transcribed exons. The first three exons encode the AT-hook domains, while the fifth exon encodes the C-terminal tail (Hauke et al. 2001, Kurose et al. 2001) (Figure 1.5 B).

Both *HMGA1* and *HMGA2* genes are widely expressed during embryogenesis while their expression is absent or low in adult tissues (Chiappetta et al. 1996). In particular, HMGA2 expression is absent both in mouse and human adult tissues, while HMGA1 expression is present in low levels in the same tissues (Chiappetta et al. 1996, Rogalla et al. 1996). However, the expression of these two genes strongly increases in high malignant cells *in vitro* and *in vivo* (Giancotti et al. 1989).

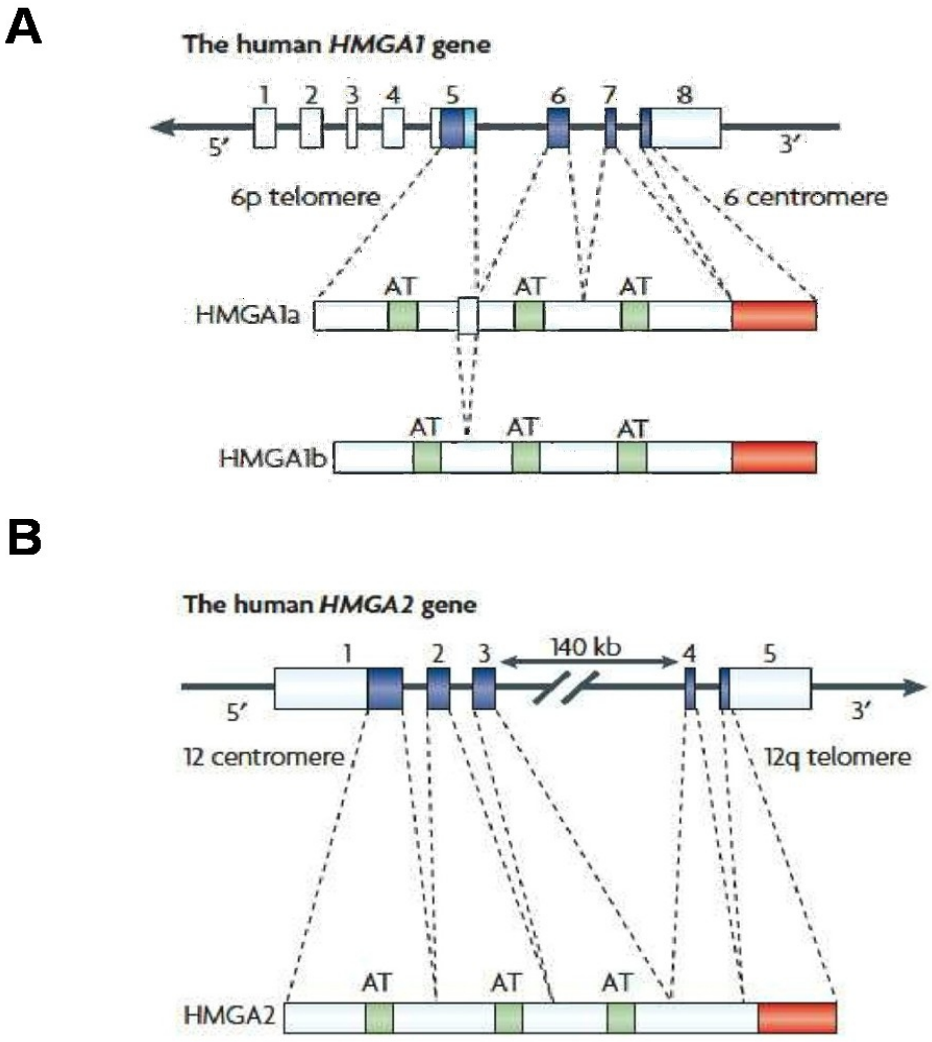

Figure 1.5 Schematic representation of HMGA proteins.
(A) HMGA1 gene is located on the chromosome 6 and gives rise to splicing variants that differ for 11 amino acids. Each of the protein contains three AT-hooks (green box), that bind to DNA, and a C-terminal tail (red box). (B) HMGA2 gene is located on the chromosome 12 and gives rise to one single protein. AT-hooks and C-terminal tail colors are described in (A).

1.6 Mechanisms of action of HMGA proteins

HMGA proteins do not have transcriptional activity *per se*, but interact with the transcription machinery and alter chromatin structure thus regulating, negatively or positively, the expression of several genes. HMGA proteins can interact both with DNA and transcriptional factors to generate multi-protein complexes bound to DNA. They play roles in assembling and modulating the formation of macromolecular complexes involved in different biological processes. HMGA proteins directly bind to the DNA and modify its conformation facilitating the binding of transcriptional factors (TFs) (Thanos et al. 1992, Thanos et al. 1993) (Figure 1.6 A). For example, through this mechanism, HMGA proteins are able to regulate the expression of the *interferon (IFN)-β* gene. In particular, the activation of *IFN-β* gene is due to a multifactor complex assembled on the nucleosome-free enhancer region of the gene. This complex includes the NFκB factor, the interferon regulatory factor, the activating transcriptional factor 2 (ATF2)/JUN and the HMGA1a protein (Thanos et al. 1992, Thanos et al. 1993).
In addition, through the study of the enhancement of transcriptional activity of TF serum-response factor mediated by HMGA1a protein, it has been demonstrated that HMGA proteins can also influence gene transcription by directly interacting with TFs and enhancing their binding affinity to DNA (Chin et al. 1998) (Figure 1.6 B).
Finally, HMGA proteins are able to interact with matrix- and scaffold- associated regions that are enriched in AT sequences and have high affinity for the nuclear matrix. These sequences anchor chromatin to the nuclear scaffold and organize topologically independent DNA domains that play functional roles both in DNA replication and transcription (Figure 1.6 C). The binding of HMGA proteins to these regions leads to activation of gene transcription through the displacement of histone H1 by the DNAmolecule (Galande et al. 2002).

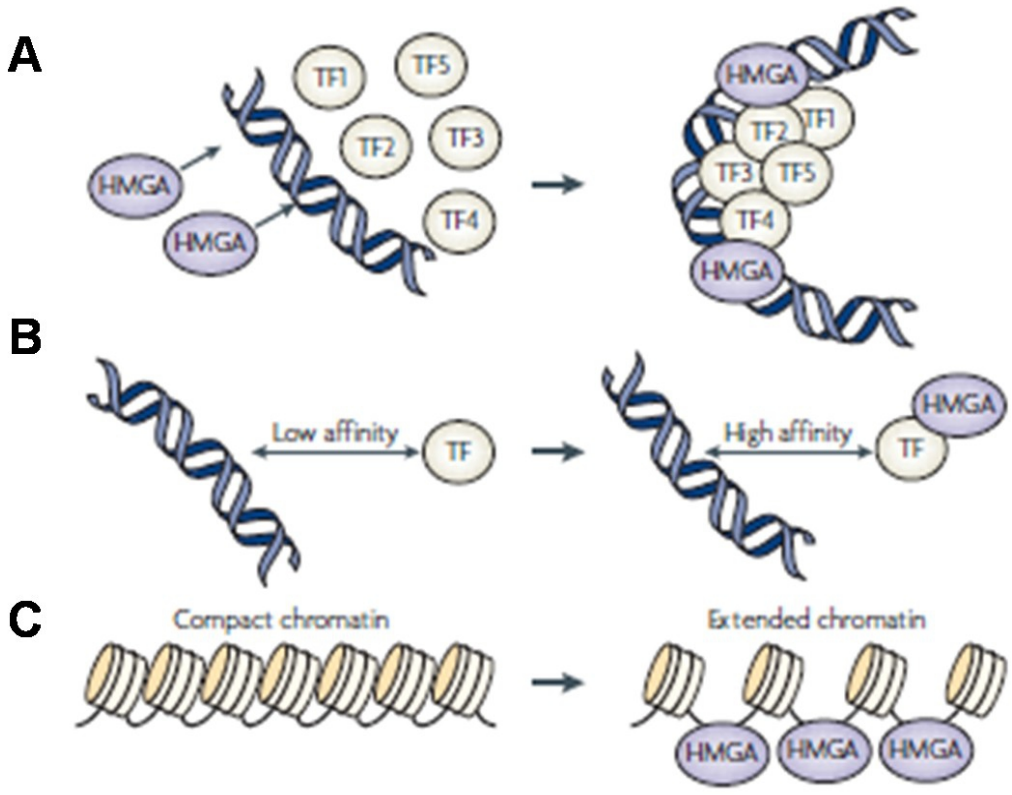

Figure 1.6 Mechanisms of action of the HMGA proteins.
HMGA proteins regulate positively or negatively gene expression through several mechanisms: (A) they are able to simultaneously interact with DNA and with transcriptional factors, thus forming macro-molecular complexes on specific chromatin regions; (B) they are able to enhance the affinity of transcriptional factors for the binding to the DNA;(C) they are able to alter the chromatin structure, thus promoting or silencing gene expression.

1.7 Characterization of the HMGA proteins role in cancer

HMGA proteins were identified for the first time in HeLa S3 cells (Lund et al. 1983), but the association between their expression and the neoplastic phenotype was found by observing changes in nuclear proteins expression following the transformation of the rat normal thyroid cell line FRTL5 through the Kirsten murine sarcoma virus (KiMSV). In particular, in this system it was observed an

increased expression of nuclear proteins showing elevated mobility on gel, that were named HMGA (Giancotti et al. 1989).
During the years, several studies have demonstrated that *HMGA1* expression is over-expressed in different neoplastic tissues, as pancreas, thyroid, colon, breast, lung, ovary, cervix, prostate, head and neck and gastric carcinomas (Fusco and Fedele 2007). This finding indicates that HMGA1 might be a candidate biomarker for cancer diagnosis and prognosis. In fact, in several papers it has been reported that there is a strong correlation between the high expression of *HMGA1* gene and the malignant tumor phenotype. Moreover, an association was also found between the over-expression of *HMGA1* and the presence of metastasis and a reduced survival. Over-expression of *HMGA1* was also observed in several kind of human leukaemias (Pierantoni et al. 2003).
However, in contrast, both heterozygous and homozygous *Hmga1*-null mice develop B-cell lymphomas (Fedele et al. 2006). The contrastating role of HMGA1 protein in cancer could be explained by the fact the HMGA1 interact with several proteins in different cellular environments, therefore, interacting with different partners, it is able to regulate gene expression. Recently it has been demonstrated that the elevated expression of *HMGA1* could be due to a complex cooperation between SP1 family members and AP1 factors, induced by the activation of Ras signaling: this represents one of the mechanisms leading to over-expression of HMGA1 gene in cancer (Cleynen et al. 2007).
Cytogenetic studies have demonstrated the presence of chromosomal rearrangements involving the HMGA 2 locus (12q13-15) in various benign tumors of mesenchymal origin, as lipomas, uterine leiomyomas, pulmonary chondroid hamartomas, breast fibroadenomas, endometrial polyps, pleomorphic adenomas of salivary glands and vulvar aggressive angiomyxoma. Chromosomal rearrangements generally involve the third intron of the HMGA2 gene and this leads to a deregulation of gene expression, truncation or, more frequently, to a generation of fusion genes. These aberrant genes encode chimeric transcripts containing the first three exons of HMGA2 and ectopic sequences of other genes. This rearrangement generates proteins that still retain the ability to bind to DNA and to interact with other proteins, but they lose the 3' untranslated region (3'UTR) that prevents the precise regulation of HMGA2 gene expression. To confirm this hypothesis, recent studies have demonstrated that the expression of the *HMGA2* gene is regulated by microRNAs (miRNAs) that bind to the 3'UTR of the gene thus repressing its translation (Lee and Dutta 2007, D'Angelo et al. 2012). Rearrangments and overexpression of the *HMGA2* gene have also been observed in non-mesenchymal human benign tumors, such as pituitary adenomas (Finelli et al. 2002). Mice expressing a truncated form of *Hmga2* under the regulatory control of the cytomegalovirus (CMV) promoter (Battista et al. 1999) or the histocompatibility complex class I H – 2Kb promoter (Arlotta et al. 2000) develop lipomas. A similar

phenotype was also observed in mice over-expressing wild type *HMGA2*. In addition, these mice develop pituitary adenomas secreting prolactin and growth hormone (Fedele et al. 2002).

1.8 Genes regulated by HMGA proteins in cancer

Recently, several studies have characterized the transforming ability of HMGA proteins. They have demonstrated that HMGA proteins are able to up- or down-regulate the expression of genes involved in cell proliferation and cancer progression through the interaction with several proteins. In fact, it has been shown that HMGA2 induces pituitary adenomas in *Hmga2* transgenic mice by binding to pRB, a key regulator of cell cycle, and enhancing the activity of E2F1. In particular, it has been shown that HMGA2 interacts with pRB, complexed with E2F1, and displaces HDAC1 from pRB-E2F1 complex. In this way, HMGA2 promotes the acetylation of E2F1, thus stabilizing its "free active" form (Fedele et al. 2006).
Moreover, HMGA2 is able to positively regulate the *CCNA2* gene expression, encoding the Cyclin A, by associating with the transcriptional repressor E4F1 (Tessari et al. 2003) and by enhancing the activity of the AP1 complex (Vallone et al. 1997). It has been demonstrated that the over-expression of HMGA2 leads to a recruitment of FRA1 on the *CCNA2* promoter, inducing the expression of JUNB that, in turn, binds to *Cyclin A* promoter (Casalino et al. 2007).
Another study has demonstrated the role of HMGA1 protein in the control of cell proliferation. HMGA1, in fact, prevents cell apoptosis by interacting with p53. HMGA1 is able to bind to p53 *in vivo* and *in vitro* interfering with p53-mediated transcription of Bcl2-associated X protein (Bax) and cyclin-dependent kinase inhibitor 1A (p21Waf1/Cip1). As well, HMGA1 cooperates with p53 to activate the transcription of the p53 inhibitor MDM2 (Pierantoni et al. 2006).
HMGA1 interferes with apoptosis by also interacting with the pro-apoptotic homeodomain-interacting protein kinase 2 (HIPK2), promoting its delocalization in the cytoplasm, thus inhibiting the p53 apoptotic function (Pierantoni et al. 2007).
The HMGA proteins are also involved in DNA repair systems. In fact, HMGA1 is able to compete with p53 and human MutS homologue proteins (MSH2-MSH6) for "Holliday junction" binding, preventing the activation of the mismatch repair response (Subramanian et al. 2002). Moreover, HMGA1 is able to negatively regulate the expression of genes involved in DNA-damage recognition and removal, as BRCA1 (Baldassarre et al. 2003).
Finally, HMGA proteins are involved in the regulation of epithelial-mesenchymal transition, as reported in a recent study demonstrating that transforming growth factor β (TGFβ) mediates EMT by inducing HMGA2 (Thuault et al. 2006).

1.9 Small integrin-binding ligand N-linked glycoproteins (SIBLINGs) family

The cell progression toward malignancy requires complex interaction with the host tissue. To survive in host tissues, tumor cells needs to elude immune surveillance and to overcome extracellular matrix barriers. All these events may be carried out through a complex interaction between host tissues and secreted proteins, as small integrin-binding ligand N-linked glycoproteins (SIBLINGs). SIBLING family consists of five glycophosphoproteins named osteopontin (OPN) (secreted phosphoprotein 1, SPP1), bone sialoprotein (BSP), dentin matrix protein 1 (DMP1), dentin sialophosphoprotein (DSPP) and matrix extracellular phosphoglycoprotein (MEPE). The genes encoding the SIBLING proteins are five identically orientated tandem genes within a 37500 bp region on chromosome 4. They encode small soluble and secreted prosphoproteins sharing common functional motifs and domains, including an Arg-Gly-Asp (RGD) motif that binds to specific receptors (Bellahcene et al. 1997). The SIBLING name originates from their common genetic and biochemical characteristics, not from functional activity. They act as modulators of cell adhesion by interacting through RGD or non-RGD motifs with cell surface receptors with members of the matrix metalloproteinase (MMP) family and with the complement factor H (CFH). By interacting with several receptors, they can localize either on cell surface, exhibiting autocrine activities, either in the extracellular space where they may function as paracrine mediators (Bellahcene et al. 2008).

SIBLINGs were initially described as glycophosphoproteins associated to mineralized tissues and involved in hydroxyapatite crystals formation. However, recent studies have found a strongly up-regulation of SIBLINGs in ephitelial tumors, frequently exhibiting pathological microcalcification and properties to metastasize to bone (Bellahcene et al. 1997). In normal tissues, all SIBLINGs undergo post-traductional modifications leading to the formation of a mature protein involved in several cellular processes. For example, SPP1 is able to promote cell adhesion and motility by interacting with a variety of integrins (Christensen et al. 2007). Moreover, through the activation of NFκB signaling, SPP1 and BSP positively affect the survival of T lymphocytes and bone marrow-derived monocytes and macrophages (Valverde et al. 2005). Recent studies have further demonstrated that SIBLING proteins are strongly over-expressed in several human carcinomas. In fact, increased expression of BSP was detected in breast (Bellahcene et al. 1994), prostate (Waltregny et al. 1998), lung (Bellahcene et al. 1997), thyroid (Bellahcene et al. 1998) and pancreas (Kayed et al. 2007) carcinomas. Also DSPP levels were found increased in human malignancies as prostate (Chaplet et al. 2006) and breast (Bucciarelli et al. 2007) cancers. On the other hand, the expression of MEPE seems to be more restricted than the other SIBLINGs, since its expressionis associated only with tumors resulting in oncogenic hypophosphatemic osteomalacia

(Rohde et al. 2007). Although these proteins play a role in carcinogenesis, the SIBLING protein mainly involved in the progression of tumors toward malignancy is the osteopontin protein.

1.10 Characteristics of the SPP1 protein

SPP1 is a 264-301 amino acids protein that is subject to several post-translational modifications, like phosphorylation, glycosylation and cleavage that lead to the production of a protein with a molecular weight ranging from 25 to 75 kDa (Young et al. 1990). This protein contains a hydrophobic sequence like other secreted proteins. In addition, it includes a calcium phosphate apatite binding region, a cell attachment RGD sequence, a thrombin cleavage site and two glutamines recognized by transglutaminase enzymes (Young et al. 1990). The human *OPN* gene contains 7 exons and the full length mRNA is named *OPN-a*. Alternative splicing of the *OPN* mRNA, occurring in a region upstream of the central integrin binding domain and the C-terminal CD44 binding domain, leads to the formation of *OPN-b* and *OPN-c*, that lack the exon 5 and the exon 4, respectively (Mirza et al. 2008). Only the isoform *OPN-c* seems to be expressed in invasive tumors as observed in breast carcinoma samples (Mirza et al. 2008). SPP1 protein can exist as an immobilized extracellular matrix molecule in mineralized tissues as well as an intracellular protein. It also shows a wide distribution in normal tissues, like kidney (Khan et al. 2002), breast (Rodrigues et al. 2007), placenta (Joyce et al. 2005) and testes (Luedtke et al. 2002). It is also expressed by leukocytes (Iwata et al. 2004), smooth muscle cells (Iwata et al. 2004) and highly metastatic cancer cells. SPP1 protein is able to mediate cell-matrix and cell-cell communication by interacting with specific receptors. In fact, the interaction between SPP1 and cell surface integrins leads to the activation of regulatory and structural proteins like focal adhesion kinase (FAK) proteins, src and other cytoskeletal proteins (Fong et al. 2009).

1.11 SPP1 is involved in cancer progression and in the formation of tumor metastasis

Tumor progression includes a sequential series of events that confer a survival advantage to transformed cells. In this context, an important role is played by SPP1 protein. SPP1 is able to regulate cell migration by interacting with different integrins, including $\alpha_v\beta_1$,$\alpha_v\beta_3$,$\alpha_v\beta_5$, $\alpha_4\beta_1$, $\alpha_9\beta_1$ and $\alpha_8\beta_1$. Among all of them, the heterodimer $\alpha_v\beta_3$ is the most common associated with the malignant properties of

SPP1 (Liaw et al. 1995). SPP1 can also interact with the surface proteoglycan CD44 and with its variants expressed by cancer cells (CD44v3-v6) in a RGD-dependent manner through its carboxy-terminal fragment. In fact, the interaction between SPP1 and CD44v6 is sufficient to induce a metastatic phenotype in pancreatic carcinoma cells (Gunthert et al. 1991) and to trigger an autocrine mechanism sustaining proliferation and invasion of transformed rat thyroid cells transformed (Castellone et al. 2004). The binding of SPP1 to CD44 induces cell migration through the activation of phospatidyl-inositol 3-kinase (PI3K) and Akt pathway, while the binding to $\alpha_v\beta_3$ is associated with the activation of mitogen-activated protein kinase (MAPK) pathway that promotes cell proliferation. Furthermore, SPP1-$\alpha_v\beta_3$ complex enhances angiogenesis by increasing VEGFs expression (Liaw et al. 1995) and prevents apoptosis through the activation of NF-κB pathway (Khan et al. 2002) (Figure 1.7).

Recent studies have demonstrated that SPP1 contributes to the invasion of extracellular matrix by promoting the production of MMP family proteins (Philip et al. 2001). It has been reported that breast cancer cell lines transfected or treated with SPP1showed an increased expression and activity of the urokinase-type plasminogen activator (uPA) that activates MMP1 and MMP2 which, in turn, digest specific extracellular matrix components (ECM), thus promoting cancer invasion and the formation of metastasis (Tuck et al. 1999).

Another important aspect of the SPP1 protein function is its involvment in the control of immunity response. Since this protein is produced by activated macrophages, leukocytes and activated T-lymphocytes, it promotes inflammation-induced cancer growth by enhancing neutrophil and macrophage infiltration. Moreover, SPP1 might avoid tumor cells-removal by down-regulating macrophage nitric oxide synthase expression and by mediating the binding of CFH to the cell surface that inhibits the complement and the cell lysis (Fedarko et al. 2000).

SPP1 was the first SIBLING found to be overexpressed in human carcinomas. The importance of this occurence is due not only to the mechanisms regulated by SPP1, but also to the correlation of its expression levels with specific stages of clinical progression. Recent studies have in fact demonstrated that high levels of SPP1 represent a poor prognostic marker in colon (Rohde et al. 2007) and renal (Matusan et al. 2006) cancer patients. Moreover, increased plasma levels of SPP1 have been found in patient with highly aggressive prostate (Ramankulov et al. 2007), lung (Chang et al. 2007), gastric (Wu et al. 2007), hepatocellular (Wu et al. 2007) and pancreatic carcinomas (Koopmann et al. 2004), suggesting a role of SPP1 as marker for cancer progression and underlining its involvement in the formation of tumor metastasis.

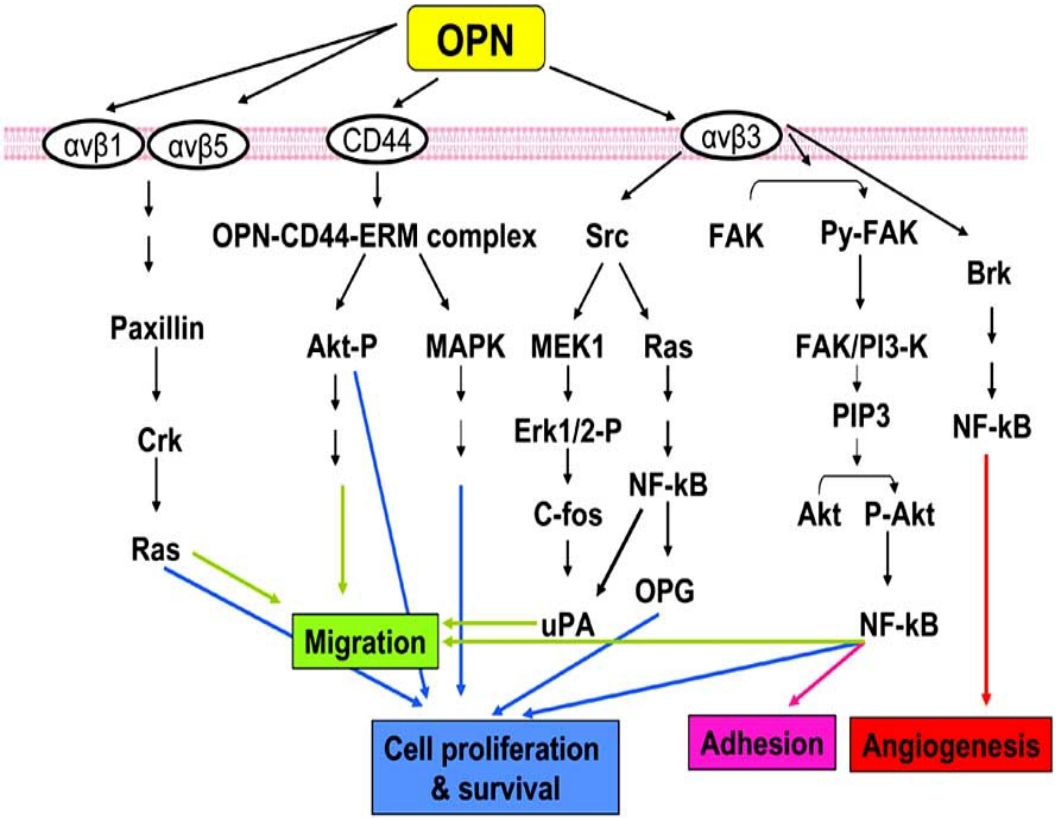

Figure 1.7 Schematic representation of the pathway activated by the osteopontin
The osteopontin is able to regulate several cellular mechanisms by interacting with different cell surface receptors. In fact, the binding to the $\alpha_v\beta_1$ and $\alpha_v\beta_5$ promotes cell migration through the activation of the Ras pathway, while the interaction with the CD44 positively regulates cell proliferation and survival through the Akt and MAPK pathway. Finally, through the interaction with the $\alpha_v\beta_3$ receptor, the osteopontin is able to activate the NF-κB pathway, thus promoting cell adhesion and angiogenesis.

1.12 Mechanisms of regulation of the *SPP1* expression

Generally, increased amount of the SPP1 protein is associated with an intense transcription of the *SPP1* gene. Several hormones, cytokines and transcriptional factors may influence the expression of this gene. *SPP1* human promoter shows a conserved region containing a conserved (TTTAAA) TATA box (-27 to -19), an inverted CCAAT box (-52 to -46), a CC box (-100 to -93) and an E-box binding factors region. Furthermore, there is one 1,25-dihydroxyvitamin D3 response

elements (VDREs) upstream the promoter region that is bound by the vitamin D3 receptor (VDR), and a consensus sequence for the AP1. Vitamin D3 is a strong stimulator of *SPP1* synthesis in bone and epidermal cells and a marked reduction of *SPP1* mRNA expression is observed in vitamin-D3-deficient rachitic mice (Chen et al. 1996). The expression of *SPP1* in bone is also increased by retinoic acid (Manji et al. 1998), while it is decreased by bisphosphonates (Sodek et al. 1995) and calcitonin (Kaji et al. 1994). Expression of *SPP1* is also up-regulated by various growth and differentiation factors. Epidermal growth factor (EGF), c-Src and 12-0-tetradecano iphorbol-l 3-acetate (TPA) enhances *SPP1* expression through the protein kinase C (PKC), which activates the early response genes JUN and FOS, that, in turn, increase *SPP1* transcription (Denhardt and Guo 1993). AP-2 is also a target of PKC-mediated signalingas well as signaling through cAMP-dependent protein kinase A (PKA).

During pre-implantation, the up-regulation of *SPP1* expression is also mediated by Oct-4 through a PORE element in the first intron of the gene, while SOX2 represses its expression by interacting with a region closely located (Botquin et al. 1998). Furthermore, Src is able to positively regulate the *SPP1* expression through the inverted CCAAT box which is bound by nuclear factor NF-Y (Kim and Sodek 1999). Since v-src is a transforming viral oncogene originally identified in the Rous sarcoma virus (RSV), this regulation established a link between neoplastic transformation and increased expression of *SPP1* gene.

More recently, RUNX2 and ETS1 were identified as important positive transcriptional regulators of *Spp1* expression in murine colorectal cancer cell line (Wai et al. 2006), while the tumor-suppressors BRCA1 (El-Tanani et al. 2006), phosphatase and tensin homologue (PTEN) (Shao et al. 2007) and the metastasis suppressor breast cancer metastasis suppressor 1 (BRMS1) have been found to be negative regulators of *SPP1* expression (Wu et al. 2012).

2. AIM OF THE STUDY

CBX7 is a chromatin-binding protein whose expression is strongly down-regulated in thyroid tumors with a progressive reduction in relation to malignant grade and neoplastic stage. Recent studies have shown that the correlation between the loss of CBX7 and a highly malignant phenotype with a consequent poor prognosis is a general event in oncology. In fact, the loss of *CBX7* expression has been shown to be associated with increasing malignancy grade of several human carcinomas whereas the retention of *CBX7* expression has been correlated with a longer survival of colon and pancreatic cancer patients (Pallante et al. 2010, Karamitopoulou et al. 2010). In this context, the aim of this study is to understand the reasons that make the loss of *CBX7* expression an important event in carcinogenesis.
Thus, it was performed an investigation of genes associated with cancer progression whose expression could be regulated by CBX7 protein. To characterize the role played by CBX7 in cancer, we considered to analyze the CBX7 interacting proteins to define the molecular mechanisms through which CBX7 is able to exert its function of gene transcriptional regulator .
Besides the study concerning the characterization of the CBX7 role in cancer, projects developed during my PhD program regarded the objects of the following publications:

1. Piscuoglio S, Zlobec I, Pallante P, **Sepe R**, Esposito F, Zimmermann A, Diamantis I, Terracciano L, Fusco A, Karamitopoulou E. **HMGA1 and HMGA2 protein expression correlates with advanced tumour grade and lymph node metastasis in pancreatic adenocarcinoma.** Histopathology 2012;60(3):397-404. (Attached at the end).

2. Pallante P, Malapelle U, Berlingieri MT, Bellevicine C, **Sepe R**, Federico A, Rocco D, Galgani M, Chiariotti L, Sanchez-Cespedes M, Fusco A, Troncone G. **UbcH10 overexpression in human lung carcinomas and its correlation with EGFR and p53 mutational status.** Eur J Cancer 2013;49(5):1117-26. (Attached at the end).

3. MATERIALS AND METHODS

3.1 Cell culture and transfections

HEK 293 (human embryonal kidney) cell line, the anaplastic thyroid carcinoma cell line FRO and the papillary thyroid carcinoma cell lines TPC-1 and BC-PAP were grown in Dulbecco's Modified Eagle Medium (DMEM, Life Technologies, Grand Island, NY) supplemented with 10% fetal bovine serum, 1% L-glutamine 10mM, 1% penicillin/streptomycin 100µg/ml (Life Technologies). Normal rat thyroid cell line PC Cl3 was cultured in modified F12 medium supplemented with 5% calf serum (Life Techonologies), 1% L-glutamine 10mM, 1% penicillin/streptomycin 100µg/ml and six growth factors (thyrotropic hormone, hydrocortisone, insulin, transferrin, somatostatin and glycyl-histidyl-lysine) (Sigma, St. Louis, MO) (Fusco et al. 1987). Mouse embryonic fibroblasts (MEFs) from *Cbx7*-knockout mice were established as described elsewhere (Forzati et al. 2012) and grown in DMEM supplemented by 1% L-glutamine 10mM, 1% penicillin/streptomycin100µg/ml and 1% gentamicin 10mg/ml (Life Technologies). All cell lines were maintained at 37°C under 5% CO_2 atmosphere.
For transfection procedures it was used Lipofectamine reagent (Life Technologies) for HEK 293 cells, Fugene HD reagent (Promega, Fitchburg, WI) for BC-PAP cells and Neon Electroporation System (Life Techologies) for FRO and TPC-1 cells, according to manifacturer's instructions. FRO cell clones were selected using geneticin (G418, Life Technologies) antibiotic at a final concentration of 1200µg/ml. For migration assays, TPC-1 cells were transfected with a short interfering RNA (siRNA) specific for the human *SPP1* gene (Flexi Tube Gene Solution, GS6696, Qiagen, Hilden, Germany) or with a non-specific siRNA control (All Stars Negative Control siRNA AF488, 1027292, Qiagen) at a final concentration of 100nM.
For the inhibition of *Cbx7* expression in PC Cl3, rat *Cbx7* siRNA (SI01495795 and SI01495802, Qiagen) and Nonsilencing Control siRNA (1022076, Qiagen) were transfected using Oligofectamine (Life Technologies) according to the manufacturer's racommandations. siRNAs were used at a final concentration of 100 nM.

3.2 Plamid and constructs

The vector encoding the CBX7 protein fused to the epitope of the P and V proteins of the paramyxovirus of simian virus 5 (V5) was constructed by cloning the human cDNA sequence in a pcDNA3.1/V5-His-TOPO ® (Life Technologies). The CBX7 cDNA was obtained by PCR using the following primers: CBX7 forward 5'-ATGGAGCTGTCAGCCATC-3' and CBX7 reverse 5'-GAACTTCCCACTGCGGTC-3'. The same PCR product was also inserted into a pCEFL-HA vector using *EcoRI* and *NotI* restriction sites, thus generating a plasmid encoding the CBX7 protein fused to the hemagglutinin tag (HA).
The vector encoding the HMGA1b protein fused to the HA tag was obtained by cloning the entire sequence of the HMGA1b in the pCEFL-HA vector using the restriction sites *EcoRI* and *NotI*, as described elsewhere (Pierantoni et al. 2006).
The expression of CBX7-V5, CBX7-HA and HMGA1-HA were assessed by western blot analysis.

3.3 Human tissue samples

The human thyroid cancer tissues, adjacent normal tissues or normal contralateral lobes, obtained from surgical specimens, were provided by the service of Pathological Anatomy of the Centre Hospitalier Lyon Sud, Pierre Bénite, France, and were immediately frozen in liquid nitrogen to subsequently perform the extraction of RNA.
"TissueScan™ Real-Time Lung Cancer Disease Panel III" of cDNAs was purchased from Origene (Origene Technologies Inc., Rockville, MD). This lung cancer cDNA panel (HLRT103) contains 8 normal lung specimens and 40 lung cancer specimens of different histotype, whose clinical pathological features are freely available at the following address: http://www.origene.com/qPCR/Tissue-qPCR-Arrays.aspx

3.4 cDNA microarray analysis

In this study we used commercially available GeneChip® Human Gene 1.0 ST Arrays (Affymetrix, Santa Clara, CA) to identify genes differentially expressed. The whole hybridization procedure was performed following the Affymetrix instructions. Briefly, the RNA was extracted from FRO-EV-1 and FRO-CBX7-1 cells and was used to obtained double strand cDNA by using oligo-dT and T7

RNA polymerase. Amplification and labeling processes were verified using a GeneChip® Eukaryotic Poly-A RNA Control Kit (Affymetrix) with exogenous positive controls. 15 µg of each biotinylated cDNA preparation was denaturated and hybridizated in a mixture containing biotinylated hybridization controls (GeneChip® Expression Hybridization Controls, Affymetrix). Samples were then hybridized onto a GeneChip® Human Gene 1.0 ST Array consisting of 12.625 probe set each representing a transcript at 45°C for 16 hours at constant rotation (60 rpm) in a Hybridization Oven (Affymetrix). Every samples was hybridized and analyzed on the microarray chip three times. Microarray scanned images were obtained with a GeneChip Scanner (Affymetrix) using the default settings. Images were analyzed with Affymetrix Gene Expression Analysis Software (Affymetrix).
The analysis was performed comparing the gene expression profiling of FRO-CBX7-1 cells to the gene expression profiling of the FRO-EV-1 cells. The fold change values obtained by this analysis indicated the relative change in the expression levels between FRO-EV-1 and FRO-CBX7-1 and were used to identify genes differentially expressed in these two clone cells.

3.5 RNA extraction and quantitative (q)RT-PCR

Total RNA was extracted from cell lines and tissues by using the Trizol reagent (Life Technologies) according to the manufacturer's instruction. The integrity of the extracted RNA was then assessed by denaturating agarose gel electrophoresis. 1µg of total RNA of each sample was used to obtained double strand cDNA with the QuantiTect Reverse Transcription Kit (Qiagen) using an optimized blend of oligo-dT and random primers according to the manufacturer's instruction. To ensure that RNA samples were not contaminated with DNA, negative controls were obtained by performing PCR on samples that were not reverse transcribed but identically processed.
The cDNA obtained in these conditions, was used to evaluate the differential gene expression levels by PCR.
Semiquantitative PCR (RT-PCR) was carried out on cDNA using the GeneAmp PCR System 9600 (Applied Biosystems, Foster City, CA). After a first denaturing step (94°C for 10 minutes), PCR amplification was performed for 25-30 (variable) cycles (94°C for 30 seconds, 55-60°C (variable) for 30 seconds, 72°C for 30 seconds).
Here are reported the primer sequences used:

MOUSE

Fos: forward 5'-CGCAGAGCATCGGCAGAAGGG-3', reverse 5'-GATTCCGGCACTTGGCTGCA-3';

Fosb: forward 5'-AGCTCATCACCCTCCGCCGA-3', reverse 5'-CGGGCATTTCCCCGAGACCG-3';

Egr1: forward 5'-GGGAGCCGAGCGAACAACCC-3'; reverse 5'-TGATGGGAGGCAACCGAGTCGT-3';

Spp1: forward 5'-GTGGCCCATGAGGCTGCAGT-3'; reverse 5'-GCCAGAATCAGTCACTTTCACCGGG-3';

Spink1: forward 5'-TCAGTGCTTTGGCCCTGCTGAGT-3', reverse 5'-TTCTGGGACATCCCGCCACTGC-3';

Steap1: forward 5'-GCCATCTTGGCTCTCTTGGCTGTG-3'; reverse 5'-CCAAAGCGTGTACTGTGCCCAGA-3';

Cbx7: forward 5'-CTGGGAGCCTATGGAGCA-3', reverse 5'-GGCCCATTGGTCAGGTCT-3';

G6pd: forward 5'-CAGCGGCAACTAAACTCAGA-3', revers 5'-TTCCCTCAGGATCCCACAC-3';

Quantitative Real-Time PCR (qRT-PCR) was carried out with the CFX96 thermocycler (Bio-Rad, Hercules, CA) in 96-well plates using a final volume of 20 µl. For each of the PCR reaction, we used 10 µl of 2X Sybr Green (Applied Biosystems, Foster City, CA), 200 nM of each primer, and 20 ng of the cDNA previously generated. Here are reported the primer sequences used:

HUMAN

FOS: forward 5'-CTACCACTCACCCGCAGACT-3', reverse 5'-AGGTCCGTGCAGAAGTCCT-3';

FOSB: forward 5'-GGCGGAGGGAGCTGACCGAC-3', reverse 5'-CGTAGGGGATCTTGCAGCCCG-3';

EGR1: forward 5'-AGCCCTACGAGCACCTGAC-3', reverse 5'-GGTTTGGCTGGGGTAACTG-3'

SPP1; forward 5'-GGCCACATGGCTAAACCCTGACC-3', reverse 5'-TGGAGTCCTGGCTGTCCACAT-3';

SPINK1: forward 5'-TAAGTGCGGTGCAGTTTTCA-3', reverse 5'-TGAGAAGAAAGATGCCTGTTACC-3'

STEAP1: forward 5'-TGGCAATACTGGCTCTGTTGGCT-3', reverse 5'-GCGTGTATTGTGCCCAGTAGAAGGG-3';

CBX7: forward 5'-CGAGTATCTGGTGAAGTGGAAA-3', reverse 5'-GGGGGTCCAAGATGTGCT-3'
G6PD: forward 5'-ACAGAGTGAGCCCTTCTTCAA-3', reverse 5'-ATAGGAGTTGCGGGCAAAG-3'

RAT

Fos: forward 5'-CAGCATGGGCTCCCCTGTCAAC-3', reverse 5'-CACTGCAGGTCTGGGCTGGTG-3';
Fosb: forward 5'-AACTTTGACACCTCGTCCCGGGGC-3', reverse 5'-TCCTCTTCGGGAGACAGCTGCTGG-3';
Egr1: forward 5'-CCTCAAGGGGAGCCGAGCGAA-3', reverse 5'-GGAGGCAACCGGGTAGTTTGGC-3';
Spp1: forward 5'-GCTTTGCAGTCTCCTGCGGCAA-3', reverse 5'-AGACAGGAGGCAAGGCCGAAC-3';
Steap1: forward 5'-AGCCTAAGGGGAACCTGGAAGATGA-3', reverse 5'-TGGACCGTGTGCGGCAAAGG-3';
Cbx7: forward 5'-ATCCGGAAGAAGCGCGTGCG-3', reverse 5'-GGCCATGACAAGGCGAGGGTC-3';
G6pd: forward 5'-GTGGCCATGGAAAAGCCTGCCT-3', reverse 5'-TGGGGTTCCCCACATACTGGCC-3'.

After a polymerase enzyme activation step at 95°C for 10 minutes, the cDNAs were denaturated at 95°C for 15 seconds and then amplified at 60°C for 30 minutes. This denaturation/amplification step was repeted for 40 cycles. At the end of the reaction, the analysis of the melting curves obtained showed the specificity of the cDNA amplified. Every reaction was carried out in duplicate. Fold mRNA overexpression was calculated according to the formula $2^{-\Delta\Delta Ct}$ as previously described (Livak et al. 2011).

3.6 Protein extraction and western blot analysis

Total protein extracts were obtained by lysing cells in RIPA buffer (20 mM Tris-HCl pH 7.5, 5 mM EDTA, 150 mM NaCl, 1% Nonidet P40, and a mix of protease inhibitors) and then centrifugating at 13000 rpm at 4°C for 30 min. The extracted proteins were separated by SDS-PAGE and then transferred onto Immobilon-P Transfer membranes (Millipore, Billerica, MA). Membranes were blocked with 5% non-fat milk proteins and incubated with antibodies (Abs) at the appropriate diluitions. Anti-V5 (Invitrogen), anti-HA (Roche Applied Science, Mannheim, Germany), anti-CBX7 (Santa Cruz Biotechnology, Inc., Santa Cruz, CA) are the

Abs used in this study. To validate that equal amounts of protein were loaded, the filters were incubated with antibodies against the γ-tubulin and α-vinculin protein (Santa Cruz Biotechnology, Inc.). Filters were then incubated with horseradish peroxidase-conjugated secondary antibody (1:3000) for 60 min at room temperature and the signals were detected by western blotting detection system (ECL) (Promega).

3.7 Luciferase transactivation assay

HEK 293 cells were transiently co-transfected with a vector encoding CBX7-HA or HMGA1b-HA protein and a vector encoding the *luciferase* gene under the transcriptional control of the CBX7-regulated genes. A region spanning 1000 bp upstream of the tanscriptional start site (TSS) of these genes was amplified by PCR using the following primers:
FOS-1K: forward 5'-ATAACCACACCTCGCACTCC-3', reverse 5'-GGCTCAGTCTTGGCTTCTCA-3';
FOSB-1K: forward 5'-TGGCAAGTGCCAAATACAAG-3', reverse 5'-TGGCCGTAGCTCTGAGTCTT-3';
EGR1-1K: forward 5'-GGGACTAGGGAACAGCCTTT-3', reverse 5'-TGGGATCTCTCGCGACTC-3';
SPP1-1K: forward 5'-TTCCAAAATCGAATCTGTTCC-3', reverse 5'-TGCTGCTGCAGACATCCTC-3';
SPINK1-1K: forward 5'-TTCCACAGGCCAATTTAAGG-3', reverse 5'-CTGGGACTGGAAGGGTCATA-3';
STEAP1-1K: forward 5'-GGGAGGGACGGAGTAAACAT-3', reverse 5'-TTCAAGGGACTCACCCACTC-3'.

PCR products where inserted in the pGL3 vector (Promega), upstream to the open reading frame of the *luciferase* gene. All the reporter constructs generated were checked for mutations by direct sequencing. A vector expressing the *Renilla* gene under the control of the cytomegalovirus (CMV) promoter was used to normalize transfection activity. Protein lysates were obtained 48 hours after transfection and luciferase activity was measured for each point by using a Lumat LB9507 luminometer (Berthold Technologies, Bad Wildbad, Germany) and the Dual-Luciferase Reporter System kit (Promega). All assays were performed in duplicate and are the results of the mean of three independent experiments.

3.8 Chromatin immunoprecipitation (ChIP) and Re-ChIP assay

ChIP and Re-ChIP experiments were performed as reported elsewhere (Federico et al. 2009). Briefly,48h after transfection $5x10^6$ HEK 293 cells were cross-linked using 1% formaldehyde at room temperature for 10 min to fix the DNA-protein complexes. The reaction was then terminated by adding glycine at a final concentration of 0.125 mol/L. Cells were lysed in 300 µl of buffer containing 10mM EDTA, 50mM Tris-HCl pH 8.0, 1% SDS and protease inhibitors and then sonicated three times for 10 minutes at maximum settings, obtaining fragments between 0.3 and 1.0 kb. The samples were cleared by centrifugation at 14000 rpm for 15 minutes at 4°C. After centrifugation, 3% of the supernatants amount was used for control of the chromatin obtained (input), and the remaining part of the samples was diluted 2.5-fold in Ip buffer (100mM NaCl, 2mM EDTA pH 8.0, 20mM Tris-HCl pH 8.0, 0.5% Triton X-100 and protease inhibitors). After 3h of pre-clearing at 4°C with Protein A Sepharose or Protein G Sepharose saturated with Salmon Sperm (Millipore), samples were mixed overnight at 4°C with the following specific antibodies: anti-HA (Santa Cruz Biotechnology, Inc.), anti-V5 (Sigma), anti-CBX7 (Santa Cruz Biotechnology, Inc.) and with aspecific IgG (Millipore). Subsequently, the DNA-protein-Antibodies complexes were immunoprecipitated with the proteins A/G previously used and the immunoprecipitated chromatin was released from the beads through 30 minutes incubation with 250 µl of 1% SDS, 0.1M $NaHCO_3$ at 37°C and finally with 200nM NaCl at 65°C overnight.
For Re-ChIP assays, complexes from the primary ChIP were eluted with 10 mmol/L of DTT for 30 minutes at 37°C and then diluted in 250 µl of Re-ChIP buffer (20mmol/L Tris-HCl pH 8.1, 1% Triton X-100, 2mmol/L EDTA, 150mmol/L NaCl). The released complexes were re-immunoprecipitated with the indicated second antibodies and then subjected again to the ChIP procedure. Crosslink was reversed by an overnight incubation at 65°C with 20 µl of 5M NaCl. Subsequently,10 µl 0.5mM EDTA, 20 µl 1M Tris-HCl pH 6.5 and 20 µg of Proteinase K were added and then the complexes were incubated for 1 h at 45°C. The chromatin immunoprecipitated was purified by phenol/chloroform (Life Techonologies), precipitated by two volumes of ethanol and 0,1M NaAc and finally analyzed by qRT-PCR using the following primers:

<u>HUMAN</u>
prom_HQ_C_FOS: forward 5'-TTAGGACATCTGCGTCAGCA-3', reverse 5'-GCCTTGGCGCGTGTCCTAATC-3';
prom_HQ_FOS_B: forward 5'-ATGGCTAATTGCGTCACAGG-3', reverse 5'-GCACTGTCCAGCAAGAGGTC-3';

prom_HQ_EGR1: forward 5'-CTTATTTGGGCAGCACCTTATTTGG-3', reverse 5'-GCTTCGGGGAAGCCTAGA-3';
prom_HQ_SPP1: forward 5'-AGGCAAGAGTGGTGCAGAT-3', reverse 5'-AGCACTTAGGGATCCCATGA-3';
prom_HQ_SPINK1: forward 5'-CCACAACCACAGAGGGAGTT-3', reverse 5'-CAGGTTCTGGGAATGTCACC-3';
prom_HQ_STEAP1: forward 5'-TAATAAGCCCCCGGGTAATC-3', reverse 5'-CCCCTCGCCTTTTGTTTAAT-3';
prom_HQ_GAPDH: forward 5'-CCCAAAGTCCTCCTGTTTCA-3', reverse 5'-GTCTTGAGGCCTGAGCTACG-3'.

MOUSE
prom_MQ_C_Fos: forward 5'-CTACACGCGGAAGGTCTAGG-3', reverse 5'-GCGCTCTGTCGTCAACTCTA-3';
prom_MQ_Fosb: forward 5'-GCCGAGCTCCTTATATGGCTA-3', reverse 5'-CACCTGCCCATAGTGTGACC-3';
prom_MQ_Egr1: forward 5'-CCACTGCTGCTGTTCCAATA-3'; reverse 5'-AGCCCTCCCATCCAAGAGT-3';
prom_MQ_Spp1: forward 5'-TCATCCCCATTGATGTTTTTC-3', reverse 5'-TGCATTTAGAATCCCGGAAG-3';
prom_MQ_Spink1: forward 5'-CTGCCCATCCATTCAGAACT-3', reverse 5'-AGCTGCATTCCTGACATCCT-3';
prom_MQ_Steap1: forward 5'-GACGGCGTAATCGCTACAGA-3', reverse 5'-CGAAATCTGCAGTTGTGCAT-3';
prom_MQ_Gapdh: forward 5'-TGAGTCCTATCCTGGGAACCATCA-3', reverse 5'-TTTGAAATGTGCACGCACCAAGCG-3'.

3.9 Cell migration assay

TPC-1 cells were used to carry out the cell migration assays. 24h after transfection, cells were counted using the TC10™ Automated Cell Counter (Bio-Rad). The transwell motility assays were performed using 8 micron pore, 6.5-mm polycarbonate transwell filters (Corning Costar Corp., Cambridge, MA). $3x10^4$cells suspended in 200 µl serum-free medium were seeded on the upper surface of the filters and allowed to migrate toward 300 µl of 10% FBS-containing media in the bottom compartment. After 24h, transwell filters were washed three times in phosphate buffered saline (PBS) at room temperature and the cells migrating to the underside of the filters were fixed and stained with crystal violet solution (0,1% crystal violet in 20% of methanol). The cells remaining on the

upper surface were removed with a cotton swab. In order to exactly quantify the crystal violet staining, samples were de-stained with 1% SDS in 500 µl of PBS. The absorbance of the eluates were measured at 540nm in microplate reader (LX 800, Universal Microplate Reader, BioTek,Winooski, VT, USA). Cell proliferation assays were performed using CellTiter96 Aqueous One (Promega) to confirm that the effects observed were due to cell migration and not to cell proliferation. Extracted RNA and proteins were analyzed to evaluate the expression of the transfected vectors.

4. RESULTS

4.1 Generation of stable clones expressing *CBX7*

In order to understand the role that the CBX7 protein plays in the process of carcinogenesis and cancer progression, we restored the *CBX7* expression in a human anaplastic thyroid carcinoma cell line (FRO) in which the expression of *CBX7* is absent. To this aim, we transfected FRO cells with a vector encoding the CBX7 protein fused to the HA epitope or with the corresponding backbone vector. By this approach, we obtained FRO cell clones stably expressing CBX7-HA (FRO-CBX7) or carrying the empty vector (FRO-EV). qRT-PCR confirmed the elevated expression of *CBX7* in the FRO-CBX7 clones compared with the levels observed in FRO-EV clones and in FRO wild type (FRO-WT) cells (Figure 4.1 A). Western blot analysis confirmed the expression of the CBX7 protein in all the FRO-CBX7 stable clones generated (Figure 4.1 B).

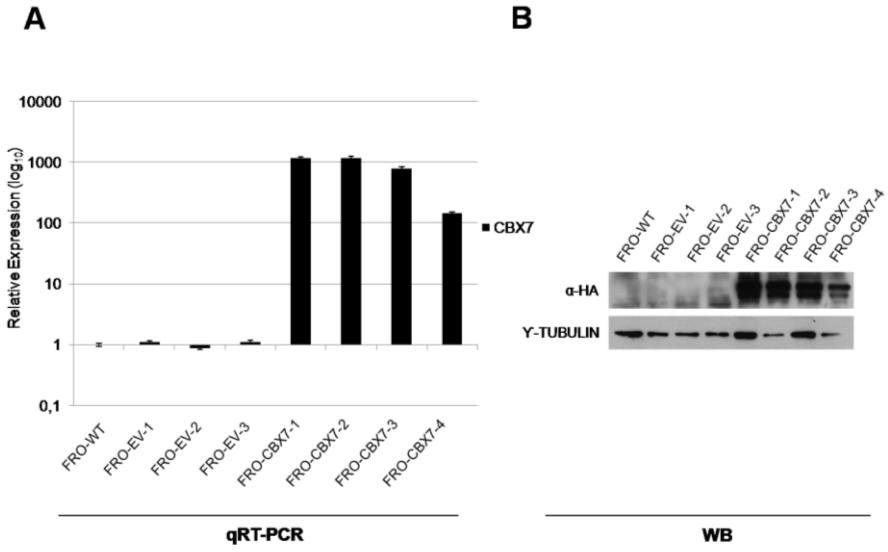

Figure 4.1 Generation of FRO clones stably expressing CBX7
CBX7 expression analysis. (A) qRT-PCR analysis of CBX7 expression in FRO cells stably expressing CBX7-HA (FRO-CBX7) or the backbone vector (FRO-EV). Relative Expression value represents the CBX7 expression levels of each sample compared to those observed in wild type cells (FRO-WT), assuming that *CBX7* expression in WT cells is equal to 1. (B) Immunoblot analysis of CBX7-HA protein expressed in FRO-CBX7, FRO-EV and FRO-WT cells confirmed the expression of the CBX7 protein in all the FRO-CBX7 clones generated. γ-tubulin was used as control of the amount of protein analyzed.

4.2 Identification of genes regulated by the CBX7 protein

To investigate the mechanism by which the loss of *CBX7* expression may contribute to the acquisition of a malignant phenotype, we analyzed the differential gene expression profiling of FRO-CBX7 and FRO-EV clones. RNAs extracted from FRO-EV-1 and FRO-CBX7-1 clones were hybridized to an Affymetrix oligonucleotide array containing probes corresponding to several thousand human transcripts. The expression profiling of the FRO-CBX7-1 cells was then compared with the FRO-EV-1 one. By this analysis, we identified several transcripts differentially expressed between FRO-CBX7-1 and FRO-EV-1. In particular, we found that 53 transcripts (17 up-regulated and 36 down-regulated) had an absolute fold change value more than 2.0, while 263 transcripts (103 up-regulated and 160 down-regulated) showed an absolute fold change value comprised from 1.5 to 2.0 in FRO-CBX7-1 respect to FRO-EV-1.

Among the whole set of genes that we found to be regulated by CBX7 in human thyroid carcinoma cells, we decided to investigate genes known to play a relevant role in the acquisition of a malignant phenotype. For this reason, we focused on *FBJ murine osteosarcoma viral oncogene homolog (FOS), FBJ murine osteosarcoma viral oncogene homolog B (FOSB)* and *early growth response 1 (EGR1)* genes that were positively regulated, and *secreted phosphoprotein (SPP1), serine peptidase inhibitor, Kazal type 1 (SPINK1)* and *six transmembrane epithelial antigen of the prostate 1 (STEAP1)* genes that, conversely, were negatively regulated by CBX7 protein (Table 4.1).

As a control of microarray analysis, we observed that CBX7 was highly expressed in the FRO-CBX7-1 clone used to carry out this experiment (Table 4.1).

Table 4.1 Analysis of the cDNA microarray

UP	Fold Change	Accession Number	Definition
CBX7	58,01	NM_175709	Chromobox homolog7
FOS	3,76	NM_005252	v-fos FBJ murine osteosarcoma viral oncogene homolog
LOC93432	2,76	NR_003715	Maltase-glucoamylase-like pseudogene
FOSB	2,67	NM_006732	FBJ murine osteosarcoma viral oncogene homolog B
C1orf88	2,65	BC101501	Chromosome 1 open reading frame 88
FLJ25778	2,49	NM_173569	Hypothetical protein FLJ25778
EGR1	2,45	NM_001964	Early growth response 1
CHN2	2,44	NM_004067	Chimaerin 2
LOC200383	2,39	BC015442	Similar to Dynein heavy chain at 16F
NEK5	2,29	NM_199289	NIMA (never in mitosis gene a)-related kinase 5
DOWN	**Fold Change**	**Accession Number**	**Definition**
SPINK1	-6,91	NM_003122	Serine peptidase inhibitor, Kazal type 1
SPP1	-4,64	NM_001040058	Secreted phosphoprotein 1 (osteopontin)
HLA-DMB	-4,6	NM_002118	Major histocompability complex, clas II, DM beta
STEAP1	-3,76	NM_012449	Six transmembrane epithelial antigen of the prostate 1
SEMA3A	-3,67	NM_006080	Semaphorin 3°
KLHL5	-3,26	NM_015990	Kelch-like 5
SGPP2	-3,22	NM_152386	Sphingosine-1-phosphate phosphatase 2
REG4	-3,10	NM_032044	Regenerating islet-derived family, member 4
NMUR2	-2,94	NM_020167	Neuromedin U receptor 2
FGL1	-2,91	NM_201553	Fibrinogen-like 1

The gene expression profiling of the FRO-CBX7-1 clone was compared to the gene expression profiling of the FRO-EV-1 clone. Fold Change value represents gene expressions in FRO-CBX7-1 cells compared with those observed in FRO-EV-1 cells. Accession number and definition are identicative of the genes identified. Up-regulated genes are indicated in green, while the down-regulated genes in red. The observation of CBX7 among the up-regulated genes represents a positive control of the experiment.

Then, by qRT-PCR, we validated the results obtained by the cDNA microarray analysis and evaluated the expression of these transcripts in several CBX7-expressing FRO cell clones. Thus, we confirmed the differential expression of these

genes in FRO-CBX7 clones compared to FRO-EV and FRO WT cells (Figure 4.2), suggesting a close association between the expression of the CBX7 protein and the expression of its regulated genes.

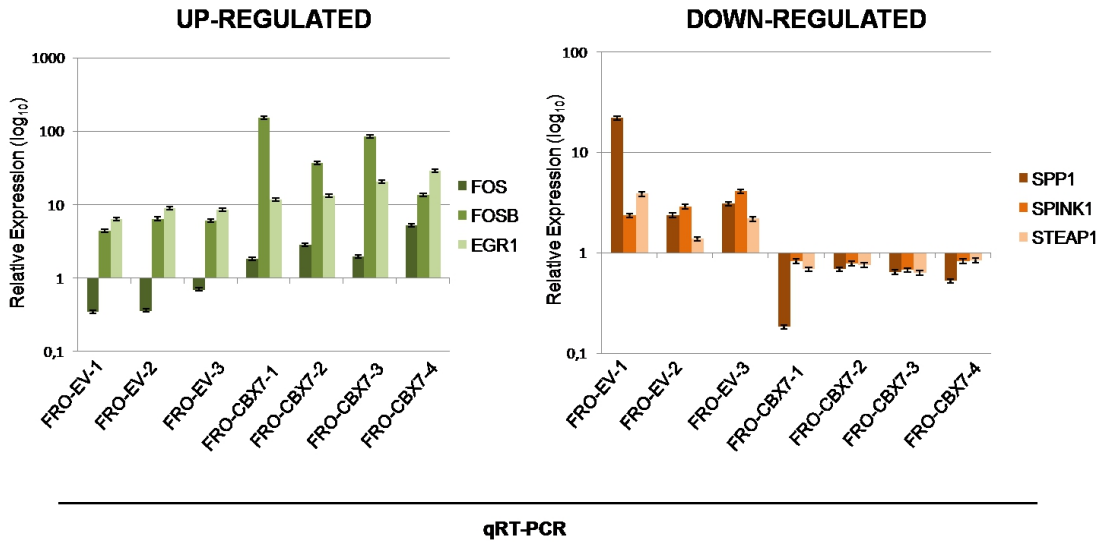

Figure 4.2 Expression analysis of the CBX7-regulated genes
The expression of the selected genes regulated by CBX7 protein was evaluated by qRT-PCR. Relative Expression value represents gene expression levels of sample compared to those observed in FRO-WT cells, assuming that gene expression in WT cells is equal to 1. (A) The expression of the CBX7 up-regulated genes is shown in green. *FOS, FOSB* and *EGR1* gene expression increased in FRO-CBX7 clones compared to FRO-EV clones and FRO WT cells. (B) The expression of the CBX7 down-regulated genes is shown in orange. *SPP1, SPINK1* and *STEAP1* gene expression decreased in FRO-CBX7 clones compared to FRO-EV clones and FRO WT cells.

4.3 Expression analysis of CBX7-regulated genes in mouse embryonic fibroblasts (MEFs) deriving from *Cbx7*$^{-/-}$ mice

Subsequently, we verified whether these genes differentially expressed in FRO-CBX7 cells showed differential expression also in other cell systems, as mouse embryonic fibroblasts (MEFs) isolated from *Cbx7*$^{-/-}$ mice (Forzati et al. 2012). To this aim, we analyzed the expression of the genes regulated by CBX7 in *Cbx7* $^{+/-}$ and *Cbx7*$^{-/-}$ MEFs. As shown in Figure 4.3, by RT-PCR we found that the expression of CBX7 down-regulated genes *Spp1, Spink1* and *Steap1* increased in MEFs heterozygous for *Cbx7* and null for *Cbx7* gene compared to WT MEFs. On the contrary, in accordance with the CBX7-positive regulation of *Fos, Fosb* and *Egr1* gene, we found that the expression of these three genes decreased in MEFs

from *Cbx7*$^{-/-}$ mice while their expression showed intermediate levels in *Cbx7*$^{+/-}$ MEFs compared to WT MEFs. These data shows that CBX7 protein is able to modulate the expression of these genes also in mouse system.

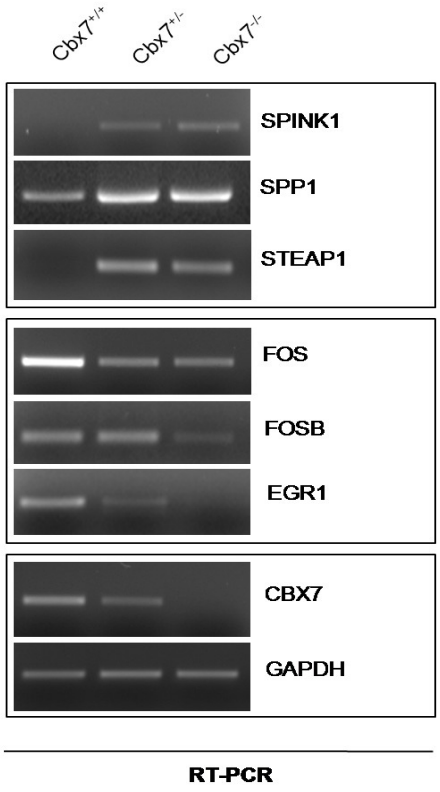

Figure 4.3 Expression analysis of the CBX7-regulated genes in mice embryonic fibroblasts (MEFs) system
Analysis of the expression of CBX7 up-regulated and down-regulated genes in MEFs obtained from *Cbx7*$^{-/-}$ mice by RT-PCR. A decreased expression of *Fos, Fosb* and *Egr1* gene was observed in MEFs *Cbx7*$^{-/-}$ compared to MEFs from *Cbx7* WT and *Cbx7* $^{+/-}$ mice. On the contrary, the expression of *Spp1, Steap1* and *Spink1* was found to be more pronunced in MEFs *Cbx7*$^{-/-}$ than in MEFs from *Cbx7* WT and *Cbx7*$^{+/-}$ mice. *Cbx7* expression was evaluated to confirm the system used. *Gapdh* expression was evaluated to normalize the amount of RNA used.

4.4 Expression analysis of CBX7-regulated genes in rat thyroid system

To further verify the role of the CBX7 protein in the regulation of these identified genes, we evaluated their expression in the normal rat thyroid cell line PC Cl3 in which *Cbx7* gene is normally expressed. *Cbx7* expression was silenced by using siRNA approach. After 24h from the siRNA treatment, we confirmed by qRT-PCR the silencing of the *Cbx7* gene. Then, we observed a reduced expression of the CBX7 up-regulated genes *Fos, Fosb* and *Egr1* expression and an increased expression of the CBX7 down-regulated genes *Spp1* and *Steap1*, in comparison with the expression levels observed in the untreated cells or in those treated with the non-silencing control siRNA (scrambled) (Figure 4.4).
The data obtained from this experiment confirmed that Cbx7 is able to modulate the transcription of these genes also in this cellular system.

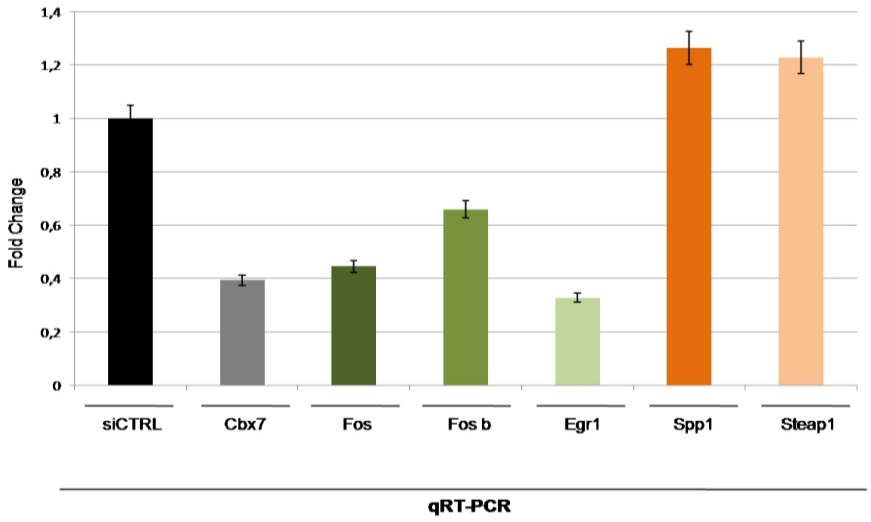

Figure 4.4 Gene expression analysis in PC Cl3 cells
qRT-PCR analysis in PC Cl3 silenced for *Cbx7* expression. After 24h from the transfection with the siRNA specific for *Cbx7,* qRT-PCR analysis showed an increased expression of *Spp1* and *Steap1* while a decreased expression of *Fos, Fosb* and *Egr1* was found in comparison to the expression levels observed in PC Cl3 cells transfected with the scrambled control siRNA (siCTRL). Fold Change value represents the gene expression levels of each sample compared to those observed in cells transfected with the control siRNA, assuming that expression levels of the control are equal to 1.

4.5 CBX7 directly modulates the activity of gene promoters

Subsequently, in order to understand whether CBX7 was directly involved in the differential expression of its regulated genes, we decided to evaluate the direct effect of CBX7 on the transcription of these genes. To this aim, we transiently co-transfected HEK 293 cells with an increasing amount of a vector encoding CBX7-HA and with a reporter vector carrying the *luciferase* gene under the control of a 1000 bp promoter region located upstream of the TSS of each one of the genes analyzed. A vector encoding the *Renilla* gene was used to normalize the luciferase signal observed. As shown in Figure 4.5 A, CBX7 enanched the transcriptional activity of *FOS, FOSB* and *EGR1* promoters, whereas it repressed the transcriptional activity of *SPP1, SPINK1* and *STEAP1* promoters (Figure 4.5 B). Interestingly, the effects of CBX7 on these promoters was dose-dependent, thus demonstrating that CBX7 is able to regulate the expression of these genes by directly modulating their promoter activity.

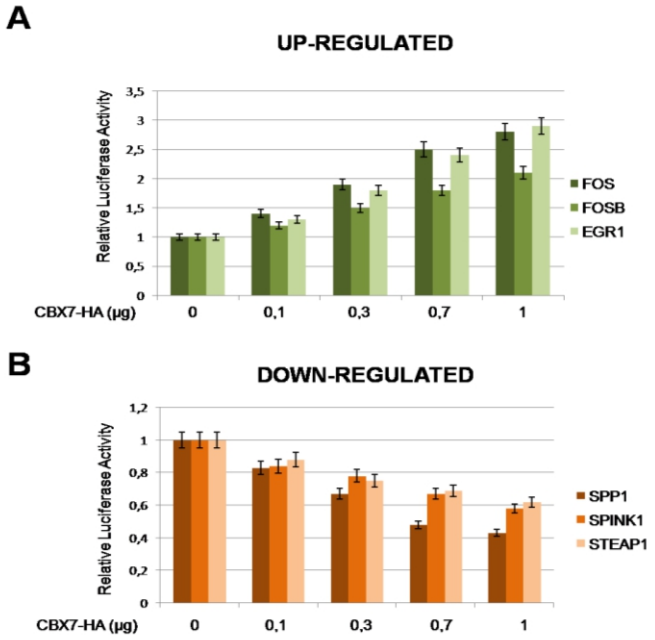

Figure 4.5 CBX7 directly modulates the activity of its regulated genes
HEK 293 cells were transiently co-transfected with increasing amount of a CBX7-expressing vector and constant amount of a vector encoding the *luciferase* gene under the control of the CBX7-regulated gene promoters. Relative luciferase activity represents the luciferase signals obtained in each samples compared to those observed in cells transfected with the backbone vector, assuming that the luciferase signals observed in backbone-expressing cells are equal to 1. (A) CBX7 was able to positively regulate the activity of the *FOS, FOSB* and *EGR1* promoter and (B) to negatively regulate the activity of *SPP1, STEAP1* and *SPINK1* promoter in a dose-dependent manner.

4.6 CBX7 protein physically interacts with the promoter region of its regulated genes

CBX7 is a chromatin protein and exerts its functional role by interacting with the DNA through its chromodomain (Bernstein et al. 2006). To characterize the molecular mechanism by which CBX7 protein acts to regulate genes transcription, we decided to evaluate whether CBX7 protein was able to bind to the promoter of its regulated genes *in vivo*. To this aim, we carried out a chromatin immunoprecipitation (ChIP) assay in HEK 293 cells transiently transfected with a vector encoding the CBX7 protein fused to the V5 tag or with the corresponding backbone vector. Cells were cross-linked and chromatin was immunoprecipitated with anti-V5 or IgG antibodies. Immunoprecipitated chromatin was subsequently analyzed by qRT-PCR using primers spanning the region of these genes promoter. We found that anti-V5 antibodies were able to precipitate region from the promoter of these genes only in cells transfected with CBX7-V5, demonstrating that CBX7 directly binds to these promoters *in vivo.* On the contrary, in cells transfected with the empty vector, we did not found any signal of chromatin immunoprecipitated. Moreover, no chromatin enrichment was found in samples immunoprecipitated with normal rabbit IgG and when primers for the human GAPDH control promoter were used (data not shown), indicating that the CBX7 binding is specific for these promoters (Figure 4.6).

To confirm the binding of endogenous CBX7 protein to the promoters of these genes, we took also advantage of tissues obtained from *Cbx7* knockout mice (Forzati et al. 2012). ChIP experiments were performed in kidney and spleen tissues obtained from $Cbx7^{+/+}$ and $Cbx7^{-/-}$ mice. Anti-CBX7 antibodies were able to recognize endogenous Cbx7 and to precipitate chromatin from $Cbx7^{+/+}$ but not from $Cbx7^{-/-}$ tissues,confirming the binding of endogenous Cbx7 to these promoter regions (Figure 4.7).

These ChIP experiments, therefore, indicated that CBX7 physically interacts with the promoter regions of these genes *in vivo*, therefore directly modulating their expression.

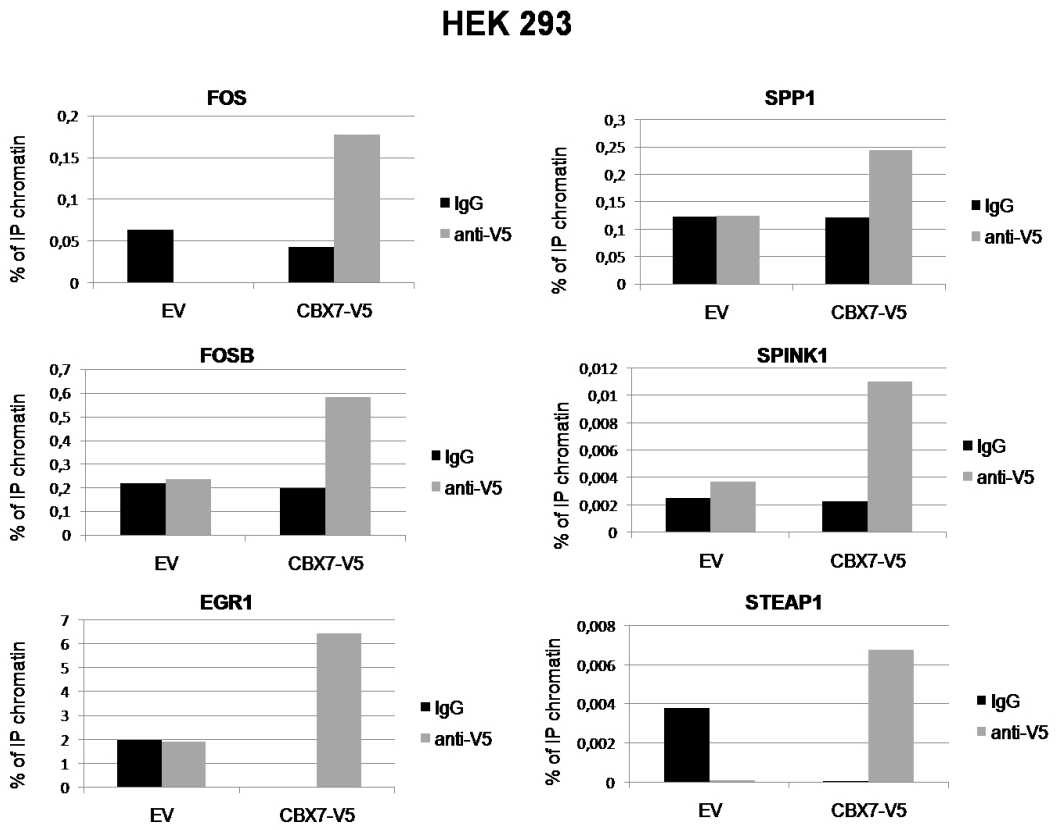

Figure 4.6 CBX7 protein binds to the promoter of its regulated genes
HEK 293 cells were transiently transfected with a vector encoding the CBX7-V5 protein or with the corresponding backbone vector. The chromatin was immunoprecipitated using antibodies against the V5 tag. IgG antibodies were used as negative control. The chromatin immunoprecipitated was analyzed by qRT-PCR using primers specific for the promoter region -300/+40 from the TSS. *GAPDH* primers were used as control of the binding specifity (data not shown). The percentage of IP chromatin represents the amount of immunoprecipitated chromatin in each sample compared to the amount of the total chromatin extracted and not immunoprecipitated (input).

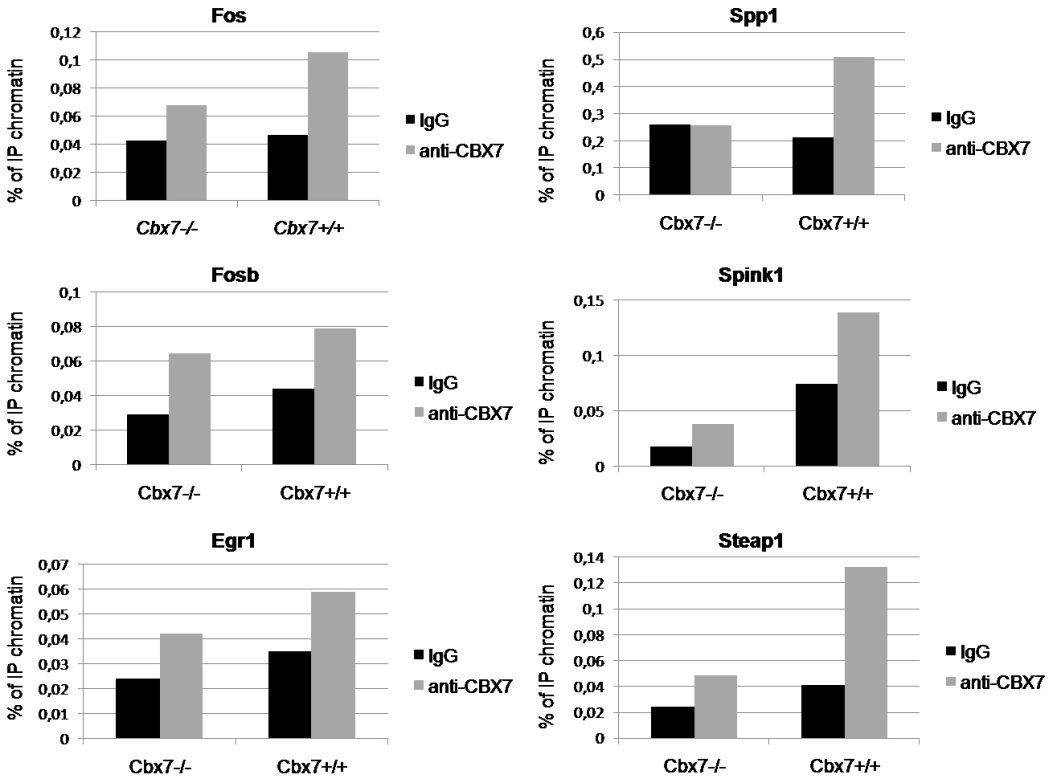

Figure 4.7 Cbx7 binds to the promoter of its regulated genes in mouse tissues
Chromatin extracted from spleen and kidney of a *Cbx7*$^{+/+}$ or *Cbx7*$^{-/-}$ mice was immunoprecipitated using anti-Cbx7 antibodies. IgG antibodies were used as negative control. The chromatin immunoprecipitated were analyzed by qRT-PCR using primers specific for the promoter region of all the genes analyzed. *GAPDH* primers were used as control of the binding specifity (data not shown). The percentage of IP chromatin represents the amount of immunoprecipitated chromatin in each sample compared to the amount of the total chromatin extracted and not immunoprecipitated (input).

4.7 The expression of CBX7-regulated genes is related to *CBX7* expression in human carcinomas

Previous studies have shown that *CBX7* expression is reduced in thyroid, colon and lung carcinomas (Pallante et al. 2008, Pallante et al. 2010, Forzati et al. 2012) with protein levels almost completely undetectable in most advanced thyroid cancers. For this reason, we hypothesized that the loss of *CBX7* gene could be involved in advanced stages of thyroid carcinogenesis through the consequent modulation of the expression of these identified genes. Therefore, we analyzed *CBX7* and the selected CBX7-regulated genes expression in a panel of human

papillary thyroid carcinomas and in lung carcinomas by qRT-PCR. As shown in Figure 4.8 A, the expression of *CBX7* is down-regulated in the PTC samples, as we expected, as well as the expression of its up-regulated genes *FOS, FOSB* and *EGR1*, while the expression of *SPP1, SPINK1* and *STEAP1* genes resulted increased. Similarly, in lung carcinoma samples we observed a positive correlation between the expression of *CBX7* and its up-regulated genes, while an inverse correlation was observed between the expression of *CBX7* and its down-regulated genes (Figure 4.8 B).
These data, therefore, strongly suggest that the loss of *CBX7* gene expression might contribute to the appearance of a malignant phenotype by modulating a set of genes critical for the progression step of carcinogenesis.

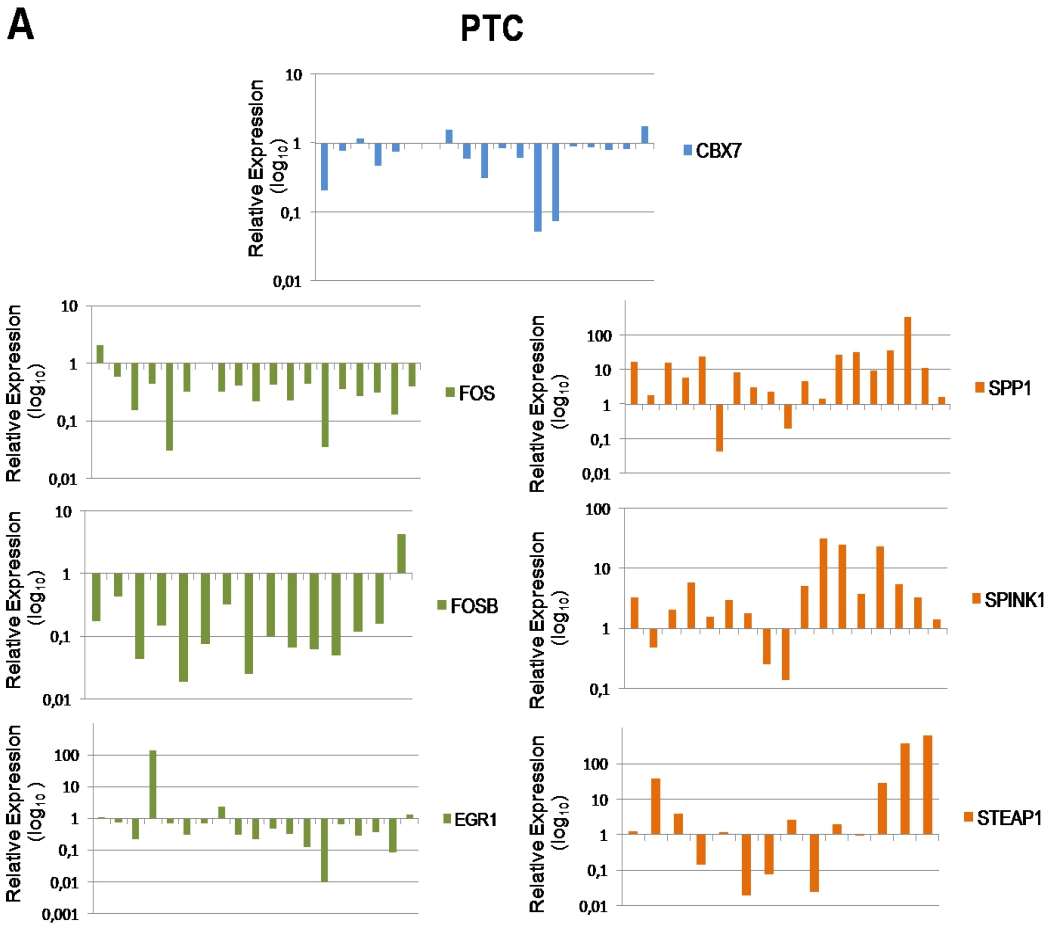

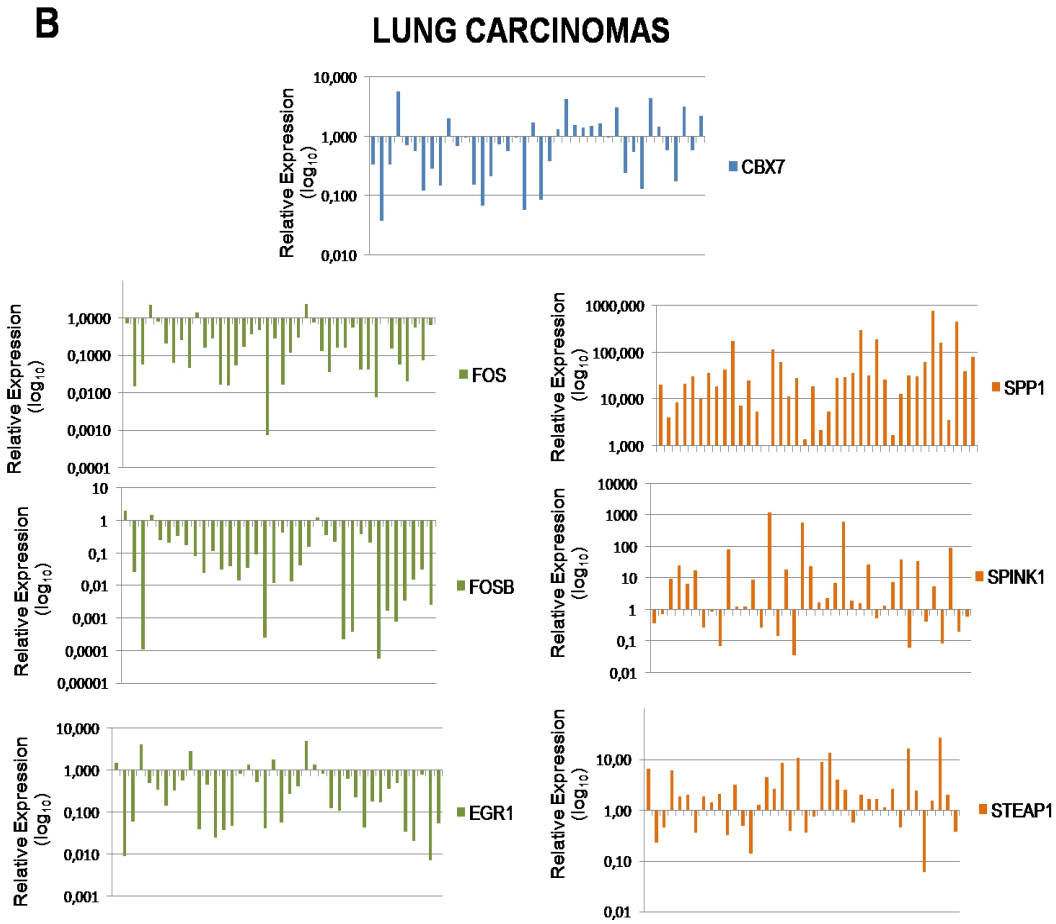

Figure 4.8 Analysis of gene expression in human carcinomas
qRT-PCR analysis. Relative Expression value represents the gene expression levels of each sample compared to those observed in the control sample, assuming that the expression level observed in the control is equal to 1. Gene expression was analyzed in a panel of (A) papillary thyroid and (B) lung carcinoma samples. A positive correlation was found between *CBX7* and its up-regulated genes (in green) while a negative correlation was found between *CBX7* and its down-regulated genes (in orange). The expression levels were compared to the mean of three normal thyroid gene expression in (A) and to the mean of eight normal lung gene expression in (B).

4.8 HMGA1 protein regulates the expression of the *SPP1* gene

In order to define the role of CBX7 in cancer and to understand why its loss could lead to malignancy, we decided to investigate the molecular mechanism by which

CBX7 regulates the expression of *SPP1,* one of its down-regulated gene. We focused on this gene because of its importance in cancer progression. Several studies, in fact, have shown that the *SPP1* gene expression strongly increases in different human carcinomas and that, the SPP1 plasma levels are well correlated with cancer progression and the formation of tumor metastasis.
Recently, it has been demonstrated that CBX7 exerts its role of transcriptional regulator by interacting with HMGA1 protein. Thus, we decided to evaluate whether this mechanism might be involved also in the regulation of the *SPP1* gene expression.
First of all, we analyzed the expression of the *Spp1* gene in MEFs system null for *Hmga1, Hmga2* or both genes. By qRT-PCR analysis we observed a decreased expression of *Spp1* in MEFs in which Hmga proteins were not expressed compared with the *Spp1* expression levels observed in WT MEFs (Figure 4.9 A). Moreover, we found that the reduction of the *Spp1* expression was more pronounced in *Hmga1*$^{-/-}$ MEFs than in *Hmga2*$^{-/-}$ ones, suggesting that the expression of the *Spp1* gene is under the transcriptional control of the Hmga1 protein. Then, to evaluate the effect of the HMGA1 protein on the expression of the *SPP1* gene, we transiently transfected the papillary thyroid carcinoma cell line BC-PAP, that shows low expression of the *SPP1* gene (Guarino et al. 2005), with increasing amount of a vector encoding HMGA1 protein fused to the HA epitope (HMGA1-HA) or with the corresponding backbone vector. By qRT-PCR analysis we found that HMGA1 protein was able to increase the *SPP1* gene expression, showing a positive transcriptional regulation of the *SPP1* gene mediated by the HMGA1 protein (Figure 4.9 B). Western blot analysis, performed with an anti-HA antibody, confirmed the expression of the HMGA1-HA protein in BC-PAP cells transfected (Figure 4.9 C).

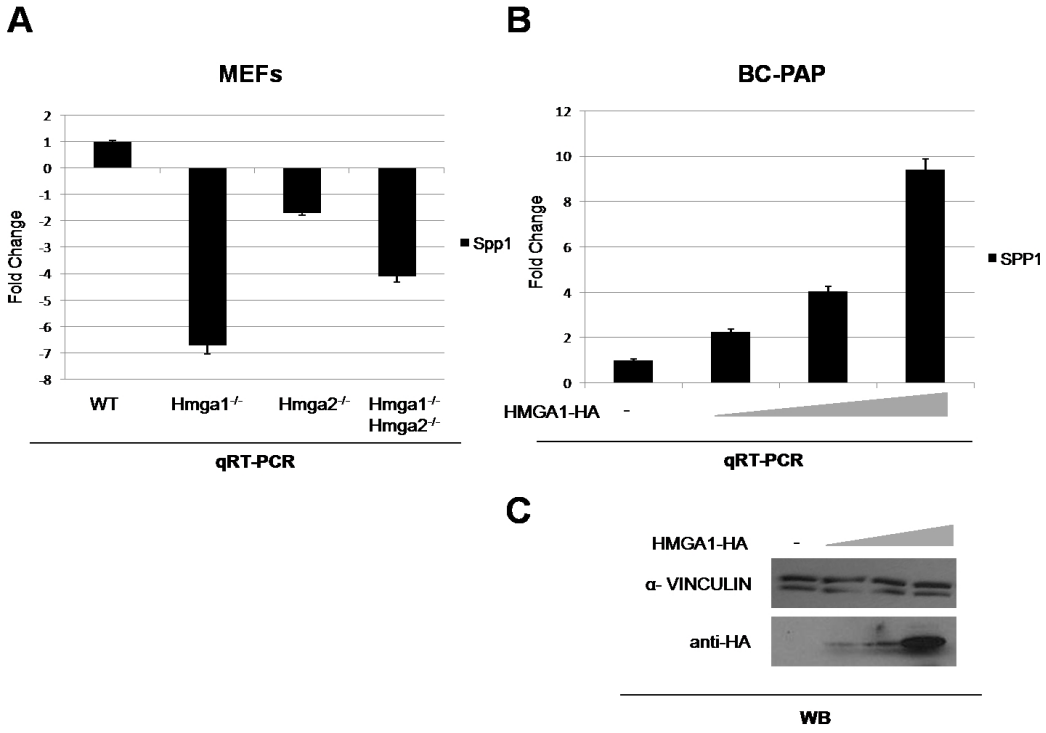

Figure 4.9 HMGA1 protein regulates the *SPP1* expression
(A) qRT-PCR analysis of *Spp1* in mouse embryonic fibroblasts (MEFs) null for Hmga1, Hmga2 or both genes showed a reduction of the *Spp1* expression levels in Hmga-null samples compared with WT cells. Fold Change value represents the *Spp1* expression levels of each sample compared with those observed in WT MEFs, assuming that the *Spp1* expression observed in WT MEFs is equal to 1. (B) Analysis of the *SPP1* gene expression by qRT-PCR in BC-PAP cells transfected with increasing amount of a vector encoding the HMGA1-HA protein showed an increase of the *SPP1* expression. Fold Change value represents the *SPP1* expression in each sample compared with the levels observed in cells transfected with the backbone vector, assuming that the *SPP1* expression observed in the sample control is equal to 1. (C) Immunoblot analysis was performed to confirm the expression of the HMGA1-HA protein. α-vinculin was used as control.

4.9 HMGA1 enhances the activity of the *SPP1* gene promoter

Subsequently, we evaluated the effect of the HMGA1 protein on the regulation of the *SPP1* promoter activity. HEK 293 cells were co-transfected with a vector encoding the luciferase gene under the control of 1000 bp region upstream the TSS of the *SPP1* promoter and with increasing amount of a vector encoding HMGA1-HA protein. A vector encoding the *Renilla* gene was used to normalize the

luciferase signals obtained. As shown in Figure 4.10, HMGA1 was able to enhance the transcriptional activity of the *SPP1* promoter in a dose-dependent manner, thus showing that HMGA1 acts by directly modulating the activity of the *SPP1* promoter.

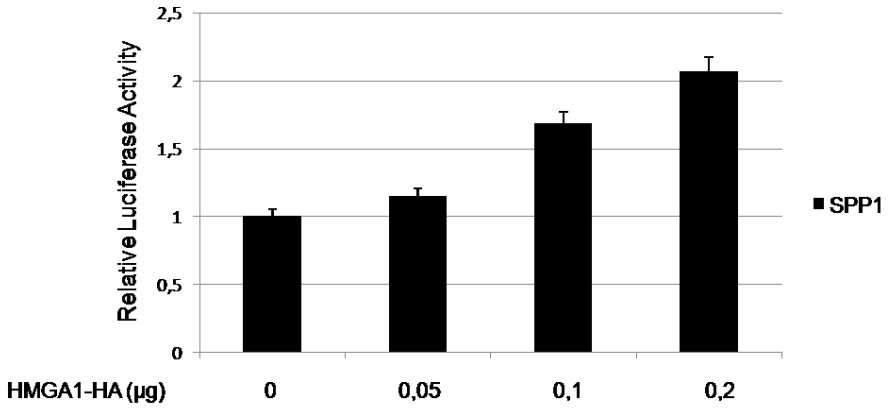

Figure 4.10 HMGA1 directly modulates the activity of the *SPP1* promoter
HEK 293 cells were transiently co-transfected with increasing amount of a vector encoding the HMGA1-HA protein and with constant amount of a vector encoding the *luciferase* gene under the control of the *SPP1* promoter. HMGA1 was able to positively regulate the *SPP1* promoter activity in a dose-dependent manner. Relative luciferase activity represents the luciferase signals obtained in each samples compared with those observed in cells transfected with the backbone vector.

4.10 CBX7 and HMGA1 compete for the binding to the *SPP1* promoter

We have demonstrated that HMGA1 protein is able to transcriptionally regulate the *SPP1* gene expression by directly modulating the activity of its promoter. Since HMGA are chromatin-interacting proteins, we asked whether HMGA1 protein was able to physically interact with the promoter region of the *SPP1* gene *in vivo*. To this aim we performed a ChIP assay in HEK 293 cell transiently transfected with a vector encoding the HMGA1-HA protein or with the corresponding backbone vector. The DNA-protein complexes were fixed and then immunoprecipitated with antibodies anti-HA epitope. The immunoprecipitated chromatin was finally extracted and analyzed by qRT-PCR using primers spanning the promoter region of the *SPP1* gene. As shown in Figure 4.11 A, we found a chromatin enrichment only in cells transfected with the vector encoding the HMGA-HA protein and immunoprecipitated with the anti-HA antibodies. No signals was obtained in cells transfected with the empty vector or in samples immunoprecipitated with aspecific IgG antibodies. Moreover, no DNA amplification was observed using primers

specific for the *GAPDH* promoter, suggesting the specificity of the HMGA1 binding to the *SPP1* promoter. Western blot analysis was carried out to confirm the expression of the HMGA1-HA protein transfected (Figure 4.11 B).

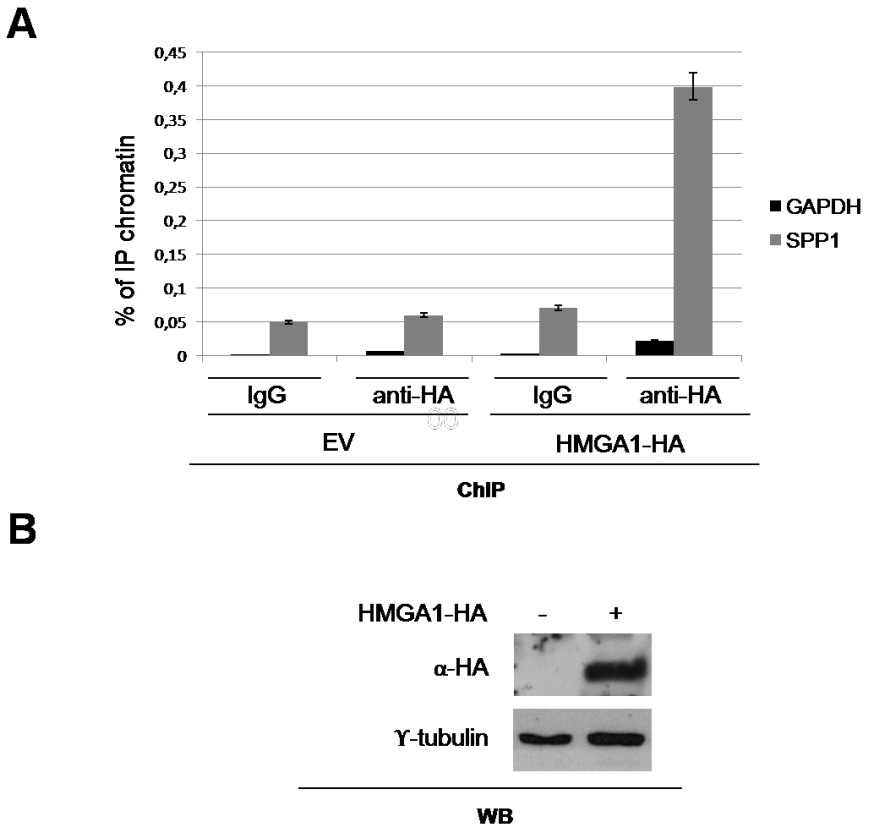

Figure 4.11 HMGA1 protein binds to the *SPP1* promoter *in vivo*
HEK 293 cells were transiently transfected with a vector encoding the HMGA1 protein (HMGA1-HA) or with the backbone vector (EV). (A) The chromatin was immunoprecipitated using antibodies against the HA tag. IgG antibodies were used as negative control. Chromatin samples immunoprecipitated were analyzed by qRT-PCR using primers specific for the *SPP1* promoter. *GAPDH* primers were used as control of the binding specifity. The percentage of IP chromatin represents the amount of immunoprecipitated chromatin in each sample compared with the amount of the total chromatin extracted and not immunoprecipitated. (B) Immunoblot analysis confirmed the expression of the HMGA1-HA protein. γ-tubulin was used as control to normalize the amount of protein used.

Since previously we have shown that CBX7 protein interacts with the *SPP1* promoter and since we have recently demonstrated that CBX7 and HMGA1 interact each other, we hypothesized that the interaction of these two proteins might take place also on the *SPP1* promoter. To test this hypothesize, we performed a ChIP assay in HEK 293 cells co-transfected with a vector encoding the CBX7-V5 protein, with a vector encoding the HMGA1-HA protein or with both vectors. The DNA-protein complexes were fixed and immunoprecipitated by using antibodies against the V5 epitope. The chromatin was then released by the immunocomplexes and finally analyzed by qRT-PCR. By this approach, we found that CBX7 was able to interact with the *SPP1* promoter region, as we expected, but, interestingly, we found that in simultaneous presence of CBX7 and HMGA1 proteins the amount of chromatin immunoprecipitated was lower than in the presence of only CBX7 protein, suggesting that CBX7 competes with and counteracts HMGA1 for the binding to the *SPP1* promoter. No DNA amplification was observed by immunoprecipitating chromatin with aspecific rabbit IgG antibodies and by performing qRT-PCR with specific primers for the *GAPDH* promoter, demonstrating that the binding is specific for the *SPP1* promoter (Figure 4.12 A). Furthermore, Re-ChIP assays showed that both CBX7 and HMGA1 protein bind together to the *SPP1* promoter (data not shown). Western blot analysis was performed to confirm the expression of the CBX7-V5 and HMGA1-HA proteins (Figure 4.12 B).

Taken together, these results demonstrate that CBX7 and HMGA1 bind together to the human *SPP1* promoter *in vivo*, and, moreover, that the CBX7 protein counteracts HMGA1 for the binding to this promoter.

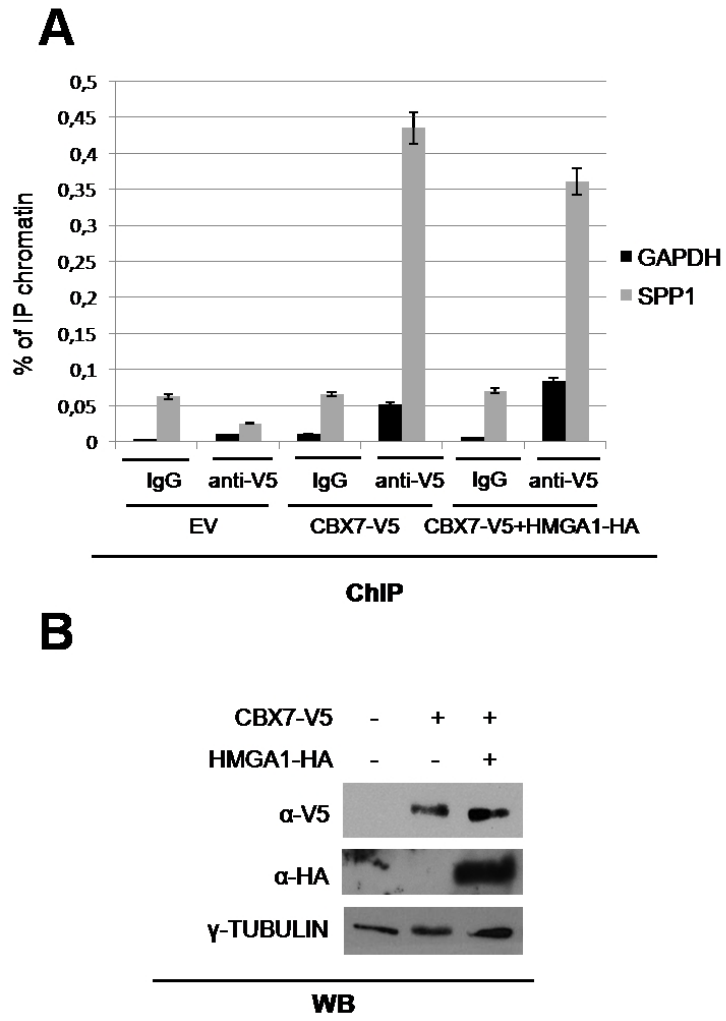

Figure 4.12 CBX7 and HMGA1 compete for the binding to the *SPP1* promoter
(A) HEK 293 cells were transfected both with a vector encoding the CBX7-V5 protein and the HMGA1-HA protein. The chromatin was immunoprecipitated using antibodies against the V5 tag and then analyzed by qRT-PCR using primers spanning the promoter region of the *SPP1* gene. Primers specific for the *GAPDH* were used as control for the specifity of the binding. The percentage of IP chromatin represents the amount of immunoprecipitated chromatin in each sample compared to the amount of the total chromatin extracted and not immunoprecipitated. (B) Immunoblot analysis was performed to confirm the expression of the CBX7-V5 and HMGA1-HA proteins. ϒ-tubulin was evaluated to normalize the amount of protein used.

4.11 CBX7 negatively regulates *SPP1* expression by counteracting the transcriptional activity of HMGA1

Then, we evaluated the effects of the simultaneous presence of CBX7 and HMGA1 proteins on the transcriptional regulation of the *SPP1* gene. To this aim,we transiently transfected the papillary thyroid carcinoma cell line TPC-1, in which the expression levels of SPP1 are elevated, with a vector encoding the CBX7-HA protein, the HMGA1-HA protein or both vectors. By qRT-PCR, we observed that the *SPP1* expression levels decreased in presence of the CBX7 protein, while it increased when the HMGA1 protein was expressed, as we expected. Interestingly, we found that when both proteins are expressed *SPP1* levels are low as well as in the presence of the only CBX7 protein, suggesting that the transcriptional activity of CBX7 protein is stronger than the HMGA1 one, and that the presence of CBX7 makes HMGA1 protein unable to exert its role of positive regulator of the expression of *SPP1* (Figure 4.13 A). Western blot analysis confirmed the expression of CBX7 and HMGA1 proteins in the samples analyzed (Figure 4.13 B).

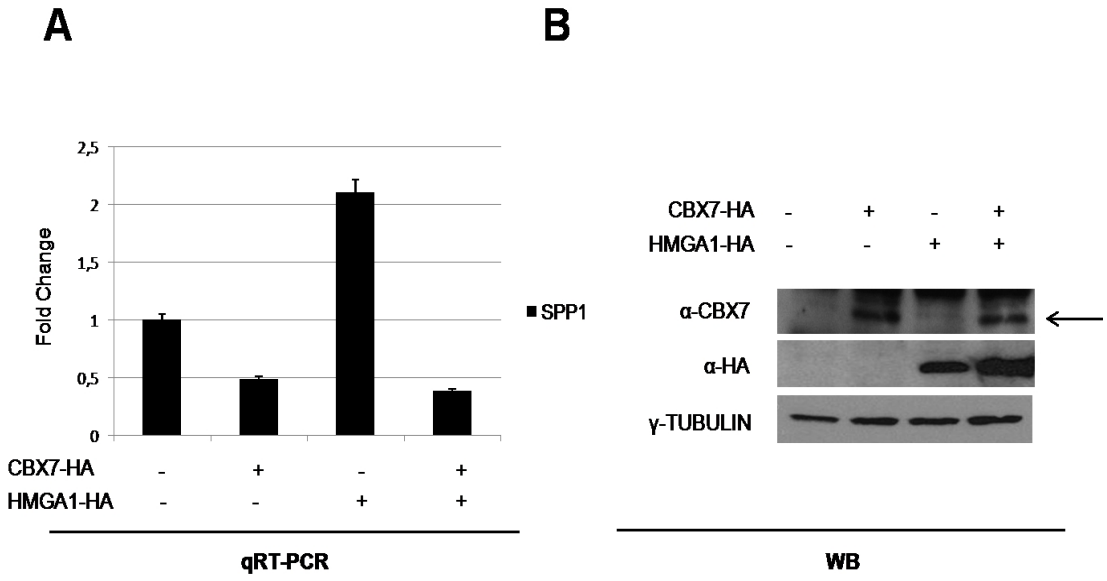

Figure 4.13 CBX7 and HMGA1 proteins compete for the transcriptional regulation of the *SPP1* gene

TPC-1 cells were transfected with a vector encoding the CBX7-HA protein, the HMGA1-HA protein or both vector. (A) The *SPP1* expression was analyzed by qRT-PCR. Fold Change value represents the *SPP1* expression levels of each sample compared to the levels observed in cells transfected with the backbone vector, assuming that *SPP1* expression in the control sample is equal to 1. (B) Immunoblot analysis confirmed the expression of the CBX7-HA (indicated by the black arrow) and the HMGA1-HA proteins. γ-tubulin was used as control.

4.12 CBX7 regulates cell migration through the block of HMGA1 and suppression of *SPP1* expression

Data obtained so far have shown that CBX7 and HMGA1 proteins are able to regulate the *SPP1* transcription. In order to evaluate the functional effect due to this mechanism, we performed a migration assay in TPC-1 cell line, highly expressing *SPP1*. TPC-1 cells were transfected with a vector encoding CBX7-HA, HMGA1-HA protein or the corresponding empty vectors. Moreover, at the same time, TPC-1 cells were transfected with a siRNA directed against the *SPP1* mRNA or with a scrambled control siRNA. 24h after transfection, cells were seeded in a transwell and the migration rate was evaluated after additional 24h. As shown in Figure 4.14 A, cells transfected with the vector encoding HMGA1-HA protein and the control siRNA showed a migration ability comparable to those observed in cells transfected with the empty vector or to wild type cells. Moreover, their ability to migrate decreased when treated with the siRNA specific for the *SPP1* mRNA.
On the contrary, cells expressing CBX7 protein and treated with the control siRNA showed a lower migration rate than wild type cells and those expressing HMGA1-HA or the empty vector.
Interestingly, when the expression of *SPP1* gene is silenced by the siRNA, cells transfected with CBX7-HA showed the same migration rate of CBX7 cells treated with the control siRNA, demonstrating that the ability of cells to migrate is due to the *SPP1* expression regulation mediated by CBX7 and HMGA1 proteins.
qRT-PCR and western blot analysis showed the differential expression levels of the *SPP1* gene (Figure 4.14 B and C). Finally, cell proliferation assays were performed to confirm that migration results observed were not due to a change of cell proliferation rate but they were a specific effect of the cell ability to migrate (data not shown).

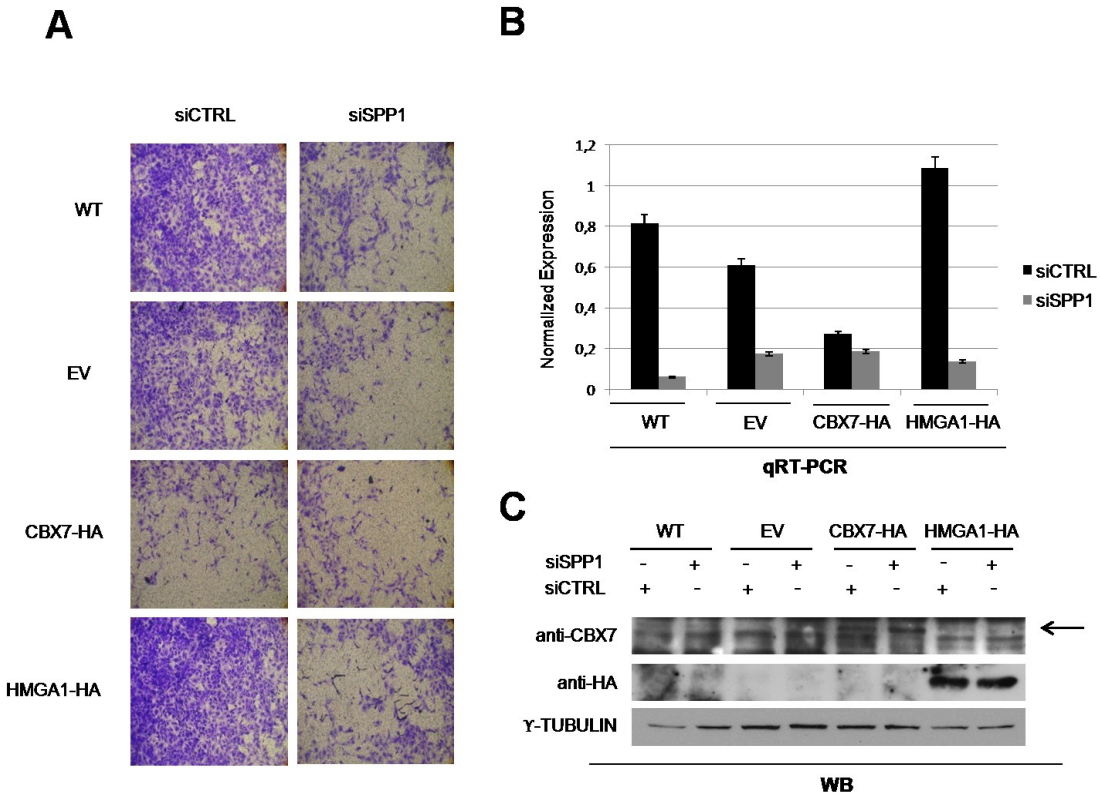

Figure 4.14 CBX7 and HMGA1 proteins modulate cell migration through the transcriptional regulation of the *SPP1* gene
Cell migration assay in TPC-1 cells. Cells were co-transfected with a vector encoding the CBX7-HA protein or the HMGA1-HA protein or both vectors and with a specific siRNA for the *SPP1* gene or the control siRNA. (A) After 24h from the transfection, $3x10^4$ cells were seeded on the upper surface of the filters and allowed to migrate to the bottom compartment. After additional 24h, cells were stained with crystal violet solution. Magnification, X40. (B) The *SPP1* expression levels were evaluated by qRT-PCR and normalized respect to the *GAPDH* expression levels of each sample. (C) Immunoblot analysis was performed to confirm the expression of CBX7-HA (indicated by the black arrow) and HMGA1-HA proteins. γ-tubulin was evaluated to normalize the amount of the protein used.

4.13 Analysis of gene expression in human thyroid carcinomas

In order to understand whether the differential expression of *CBX7, HMGA1* and *SPP1* might play a role in thyroid carcinogenesis, we analyzed by qRT-PCR the expression of these three genes in a panel of human thyroid carcinomas of different

histotypes. As shown in Figure 4.15, we found a positive correlation between the expression of *HMGA1* and *SPP1*, while an inverse correlation was observed between these two genes and *CBX7*. In fact, *CBX7* expression levels decreased in PTC and follicular-variant papillary thyroid carcinoma (FVPTC) samples and more strongly in ATC, while the expression of *HMGA1* and *SPP1* increased in all samples analyzed reaching the highest level in ATC samples.
These results demonstrated that the expression levels of these three proteins are effectively related and tumor progression might be due to the loss of CBX7/HMGA1 regulation that, in turn, could lead to the enhancement of the *SPP1* gene expression.

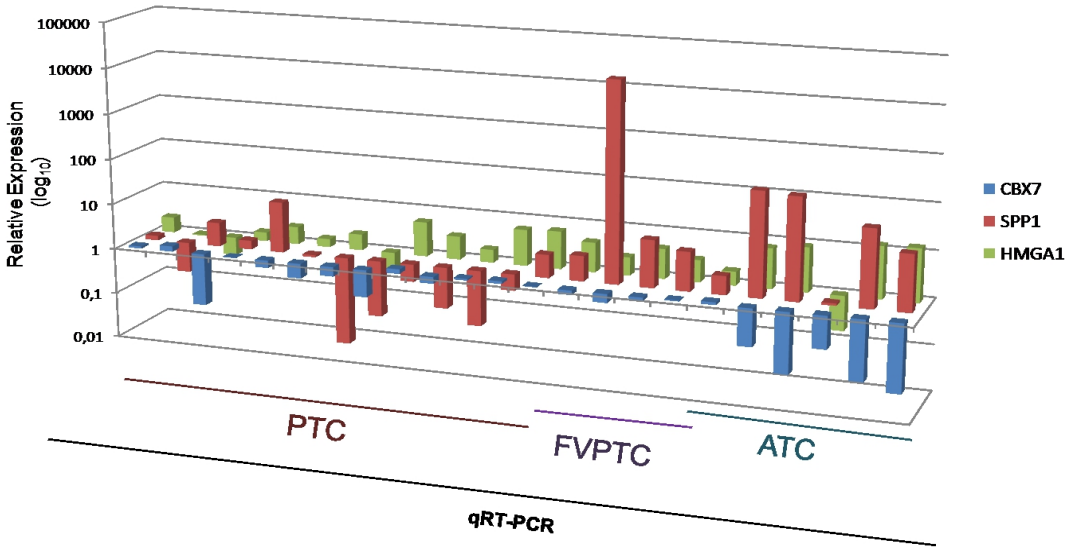

Figure 4.15 Expression analysis in human thyroid carcinomas
qRT-PCR analysis of *CBX7, HMGA1* and *SPP1* expression in human papillary thyroid carcinomas (PTC), follicular variant of papillary carcinomas (FVPTC) and anaplastic carcinomas (ATC). A positive correlation was found between *SPP1* and *HMGA1* gene expression (in red and green, respectively), while a negative correlation was found between the expression of these two genes and that of *CBX7* (in blue). Relative Expression value represents gene expression levels of each sample compared to those obtained in the mean of three normal thyroid samples, assuming that the gene expression of the control is equal to 1.

5. DISCUSSION

CBX7 is a novel Polycomb protein that regulates gene expression by taking part into the formation of macro-molecular complexes thus binding to the chromatin structure. The role of CBX7 in carcinogenesis is still not completely defined. Recent studies have shown that the expression of CBX7 decreases in thyroid carcinomas and that its reduction is more pronounced going from benign adenomas to more aggressive carcinomas (Pallante et al. 2008).
The reduction of CBX7 expression levels seems to be a general feature in human carcinogenesis. In fact, it has been observed in several human carcinomas, as colon, bladder, breast, pancreatic and lung, and the completely loss of CBX7 expression results associated with the most advanced stages and grades of malignancies. Indeed, we have found that the loss of CBX7 expression is a marker of poor prognosis and shorter survival time of colorectal and pancreatic carcinoma patients (Pallante et al. 2010, Karamitopoulou et al. 2010). Therefore, it is reasonable to hypothesize that the reduced expression levels of CBX7 might play a key role in the process of carcinogenesis and in cancer progression.
According to this hypothesis, our laboratory has demonstrated that CBX7 is able to positively regulate the expression of the *E-cadherin* gene, a key mediator of the EMT (Federico et al. 2009). By this mechanism, CBX7 contributes to prevent the acquisition of the malignant features associated with the loss of epithelial characteristics and with the acquisition of a mesenchymal phenotype.
The tumor-suppresor role exerted by CBX7 in cancer is also supported by another study regarding the repression of *CCNE1* gene, encoding the Cyclin E. By this mechanism, CBX7 attenuates the transition from the phase G1 to S of the cell cycle, thus negatively regulating cell proliferation (Forzati et al. 2012).
However, recent studies have demonstrated a correlation between the expression of *CBX7* and the development of B-cell lymphomas *in vivo* (Scott et al. 2007) and the over-expression of CBX7 was found to be associated with gastric cancer (Zhang at al. 2010) and with the expansion of cellular lifespan in human prostate primary epithelial cells (Bernard et al. 2005) and in mouse fibroblasts (Gil et al. 2004), thus suggesting an oncogenic role of the CBX7 protein.
In order to better understand the role of the loss of CBX7 gene expression in carcinogenesis, we searched for genes whose expression might be regulated by the CBX7 protein. To this aim, we restored the CBX7 expression in the thyroid carcinoma cell line FRO in which CBX7 is not expressed. Then, we generated FRO stably expressing CBX7 (FRO-CBX7) or carrying the corresponding backbone vector (FRO-EV), and used the RNA obtained from this cell clones to analyze the differential expression profiling through the hybridization of an Affymetrix cDNA

microarray. By this approach, we identified several genes involved in the process of carcinogenesis whose expression is regulated by CBX7 protein.
Among the genes that we found to be up-regulated by CBX7, we concentrated our attention on the *FOS, FOSB* and *EGR1* genes.
FOS and FOSB are transcriptional co-factors that dimerise with the members of the JUN family to form the AP-1 complex (Milde-Langosch 2005), an important multi-protein complex that regulates gene transcription. The role of FOS protein is well characterized in different processes, as signal transduction, cell differentiation and cell proliferation (Shaulian and Karin 2001). Many studies have described FOS as a protein involved in cellular oncogenic transformation, able to modulate the expression of several genes important for tumorigenesis, thus causing the down-regulation of tumor-suppressor genes (Bakin and Curran 1999) and leading to invasive growth of cancer cells (Hu et al. 1994). However, recent studies have demonstrated that FOS protein has a role in the positive regulation of apoptosis, suggesting that this protein may also have tumor-suppressor activities (Mahner et al. 2008).
In addition to FOS, FOSB has been shown to have a role in the progression of tumors from different tissues, being down-regulated in poorly differentiated mammary carcinomas (Milde-Langosch et al. 2005). Interestingly, the expression of the *FOS-like antigen 1 (FOSL1)* and *2 (FOSL2)* genes, that encode other two proteins of the FOS family positively involved in tumor cell motility and invasion in breast, colorectal and mesothelioma carcinomas (Milde-Langosch et al. 2005), were not regulated by CBX7 protein (data not shown). Therefore, the loss of CBX7 expression may affect the composition of the AP-1 complex, which in turn triggers an altered transcription program leading to the appearance of a neoplastic phenotype.
EGR1 is a DNA-binding transcription factor. Several studies have demonstrated that the expression of *EGR1* is strongly and rapidly induced in response to a wide spectrum of stimuli such as serum, growth factors, radiations and stress (Liu et al. 1998). Moreover, EGR1 exerts its tumor-suppressor role by suppressing growth, differentiation and migration of several kind of carcinoma cells (Calogero et al. 2004, Wu et al. 2001).
Among all the genes that resulted down-regulated by CBX7 protein, we focused on the *SPP1, SPINK1* and *STEAP1* genes since their elevated expression and involvement in human carcinomas.
SPP1 is a secreted intregrin-binding phosphoprotein involved in the regulation of different processes and whose expression has been found strongly over-expressed during tumor progression, as observed in colon (Rohde et al. 2007) and renal (Matusan et al. 2006) cancer. In particular, elevated plasma levels of the SPP1 protein are associated with breast advanced tumor stages and poor patient prognosis (Tuck et al. 1999). Experimental studies have shown that the SPP1 protein

functionally contributed to malignancy, by directly influencing cell and tissue properties such as migration and invasion (Tuck et al. 1999), tumor angiogenesis (Liaw et al. 1995), and cell survival through the inhibition of apoptosis (Khan et al. 2002).

SPINK1 is an enzyme produced by the pancreatic gland and its mainly function is to inhibit the effect of the trypsin protein. Recent evidences have shown its role in the regulation of cell migration and in tissue repair (Stenman 2002). The over-expression of SPINK1 is able to promote cell growth in pancreatic cancer by stimulating the epidermal growth factor receptor (EGFR) (Ozaki et al. 2009) and altered SPINK1 expression has been associated with decreased survival time in ovarian and colorectal carcinomas (Paju et al. 2004, Gaber et al. 2009).

STEAP1 protein is a membrane protein of 339 amino-acids characterized by six transmembrane domains. The expression of *STEAP1* is low in normal human tissues, while it appears to be elevated in all steps of prostate cancer (Hubert et al. 1999) and in several human cancer cell lines (Alves et al. 2006). However, the role of STEAP1 in cancer is not well reported, but it seems that its oncogenic functions are due to its role of transporter protein or ion channel in epithelial cells (Prevarskaya et al. 2007).

We first validated the data obtained from the cDNA microarray analysis in all the FRO-CBX7 and FRO-EV clones generated and then confirmed the CBX7 mediated-regulation of all these genes in MEFs system null for the *Cbx7* gene. By this analysis, we found that the expression of CBX7 up-regulated genes decreased more in the $Cbx7^{-/-}$ MEFs (or it is completely silenced, as *Egr1)* than in $Cbx7^{+/-}$ MEFs compared to the WT MEFs in which the *Cbx7* protein is expressed. In contrast, in accordance to the CBX7 gene modulation, we found that the expression of *Spp1, Spink1* and *Steap1* gene increased in $Cbx7^{-/-}$ MEFs in which the *Cbx7* expression is silenced. Furthermore, to enforce the data obtained, we analyzed the expression of the CBX7-gene regulated also in the rat normal thyroid cell line PC Cl3 in which the *Cbx7* expression was silenced. Also in this case, we found a positive correlation between the expression of *Cbx7* and the expression of its up-regulated genes, while a negative correlation was found between the expression of *Cbx7* and the expression of its down-regulated genes, confirming that the expression of these genes is regulated by the CBX7 protein.

Subsequently, we evaluated the effect of the CBX7 protein on the transcriptional regulation of these genes and found that CBX7 is able to positively modulate the promoter activity of its up-regulated genes and to negatively modulate the promoter activity of its down-regulated genes in a dose-dependent manner. Next, ChIP assay showed that CBX7 was able to physically bind to the promoter region of its regulated genes *in vivo*. This data was also confirmed by ChIP assay performed in tissues obtained from $Cbx7^{-/-}$ and WT mice, showing that only in WT tissues, expressing *Cbx7,* and not in $Cbx7^{-/-}$ ones, we found an enrichment of the

immunoprecipitated chromatin, confirming the ability of CBX7 to modulate transcription by directly binding to the promoter of its regulated genes. Finally, the analysis of *CBX7* and the selected CBX7-regulated gene expression in human papillary thyroid and lung carcinomas showed a positive or negative correlation between *CBX7* and the selected CBX7-regulated genes, indicating that the loss of CBX7 expression and the consequent de-regulation of several genes is one of the processes that finally leads to cancer progression.

CBX7 is a transcriptional co-factor that exerts its tumor-suppressor activity in relation to the interacting proteins localized in the macro-molecular complexes and in relation to the tissue compartments in which these different complexes take place (Gil and Peters 2006, Whitcomb et al. 2007). To better understand the transcriptional regulation exerted by CBX7, we decided to characterize the molecular mechanism by which CBX7 is able to regulate the expression of one of its down-regulated gene, the *SPP1* gene. In particular, we concentrated also on proteins that interact with CBX7 leading to the regulation of *SPP1*. Since we have recently demonstrated that CBX7 protein is able to repress the expression of the *CCNE1* gene by interacting with and counteracting the activity of HMGA1 on the *CCNE1* promoter (Forzati et al. 2012), we asked whether the same molecular mechanism could be involved in the transcriptional regulation of the *SPP1* gene.

HMGA proteins are non-histone chromatin proteins that do not have transcriptional activities *per se*, but they regulate, positively or negatively, gene expression by interacting with the DNA structure through their "AT-hooks", thus modifying the conformation of chromatin and promoting the binding of transcriptional factors to the DNA (Thanos et al. 1992, Thanos et al. 1993). Indeed, HMGA proteins can also influence gene transcription by simultaneously interacting with the DNA and the transcriptional factors (Thanos et al. 1992, Thanos et al. 1993) or by enhancing the binding affinity of TFs to the chromatin structure (Chin et al. 1998).

The HMGA expression is high during the development while it appears low or absent in adult tissues (Chiappetta et al. 1996, Rogalla et al. 1996). However, the expression of HMGA proteins strongly increases in several human and mouse carcinomas, suggesting the critical role that these proteins play in human and mouse carcinogenesis (Giancotti et al. 1989). Several studies have shown a strong association between the over-expression of HMGA proteins and a poorer patient prognosis and lower survival time of different carcinomas. The altered HMGA expression leads to an anomalous transcriptional regulation of genes involved in the control of cell proliferation and migration. In fact, it has been demonstrated that HMGA2 protein is able to promote the expression of the *CCNA2* gene by interacting with E4F1 (Tessari et al. 2003) and by enhancing the AP-1 complex activity (Vallone et al. 1997). Moreover, HMGA1 prevents the apoptosis by interacting with p53 (Pierantoni et al. 2006) and by re-localizing HIPK2 to the cytoplasm, thus inhibiting the apoptosis (Pierantoni et al. 2007).

In order to evaluate whether HMGA regulates the expression of the *SPP1* gene, by qRT-PCR we analyzed the *Spp1* expression in MEFs null for *Hmga1*, *Hmga2*, or both genes. By this analysis, we observed a decreased expression of *Spp1* when Hmga1, Hmga2 or both proteins were not expressed compared with the *Spp1* expression levels observed in WT MEFs. In particular, we found that the *Spp1* expression reduction was stronger in *Hmga1*$^{-/-}$ MEFs than in *Hmga2*$^{-/-}$ ones, suggesting that, among the Hmga proteins, Hmga1 had a more effect on the regulation of *Spp1* transcription. To confirm this data, then we transfected different amount of a vector encoding HMGA1-HA protein in the BC-PAP cell line (that expresses low levels of the SPP1 protein) and found that *SPP1* expression increased in relation to the amount of HMGA1 expressed, showing that HMGA1 is able to positively regulate the expression of the *SPP1* gene. Then, we evaluated the effect of the HMGA1 protein on the transcriptional regulation of the *SPP1* promoter activity and we found that HMGA1 was able to directly increase the transcriptional activity of the *SPP1* gene in a dose-dependent manner.

Since HMGA1 is a protein that affects gene expression by interacting with CBX7 and altering the chromatin structure (Forzati et al. 2012), we asked whether the same protein interaction could take place on the *SPP1* promoter and whether the same transcriptional mechanism could be involved in the regulation of the *SPP1* gene expression. First, ChIP assays showed that HMGA1 physically interacts with the promoter region of the *SPP1* gene *in vivo*. Then, interestingly, we found that CBX7 and HMGA1 proteins displace each other and compete for the binding to this promoter. Moreover, Re-ChIP assays showed that both CBX7 and HMGA1 protein bind simultaneously the *SPP1* promoter (data not shown). Then, to evaluate the transcriptional effect of this binding on the *SPP1* gene, we analyzed the expression of *SPP1* in TPC-1 cells expressing CBX7, HMGA1 or both proteins. By this analysis, we found that the *SPP1* expression decreased in presence of the CBX7 protein, whereas it increased after HMGA1 expression. Interestingly, we observed that, when both CBX7 and HMGA1 proteins are transfected, the *SPP1* gene expression decreased reaching expression levels comparable to those observed when only CBX7 protein was transfected. This result suggests that the CBX7-HMGA1 complex is involved in modulation of *SPP1* expression, and that, in this complex, the CBX7 protein had a strong effect on the transcriptional regulation of *SPP1*.

Furthermore, by functional assays we showed that CBX7 and HMGA1 proteins are able to modulate cell migration through the regulation of the *SPP1* expression. In fact, we found that HMGA1 is able to promote cell migration by enhancing *SPP1* transcription whereas the transfection of CBX7 protein reduces cell motility and the *SPP1* expression levels. Moreover, when cells expressing the CBX7-HA protein were transfected with a siRNA specific for the *SPP1* gene, we found a low migration rate comparable to that observed in cells CBX7-expressing transfected

with the control aspecific siRNA, suggesting that CBX7 negatively regulates *SPP1* gene expression, preventing the cell ability to migrate.
Finally, expression analysis of the *CBX7, HMGA1* and *SPP1* gene in a panel of thyroid tumors of different histotypes showed a positive correlation between *SPP1* and *HMGA1* expression, and a negative correlation between the expression of these two genes and the *CBX7* gene, suggesting the involvement of the altered expression of these genes in the neoplastic transformation of the thyroid gland.

6. CONCLUSION

Previous studies have demonstrated that *CBX7* expression decreases during the neoplastic transformation of different human tissues and that its reduction is associated to malignant grade and neoplastic stage. The loss of *CBX7* expression is a marker of poorer prognosis and survival time of cancer patients.

The purpose of our study was to define the role of CBX7 in cancer and the mechanisms by which CBX7 protein is able to exert its function of transcriptional regulator. To this aim, we analyzed six genes de-regulated in several human carcinomas whose expression is modulated by CBX7 protein. We demonstrated that CBX7 is able to regulate the transcriptional activity of these genes by directly binding to their promoters. Moreover, by analyzing the expression of *CBX7* and its up- and down-regulated genes we have found a positive or negative correlation, respectively, in a panel of human carcinomas deriving from different tissues. Finally, we characterized a molecular mechanism by which CBX7 represses the expression of the *SPP1* gene, encoding a key mediator of cell migration. We found that CBX7 is able to negatively regulate the *SPP1* expression by counteracting the effect of HMGA1 on the promoter of this gene and counteracting its positive effect on the *SPP1* gene transcription.

In conclusion, our data shows the importance of the role played by the CBX7 protein on the transcriptional regulation of several cancer-related genes, suggesting that the loss of CBX7 expression during carcinogenesis may contribute to the acquisition of a malignant phenotype.

7. ACKNOWLEDGEMENTS

At the end of my PhD journey, I want to thank Prof. Massimo Santoro, coordinator of the Molecular Oncology and Endocrinology Doctorate program, that gave me the opportunity to work at the Department of Molecular Medicine and Medical Biotechnology at the University of Naples "Federico II".

I want to warmly thank Prof. Alfredo Fusco that gave me the professional opportunity to work in his laboratory during these years.

I thank Dr. Pierlorenzo Pallante that has been my tutor since my first day in lab. Your guide and your encouragement made me grow both professionally and personally.

I want to thank all my lab's friends and all the people I met along my way: each of you has been an important tile of this mosaic long three years.

Thanks to Chiara, Nunzio and Umberto that helped me to go on and to realize this project both with hard work and with laughs.

A special thank to Antonella, Daniela, Enza, Floriana and Mara that have supported me and accompanied me every moment of my travel. You are for me precious friends more than colleagues.

I want to thank my parents and my brother, the columns of my life. Because they believe in what we do and because they hope, as me, that one day we will be able to help someone who we could not help in the past.

Thanks to Vittorio, the people that has lived this adventure with me day by day. Thanks for having climbed with me the highest mountains and for having always helped me to fly.

Finally, I want to thank Elisabetta and Fabio, the travel companions of my life. And wherever our roads will bring us. Always.

8. REFERENCES

1. Alves PM, Faure O, Graff-Dubois S, Cornet S, Bolonakis I, Gross DA, Miconnet I, Chouaib S, Fizazi K, Soria JC, Lemonnier FA, Kosmatopoulos K. STEAP, a prostate tumor antigen, is a target of human CD8+ T cells. Cancer Immunol Immunother 2006;55:1515-23.
2. Arlotta P, Tai AK, Manfioletti G, Clifford C, Jay G, Ono SJ. Transgenic mice expressing a truncated form of the high mobility group I-C protein develop adiposity and an abnormally high prevalence of lipomas. J. Biol. Chem 2000;275:14394–14400.
3. Bakin AV, Curran T. Role of DNA 5-methylcytosine transferase in cell transformation by fos. Science 1999;283:387-90.
4. Baldassarre G, Battista S, Belletti B, Thakur S, Pentimalli F, Trapasso F, Fedele M, Pierantoni G, Croce CM, Fusco A. Negative regulation of BRCA1 gene expression by HMGA1 proteins accounts for the reduced BRCA1 protein levelsin sporadic breast carcinoma. Mol Cell Biol 2003; 323: 2225-2238.
5. Battista S, Fidanza V, Fedele M, Klein-Szanto AJ, Outwater E, Brunner H, Santoro M, Croce CM, Fusco A. The expression of a truncated HMGIC gene induces gigantism associated with lipomatosis.Cancer Res 1999;59:4793–4797.
6. Bellahcene A, Albert V, Pollina L, Basolo F, Fisher LW, Castronovo V. Ectopic expression of bone sialoprotein in human thyroid cancer. Thyroid 1998;8:637–641
7. Bellahcene A, Castronovo V, Ogbureke KU, Fisher LW, Fedarko NS.Small integrin-binding ligand N-linked glycoproteins (SIBLINGs): multifunctional proteins in cancer.Nat. Rev. Cancer 2008;8:212-226.
8. Bellahcene A, Maloujahmoum N, Fisher LW, Pastorino H, Tagliabue E, Ménard S, Castronovo V. Expression of bone sialoprotein in human lung cancer. Calcif. Tissue Int 1997;61:183–188.
9. Bellahcene, A, Merville MP, Castronovo V. Expression of bone sialoprotein, a bone matrix protein, in human breast cancer. Cancer Res 1994;54:2823–2826.
10. Bernard D, Martinez-Leal JF, Rizzo S, Martinez D, Hudson D, Visakorpi T, Peters G, Carnero A, Beach D, Gil J. CBX7 controls the growth of normal and tumor-derived prostate cells by repressing the Ink4a/Arf locus. Oncogene 2005;24(36):5543-51.
11. Bernstein E, Duncan EM, Masui O, Gil J, Heard E, et al. Mouse polycomb proteins bind differentially to methylated histone H3 and RNA and are enriched in facultative heterochromatin. Mol Cell Biol 2006;26:2560–2569.

12. Botquin V, Hess H, Fuhrmann G, Anastassiadis C, Gross MK, Vriend G, Schöler HR. New POU dimer configuration mediates antagonistic control of an osteopontin preimplantation enhancer by Oct-4 and Sox-2. GenesDev 1998;12:2073-2090.
13. Bracken AP, Dietrich N, Pasini D, Hansen KH, Helin K. Genome-wide mapping of Polycomb target genes unravels their roles in cell fate transitions. Genes Dev 2006;20:1123–1136.
14. Bucciarelli E, Sidoni A, Bellezza G, Cavaliere A, Brachelente G, Costa G, Chaplet M, Castronovo V, Bellahcène A. Low dentin matrix protein 1 expression correlates with skeletal metastases development in breast cancer patients and enhances cell migratory capacity in vitro. Breast Cancer ResTreat2007;105:95–104.
15. Calogero A, Lombari V, De Gregorio G, Porcellini A, Ucci S, Arcella A, Caruso R, Gagliardi FM, Gulino A, Lanzetta G, Frati L, Mercola D, Ragona G. Inhibition of cell growth by EGR-1 in human primary cultures from malignant glioma. Cancer Cell Int 2004;4:1.
16. Cao R, Tsukada Y, Zhang Y. Role of Bmi-1 and Ring1A in H2A ubiquitylation and Hox gene silencing. Mol Cell 2005;20:845–854.
17. Casalino L, Bakiri L, Talotta F, Weitzman JB, Fusco A, Yaniv M, Verde P. Fra-1 promotes growth and survival in RAS-transformed thyroid cells by controlling cyclinA transcription. EMBO J 2007;26:1878–1890.
18. Castellone MD, Celetti A, Guarino V, Cirafici AM, Basolo F, Giannini R, Medico E, Kruhoffer M, Orntoft TF, Curcio F, Fusco A, Melillo RM, Santoro M. Autocrine stimulation by osteopontin plays a pivotal role in the expression of the mitogenic and invasive phenotype of RET/PTC-transformed thyroid cells. Oncogene 2004;23(12):2188-96.
19. Centelles JJ. General aspects of colorectal cancer.ISRN Oncol 2012;2012:139268.
20. Chang YS, Kim HJ, Chang J, Ahn CM, Kim SK. Elevated circulating level of osteopontin is associated with advanced disease state of non-small cell lung cancer. Lung Cancer 2007;57:373–380.
21. Chaplet M, Waltregny D, Detry C, Fisher LW, Castronovo V, Bellahcène A. Expression of dentin sialophosphoprotein in human prostate cancer and its correlation with tumor aggressiveness. Int. J. Cancer 2006;118:850–856.
22. Chen J, Thomas HF, Sodek J. Regulation of bone sialoprotein and osteopontin mRNA expression by dexamethasone and 1,25-dihydroxyvitamin D3 in ratbone organ cultures. Connect Tissue Res 1996;34:41 -5 1.
23. Chiappetta G, Avantaggiato V, Visconti R, Fedele M, Battista S, Trapasso F, Merciai BM, Fidanza V, Giancotti V, Santoro M, Simeone A, Fusco A. High level expression of the HMGI (Y) gene during embryonic development.Oncogene 1996;13:2439-2446.

24. Chieffi P, Battista S, Barchi M, Di Agostino S, Pierantoni GM, Fedele M, Chiariotti L, Tramontano D, Fusco A. HMGA1 and HMGA2 protein expression in mouse spermatogenesis. Oncogene 2002;21:3644-3650.
25. Chin MT, Pellacani A, Wang H, Lin SS, Jain MK, Perrella MA, Lee ME. Enhancement of serum-response factor-dependent transcription and DNA binding by the architectural transcription factor HMG-I(Y). J Biol Chem 1998;273:9755-9760.
26. Christensen B, Kazanecki CC, Petersen TE, Rittling SR, Denhardt DT, Sørensen ES. Cell type-specific posttranslational modifications of mouse osteopontin are associated with different adhesive properties. J. Biol.Chem.2007;282:19463–19472.
27. Christiani DC. Genetic susceptibility to lung cancer. J Clin Oncol 2006;24(11):1651-2.
28. Cleynen I, Huysmans C, Sasazuki T, Shirasawa S, Van de Ven W, Peeters K.Transcriptional control of the humanhigh mobility group A1 gene: basal and oncogenic Rasregulatedexpression. Cancer Res 2007;15, 4620–4629.
29. D'Angelo D, Palmieri D, Mussnich P, Roche M, Wierinckx A, Raverot G, Fedele M, Croce CM, Trouillas J, Fusco A. Altered microRNA expression profile in human pituitary GH adenomas: down-regulation of miRNA targeting HMGA1, HMGA2, and E2F1.J Clin Endocrinol Metab 2012;97(7):E1128-38.
30. Denhardt DT, Guo X. Osteopontin: a protein withdiverse functions. FASEB J 1993;7:1475- 1482. Review.
31. Egger G, Liang G, Aparicio A, Jones PA. Epigenetics in human disease and prospects for epigenetic therapy. Nature 2004;429(6990):457-63. Review.
32. El-Tanani MK, Campbell FC, Crowe P, Erwin P, Harkin DP, Pharoah P, Ponder B, Rudland PS. BRCA1 suppresses osteopontin-mediated breast cancer. J Biol Chem 2006;281(36):26587-601.
33. Fedarko NS, Fohr B, Robey PG, Young MF,Fisher LW. Factor H binding to bone sialoprotein and osteopontin enables tumor cell evasion of complement-mediated attack. J. Biol. Chem.2000;275:16666–16672.
34. Fedele M, Battista S, Kenyon L, Baldassarre G, Fidanza V, Klein-Szanto AJ, Parlow AF, Visone R, Pierantoni GM, Outwater E, Santoro M, Croce CM, Fusco A. Overexpression of the HMGA2 gene in transgenic mice leads to theonset of pituitary adenomas. Oncogene 2002;21:3190-3198.
35. Fedele M, Visone R, De Martino I, Troncone G, Palmieri D, Battista S, Ciarmiello A, Pallante P, Arra C, Melillo RM, Helin K, Croce CM, Fusco A.HMGA2 induces pituitary tumorigenesis by enhancing E2F1 activity. Cancer Cell 2006; 9:459-471.
36. Federico A, Pallante P, Bianco M, Ferraro A, Esposito F, Monti M, Cozzolino M, Keller S, Fedele M, Leone V, Troncone G, Chiariotti L, Pucci P, Fusco A. Chromobox protein homologue 7 protein, with decreased expression in

human carcinomas, positively regulates E-cadherin expression by interacting with the histone deacetylase 2 protein.Cancer Res. 2009;69(17):7079-87.
37. Finelli P, Pierantoni GM, Giardino D, Losa M, Rodeschini O, Fedele M, Valtorta E, Mortini P, Croce CM, Larizza L, Fusco A. The High Mobility Group A2 gene is amplified and overexpressed in human prolactinomas. Cancer Res 2002;62:2398-2405.
38. Fisher LW, Jain A, Tayback M, Fedarko NS. Small integrin binding ligand N-linked glycoprotein gene family expression in different cancers. Clin.Cancer Res 2004;10:8501–8511.
39. Fong YC, Liu SC, Huang CY, Li TM, Hsu SF, Kao ST, Tsai FJ, Chen WC, Chen CY, Tang, CH. Osteopontin increases lung cancer cells migration via activation of the alphavbeta3 integrin/FAK/Akt and NF-kappaB-dependent pathway. Lung Cancer 2009;64:263-70.
40. Forzati F, Federico A, Pallante P, Abbate A, Esposito F, Malapelle U, Sepe R, Palma G, Troncone G, Scarfò M, Arra C, Fedele M, Fusco A. CBX7 is a tumor suppressor in mice and humans. J Clin Invest 2012;122(2):612-23.
41. Friedmann M, Holth LT, Zoghbi HY, Reeves R. Organization, inducibleexpressionand chromosome localization of the human HMG-I(Y) nonhistoneprotein gene. Nucleic Acids Res 1993;21:4259-4267.
42. Fusco A, Berlingieri MT, Di Fiore PP, Portella G, Grieco M, Vecchio G. One-and two-step transformations of rat thyroid epithelial cells by retroviral oncogenes. Mol Cell Biol 1987;7(9):3365-70.
43. Fusco A, Fedele M. Roles of HMGA proteins in cancer. Nat Rev Cancer. 2007;7(12):899-910.Review.
44. Gaber A, Johansson M, Stenman UH, Hotakainen K, Pontén F, Glimelius B, Bjartell A, Jirström K, Birgisson H. High expression of tumour-associated trypsin inhibitor correlates with liver metastasis and poor prognosis in colorectal cancer. Br J Cancer 2009;100:1540-8.
45. Galande, S. Chromatin (dis)organization and cancer: BUR-binding proteins asbiomarkers for cancer. Curr Cancer Drug Targets 2002;2:157-190.
46. Giancotti V, Buratti E, Perissin L, Zorzet S, Balmain A, Portella G, Fusco A, Goodwin GH. Analysis of the HMGI nuclear proteins in mouse neoplastic cellsinduced by different procedures. Exp Cell Res 1989;184:538-545.
47. Giancotti V, Buratti E, Perissin L, Zorzet S, Balmain A, Portella G, Fusco A,Goodwin GH. Analysis of the HMGI nuclear proteins in mouse neoplastic cellsinduced by different procedures. Exp Cell Res 1989;184:538-545.
48. Gil J, Bernard D, Martínez D, Beach D. Polycomb CBX7 has a unifying role in cellular lifespan. Nat Cell Biol 2004;6(1):67-72.
49. Gil J, Peters G. Regulation of the INK4b-ARF-INK4a tumour suppressor locus: all for one or one for all. Nat Rev Mol Cell Biol 2006;7:667–677.

50. Guarino V, Faviana P, Salvatore G, Castellone MD, Cirafici AM, De Falco V, Celetti A, Giannini R, Basolo F, Melillo RM, Santoro M. Osteopontin is overexpressed in human papillary thyroid carcinomas and enhances thyroid carcinoma cell invasiveness. J Clin Endocrinol Metab. 2005;90(9):5270-8. 5.
51. Gunthert U, Hofmann M, Rudy W, Reber S, Zoller M, Haussmann I, Matzku S, Wenzel A, Ponta H, Herrlich P. A new variant of glycoprotein CD44 confers metastatic potential to rat carcinoma cells.Cell 1991;65:13-24.
52. Hannafon BN, Sebastiani P, de las Morenas A, Lu J, Rosenberg CL. Expression of microRNA and their gene targets are dysregulated in preinvasive breast cancer.Breast Cancer Res 2011;13(2):R24.
53. Hauke S, Rippe V, Bullerdiek J. Chromosomal rearrangements leading to abnormal splicing within intron 4 of HMGIC? Genes Chromosomes Cancer2001;30:302-304.
54. Hinz S, Kempkensteffen C, Christoph F, Krause H, Schrader M, Schostak M, Miller K, Weikert S. Expression parameters of the polycomb group proteins BMI1, SUZ12, RING1 and CBX7 in urothelial carcinoma of the bladder and their prognostic relevance. Tumour Biol. 2008;29(5):323-9.
55. Hinz S, Kempkensteffen C, Christoph F, Krause H, Schrader M, Schostak M, Miller K, Weikert S, Jones DO, Cowell IG, Singh PB. Mammalian chromodomain proteins: their role in genome organisation and expression. Bioessays 2000;22(2):124-37. Review.
56. Hu E, Mueller E, Oliviero S, Papaioannou VE, Johnson R, Spiegelman BM. Targeted disruption of the c-fos gene demonstrates c-fos-dependent and -independent pathways for gene expression stimulated by growth factors or oncogenes. EMBO J 1994;13:3094-103.
57. Hubert RS, Vivanco I, Chen E, Rastegar S, Leong K, Mitchell SC, Madraswala R, Zhou Y, Kuo J, Raitano AB, Jakobovits A, Saffran DC, Afar DE. STEAP: a prostate-specific cell-surface antigen highly expressed in human prostate tumors. Proc Natl Acad Sci U S A 1999;96:14523-8.
58. Iwata M, Awaya N, Graf L, Kahl C, Torok-Storb B. Human marrow stromal cells activate monocytes to secrete osteopontin, which down-regulates Notch1 gene expression in CD34+ cells. Blood 2004;103:4496-4502.
59. Johnson KR, Disney JE, Wyatt CR, Reeves R. Expression of mRNAs encoding mammalian chromosomal proteins HMG-I and HMG-Y during cellularproliferation. Exp Cell Res 1990;187:69-76.
60. 47. Jones DO, Cowell IG, Singh PB. Mammalian chromodomain proteins: their role in genome organisation and expression. Bioessays 2000;22(2):124-37. Review.
61. Joyce MM, Gonzalez JF, Lewis S, Woldesenbet S, Burghardt RC, Newton GR, Johnson GA. Caprine uterine and placental osteopontin expression is distinct among epitheliochorial implanting species.Placenta 2005;26:160-170

62. Kaji H, Sugimoto T, Miyauchi A, Fukase M, Tezuka K, Hakeda Y, Kumegawa M, Chihara K. Calcitonin inhibits osteopontin mRNA expression in isolated rabbit osteoclasts.Endocrinology1994;135:484-487.
63. Kanno M, Hasegawa M, Ishida A, Isono K, Taniguchi M. mel-18, a Polycomb group-related mammalian gene, encodes a transcriptional negative regulator with tumor suppressive activity. EMBO J 1995;14:5672–8.
64. Karamitopoulou E, Pallante P, Zlobec I, Tornillo L, Carafa V, Schaffner T, Borner M, Diamantis I, Esposito F, Brunner T, Zimmermann A, Federico A, Terracciano L, Fusco A. Loss of the CBX7 protein expression correlates with a more aggressive phenotype in pancreatic cancer.Eur J Cancer 2010;46(8):1438-44.
65. Kayed H, Kleeff J, Keleg S, Felix K, Giese T, Berger MR, Büchler MW, Friess H.. Effects of bone sialoprotein on pancreatic cancer cell growth, invasion andmetastasis. Cancer Lett 2007;245:171–183.
66. Khan SR, Johnson JM, Peck AB, Cornelius JG, Glenton PA. Expression of osteopontin in rat kidneys: induction during ethylene glycol induced calcium oxalate nephrolithiasis. J. Urol 2002;168:1173-1181.
67. Kim RH, Sodek J. Transcription of the bone sialoprotein gene is stimulated by v-Src acting through aninverted CCAAT box. Cancer Res 1999;59:565-571.
68. Kirmizis A, Bartley SM, Kuzmichev A, Margueron R, Reinberg D, Green R, Farnham PJ. Silencing of human polycomb target genes is associated with methylation of histone H3 Lys 27. Genes Dev 2004;18:1592-605.
69. Kirmizis A, Santos-Rosa H, Penkett CJ, et al. Arginine methylation at histone H3R2 controls deposition of H3K4 trimethylation. Nature 2007;449:928–32.
70. Kondo T, Ezzat S, Asa SL. Pathogenetic mechanisms in thyroid follicular-cell neoplasia. Nat Rev Cancer 2006;6:292–306.
71. Koopmann J, Fedarko NS, Jain A, Maitra A, Iacobuzio-Donahue C, Rahman A, Hruban RH, Yeo CJ, Goggins M. Evaluation of osteopontin as biomarker for pancreatic adenocarcinoma. CancerEpidemiol. Biomarkers Prev 2004;13:487–491.
72. Kurose K, Mine N, Iida A, Nagai H, Harada H, Araki T, Emi M. Three aberrant splicing variants of the HMGIC gene transcribed in uterine leiomyomas. GenesChromosomes Cancer 2001;30:212-7.
73. Kuzmichev A, Nishioka K, Erdjument-Bromage H, Tempst P, Reinberg D. Histone methyltransferase activity associated with a human multiprotein complex containing the Enhancer of Zeste protein. Genes Dev 2002;16(22):2893-905.
74. Lee YS, Dutta A. The tumor suppressor microRNA let-7 represses the HMGA2 oncogene. Genes Dev 2007;21:1025–1030.
75. Lessard J, Sauvageau G. Bmi-1 determines the proliferative capacity of normal and leukaemic stem cells. Nature 2003;423:255–260.

76. Liaw L, Lindner V, Schwartz SM, Chambers AF, Giachelli CM. Circ. Res 1995;77:665-672.
77. Liu C, Rangnekar VM, Adamson E, Mercola D. Suppression of growth and transformation and induction of apoptosis by EGR-1. Cancer Gene Ther 1998;5:3-28.
78. Livak KJ, Schmittgen TD. Analysis of relative gene expression data using real-time quantitative PCR and the 2(-Delta Delta C(T)) Method Methods 2001;(4):402-8.
79. Luedtke CC, McKee MD, Cyr DG, Gregory M, Kaartinen MT, Mui J, Hermo L. Osteopontin expression and regulation in the testis, efferent ducts, and epididymis of rats during postnatal development through to adulthood.Biol. Reprod 2002;66:1437-1448.
80. Lund AH, van Lohuizen M. Polycomb complexes and silencing mechanisms. Curr Opin Cell Biol 2004;16:239–46.
81. Lund T, Holtlund J, Fredriksen M, Laland SG. On the presence of two new high mobility group-like proteins in HeLa S3 cells. FEBS Lett.1983; 21:163–167.
82. Mahner S, Baasch C, Schwarz J, Hein S, Wölber L, Jänicke F, Milde-Langosch K. C-Fos expression is a molecular predictor of progression and survival in epithelial ovarian carcinoma. Br J Cancer 2008;99:1269-75.
83. Manji SS, Ng KW, Martin TI, Zhou H. Transcriptional and posttranscriptional regulation of osteopontin gene expression in preosteoblasts byretinoic acid. Cell Physiol 1998;76:1-9.
84. Mansueto G, Forzati F, Ferraro A, Pallante P, Bianco M, Esposito F, Iaccarino A, Troncone G, Fusco A. Identification of a New Pathway for Tumor Progression: MicroRNA-181b Up-Regulation and CBX7 Down-Regulation by HMGA1 Protein.Genes Cancer 2010;1(3):210-24.
85. Marks P, Rifkind RA, Richon VM, Breslow R, Miller T, Kelly WK. Histone deacetylases and cancer: causes and therapies. Nat Rev Cancer2001; 1:194-202.
86. Matusan K, Dordevic G, Stipic D, Mozetic V, Lucin K. Osteopontin expression correlates with prognostic variables and survival in clear cell renal cellcarcinoma. J. Surg. Oncol 2006;94:325–331.
87. Milde-Langosch K, Bamberger AM, Rieck G,Grund D, Hemminger G, Müller V, Löning T. Expression and prognostic relevance of activated extracellular-regulated kinases (ERK1/2) in breast cancer. Br J Cancer 2005;92:2206-15.
88. Milde-Langosch K. The Fos family of transcription factors and their role in tumourigenesis. Eur J Cancer 2005;41:2449-61.
89. Min J, Zhang Y, Xu RM. Structural basis for specific binding of Polycomb chromodomain to histone H3 methylated at Lys 27. Genes Dev 2003;17(15):1823-8.

90. Mirza M, Shaughnessy E, Hurley JK, Vanpatten KA, Pestano GA, He B, Weber GF. Osteopontin-c is a selective marker of breast cancer.Int J Cancer. 2008;122(4):889-97.
91. Mohammad HP, Cai Y, McGarvey KM, Easwaran H, Van Neste L, Ohm JE, O'Hagan HM, Baylin SB. Polycomb CBX7 promotes initiation of heritable repression of genes frequently silenced with cancer-specific DNA hypermethylation. Cancer Res 2009;69(15):6322-30
92. Nakao M, Minami T, Ueda Y, Sakamoto Y, Ichimura T. Epigenetic system: a pathway to malignancies and a therapeutic target. Int J Hematol 2004;80(2):103-7.
93. Napgal S, Ghosn C, DiSepio D, Molina Y, Sutter M, Klein ES, Chandraratna RA. Retinoid-dependent recruitment of a histone H1 displacement activity byretinoic acid receptor. J Biol Chem 1999;274:22563-22568.
94. Otte AP, Kwaks TH. Gene repression by Polycomb group protein complexes: a distinct complex for every occasion? Curr Opin Genet Dev 2003;13:448–54.
95. Ozaki N, Ohmuraya M, Hirota M, , Ida S, Wang J, Takamori H, Higashiyama S, Baba H, Yamamura K. Serine protease inhibitor Kazal type 1 promotes proliferation of pancreatic cancer cells through the epidermal growth factor receptor. Mol Cancer Res 2009;7:1572-81.
96. Paju A, Vartiainen J, Haglund C, Itkonen O, von Boguslawski K, Leminen A, Wahlström T, Stenman UH. Expression of trypsinogen-1, trypsinogen-2, and tumor-associated trypsin inhibitor in ovarian cancer: prognostic study on tissue and serum. Clin Cancer Res 2004;10:4761-8.
97. Pallante P, Federico A, Berlingieri MT, Bianco M, Ferraro A, Forzati F, Iaccarino A, Russo M, Pierantoni GM, Leone V, Sacchetti S, Troncone G, Santoro M, Fusco A. Loss of the CBX7 gene expression correlates with a highly malignant phenotype in thyroid cancer. Cancer Res 2008;68(16):6770-8.
98. Pallante P, Terracciano L, Carafa V, Schneider S, Zlobec I, Lugli A, Bianco M, Ferraro A, Sacchetti S, Troncone G, Fusco A, Tornillo L. The loss of the CBX7 gene expression represents an adverse prognostic marker for survival of colon carcinoma patients. Eur J Cancer 2010;46(12):2304-13.
99. Park IK, Qian D, Kiel M, Becker MW, Pihalja M, et al. Bmi-1 is required for maintenance of adult self-renewing haematopoietic stem cells. Nature 2003;423:302–305.
100. Paro R, Hogness DS. The Polycomb protein shares a homologous domain with a heterochromatin-associated protein of Drosophila. Proc Natl Acad Sci U S A 1991;88(1):263-7.
101. Philip S, Bulbule A, Kundu GC. Osteopontin stimulates tumor growth and activation of promatrix metalloproteinase-2 through nuclear factor-kappa B-

mediated induction of membrane type 1 matrix metalloproteinase in murine melanoma cells.J BiolChem2001;276:44926-44935.
102. Pierantoni GM, Rinaldo C, Esposito F, Mottolese M, Soddu S, Fusco A. High Mobility Group A1 (HMGA1) proteins interact with p53 and inhibit its apoptoticactivity. Cell Death Differ 2006;13:1554-1563.
103. Pierantoni GM, Rinaldo C, Mottolese M, Di Benedetto A, Esposito F, Soddu S, Fusco A. High-mobility group A1 inhibits p53 by cytoplasmic relocalization of its proapoptotic activator HIPK2. J Clin Invest 2007;117:693-702.
104. Pierantoni GM, Santulli B, Caliendo I, Pentimalli F, Chiappetta G, Zanesi N,Santoro M, Bulrich F, Fusco A. HMGA2 locus rearrangement in a case of acute lymphoblastic leukemia. Int J Oncol 2003;23:363-367.
105. Piunti A., Pasini D. Epigenetic factors in cancer development: polycomb group proteins. Future Oncol 2011;7:57–75.
106. Prevarskaya N, Skryma R, Bidaux G, Flourakis M, Shuba Y. Ion channels in death and differentiation of prostate cancer cells. Cell Death Differ 2007;14:1295-304.
protein gene. Nucleic Acids Res 1993;21:4259-4267.
107. Raaphorst FM, van Kemenade FJ, Blokzijl T, Fieret E, Hamer KM, Satijn DP, Otte AP, Meijer CJ. Coexpression of BMI-1 and EZH2 polycomb group genes in Reed-Sternberg cells of Hodgkin's disease. Am J Pathol 2000;157(3):709-15.
108. Raaphorst FM, Vermeer M, Fieret E, Blokzijl T, Dukers D, Sewalt RG, Otte AP, Willemze R, Meijer CJ. Site-specific expression of polycomb-group genes encoding the HPC-HPH/PRC1 complex in clinically defined primary nodal and cutaneous large B-cell lymphomas. Am J Pathol 2004;164(2):533-42.
109. Ramankulov A, Lein M, Kristiansen G, Loening SA, Jung K. Plasma osteopontin in comparison with bone markers as indicator of bone metastasis and survival outcome in patients with prostate cancer. Prostate 2007;67:330–340.
110. Reeves R, Beckerbauer L. HMGI/Y proteins: flexible regulators of transcription and chromatin structure. Biochim Biophys Acta 2001;1519:13-29.
111. Rodrigues LR, Teixeira JA, Schmitt FL, Paulsson M, Lindmark-Mansson H. Cancer Epidemiol.The role of osteopontin in tumor progression and metastasis in breast cancer.Biomarkers Prev 2007;16:1087-1097.
112. Rogalla, P, Drechsler K, Frey G, Hennig Y, Helmke B, Bonk U, Bullerdiek J.HMGI-C expression patterns in human tissues. Implications for the genesis of frequent mesenchymal tumors. Am J Pathol 1996;149(3):775-779.
113. Rohde F, Rimkus C, Friederichs J, Rosenberg R, Marthen C, Doll D, Holzmann B, Siewert JR, Janssen KP.. Expression of osteopontin, a target gene of de-regulated Wnt signaling, predicts survivalin colon cancer. Int. J. Cancer 2007;121(8):1717-23.

114. Saltman B, Singh B, Hedvat CV, Wreesmann VB, and Ghossein R. Patterns of expression of cell cycle/apoptosis genes along the spectrum of thyroid carcinoma progression. Surgery 2006;140:899-905.
115. Saurin AJ, Shao Z, Erdjument-Bromage H, Tempst P, Kingston RE. A Drosophila Polycomb group complex includes Zeste and dTAFII proteins. Nature 2001;412:655–660.
116. Saurin AJ, Shiels C, Williamson J, Satijn DP, Otte AP, Sheer D, Freemont PS. The human polycomb group complex associates with pericentromeric heterochromatin to form a novel nuclear domain. J Cell Biol 1998;142:887–98.
117. Schwartz YB, Pirrotta V. Polycomb silencing mechanisms and the management of genomic programmes. Nat Rev Genet 2007;8:9–22.
118. Scott CL, Gil J, Hernando E, et al. Role of the chromobox protein CBX7 in lymphomagenesis. Proc Natl Acad Sci U S A 2007;104:5389–94.
119. Shao J, Washington MK, Saxena R, Sheng H. Heterozygous disruption of the PTEN promotes intestinal neoplasia in APCmin/+ mouse: roles of osteopontin. Carcinogenesis 2007;28(12):2476-83.
120. Shao Z, Raible F, Mollaaghababa R, Guyon JR, Wu CT, et al. Stabilization of chromatin structure by PRC1, a Polycomb complex. Cell 1999;98:37–46.
121. Shaulian E, Karin M. AP-1 in cell proliferation and survival. Oncogene 2001;20:2390-400.
122. Sodek I, Chen J, Nagata T, Kasugai S, Todescan R Ir, Li IWS, Kim RH. Regulation of osteopontin expressionin osteoblasts. Ann NY Acad Sci 1995;760:223-241.
123. Sparmann A, van Lohuizen M. Polycomb silencers control cell fate, development and cancer. Nat Rev Cancer 2006;6:846–856.
124. Stenman UH. Tumor-associated trypsin inhibitor. Clin Chem 2002;48:1206-9.
125. Subramanian D, Griffith JD. Interactions between p53, hMSH2-hMSH6 and HMGI(Y) on Holliday junctions and bulged bases. Nucleic Acids Res 2002;30:2427–2434.
126. Tavares L, Dimitrova E, Oxley D, Webster J, Poot R, Demmers J, Bezstarosti K, Taylor S, Ura H, KoideH, Wutz A, Vidal M, Elderkin S, Brockdorff N. RYBP-PRC1complexes mediate H2A ubiquitylation at polycomb target sites independentlyof PRC2 and H3K27me3. Cell 2012;148:664–678.
127. Tessari MA, Gostissa M, Altamura S, Sgarra R, Rustighi A, Salvagno C, Caretti G, Imbriano C, Mantovani R, Del Sal G, Giancotti V, Manfioletti G.Transcriptional activation of the cyclin A gene by architectural transcriptional factorHMGA2. Mol. Cell Biol 2003;23:9104–9116.
128. Thanos D, Maniatis T. The high mobility group protein HMG I(Y) is required for NF-kappa B-dependent virus induction of the human IFN-beta gene. Cell1992; 71:777-789.

129. Thanos D, Du W, Maniatis T. The high mobility group protein HMG I(Y) is an essential structural component of a virus-inducible enhancer complex. ColdSpring Harb Symp Quant Biol 1993;58:73-81.
130. Thuault S, Valcourt U, Petersen M, Manfioletti G, Heldin CH, Moustakas A. Transforming growth factor-β employs HMGA2 to elicit epithelialmesenchymaltransition. J. Cell Biol 2006;174:175–183.
131. Tolhuis B, Muijrers I, de Wit E, Teunissen H, Talhout W, van Steensel B, van Lohuizen M. Genome-wide profiling of PRC1 and PRC2 Polycomb chromatin binding in Drosophila melanogaster. Nat Genet 2006;38(6):694-9.
132. Tuck AB, Arsenault DM, O'Malley FP, Hota C, Ling MC, Wilson SM, Chambers AF. Osteopontin induces increased invasiveness and plasminogen activator expression of human mammary epithelial cells.Oncogene 1999;18:4237-4246.
133. Vallone D, Battista S, Pierantoni GM, Fedele M, Casalino L, Santoro M, Viglietto G, Fusco A, Verde P. Neoplastic transformation of rat thyroid cells requires the JunB and Fra1 gene induction which is dependent on the HMGI-C geneproducts. EMBO J 1997;17:5310–5321.
134. Valverde P, Tu Q, Chen J. BSP and RANKL induce osteoclastogenesis and bone resorption synergistically.J. Bone Miner. Res.2005;20:1669–1679.
135. Van der Laan BF, Freeman JL, Tsanq RW, Asa SL.The association of well-differentiated thyroid carcinoma with insular or anaplastic thyroid carcinoma; evidence for dedifferentiation in tumor progression. Endocrine Pathology1993;4:215-221.
136. Wai PY, Mi Z, Gao C, Guo H, Marroquin C, Kuo PC. ETS-1 and RUNX2 regulate transcription of a metastatic gene, osteopontin, in murine colorectal cancer cells. J Biol Chem 2006;281:18973–18982.
137. Walker S. Updates in non-small cell lung cancer. Clin J Oncol Nurs. 2008. 12(4):587-96.
138. Waltregny D, Bellahcène A, Van Riet I, Fisher LW, Young M, Fernandez P, Dewé W, de Leval J, Castronovo V. Prognostic value of bone sialoprotein expression in clinically localized human prostate cancer. J. Natl Cancer Inst1998;90:1000–1008.
139. Wang H, Wang L, Erdjument-Bromage H, Vidal M, Tempst P, et al. Role of histone H2A ubiquitination in Polycomb silencing. Nature 2004;431:873–878.
140. Whitcomb SJ, Basu A, Allis CD, Bernstein E. Polycomb Group proteins: an evolutionary perspective. Trends Genet 2007;23:494–502.
141. WuCY, Wu MS, Chiang EP, Wu CC, Chen YJ, Chen CJ, Chi NH, Chen GH, Lin JT. Elevated plasma osteopontin associated with gastric cancer development, invasion and survival. Gut 2007;56:782–789.

142. Wu MY, Chen MH, Liang YR, Meng GZ, Yang HX, Zhuang CX. Experimental and clinicopathologic study on the relationship between transcription factor Egr-1 and esophageal carcinoma. World J Gastroenterol 2001;7:490-5.
143. Wu Y, Jiang W, Wang Y, Wu J, Saiyin H, Qiao X, Mei X, Guo B, Fang X, Zhang L, Lou H, Wu C, Qiao S. Breast cancer metastasis suppressor 1 regulates hepatocellular carcinoma cell apoptosis via suppressing osteopontin expression.PLoS One 2012;7(8):e42976.
144. Yap KL, Li S, Muñoz-Cabello AM, Raguz S, Zeng L, Mujtaba S, Gil J, Walsh MJ, Zhou MM.Molecular interplay of the noncoding RNA ANRIL and methylated histone H3 lysine 27 by polycomb CBX7 in transcriptional silencing of INK4a. Mol Cell 2010;38(5):662-74.
145. Young MF, Kerr IM, Termine ID, Wewer UM, Wang MG, McBride OW, Fisher LW. cDNA cloning, mRNA distribution and heterogeneity, chromosomal location, and RFLP analysis of human osteopontin (OPN).Genomics 1990;7:491-502.
146. Zhang XW, Zhang L, Qin W, Yao XH, Zheng LZ, Liu X, Li J, Guo WJ. Oncogenic role of the chromobox protein CBX7 in gastric cancer.J Exp Clin Cancer Res 2010;29:114.

Histopathology 2012, **60**, 397–404. DOI: 10.1111/j.1365-2559.2011.04121.x

HMGA1 and HMGA2 protein expression correlates with advanced tumour grade and lymph node metastasis in pancreatic adenocarcinoma

Salvatore Piscuoglio, Inti Zlobec, Pierlorenzo Pallante,[1] Romina Sepe,[1] Francesco Esposito,[1] Arthur Zimmermann,[2] Ioannis Diamantis,[3] Luigi Terracciano, Alfredo Fusco[1] & Eva Karamitopoulou[2]

Institute of Pathology, University of Basel, Basel, Switzerland, [1]Istituto di Endocrinologia ed Oncologia Sperimentale del CNR c/o Dipartimento di Biologia e Patologia Cellulare e Molecolare, Università degli Studi di Napoli 'Federico II', Naples, Italy, [2]Institute of Pathology, University of Bern, Bern, and [3]Department of Internal Medicine and Gastroenterology, Zofingen Hospital, AG, Switzerland

Date of submission 10 November 2010
Accepted for publication 9 February 2011

Piscuoglio S, Zlobec I, Pallante P, Sepe R, Esposito F, Zimmermann A, Diamantis I, Terracciano L, Fusco A & Karamitopoulou E

(2012) *Histopathology* **60**, 397–404

HMGA1 and HMGA2 protein expression correlates with advanced tumour grade and lymph node metastasis in pancreatic adenocarcinoma

Aims: Pancreatic ductal adenocarcinoma follows a multistep model of progression through precursor lesions called pancreatic intraepithelial neoplasia (PanIN). The high mobility group A1 (HMGA1) and high mobility group A2 (HMGA2) proteins are architectural transcription factors that have been implicated in the pathogenesis and progression of malignant tumours, including pancreatic cancer. The aim of this study was to explore the role of HMGA1 and HMGA2 in pancreatic carcinogenesis.

Methods and results: HMGA1 and HMGA2 expression was examined in 210 ductal pancreatic adenocarcinomas from resection specimens, combined on a tissue microarray also including 40 examples of PanIN and 40 normal controls. The results were correlated with the clinicopathological parameters of the tumours and the outcome of the patients. The percentage of tumour cells showing HMGA1 and HMGA2 nuclear immunoreactivity correlated positively with increasing malignancy grade and lymph node metastasis. Moreover, HMGA1 and HMGA2 expression was significantly higher in invasive carcinomas than in PanINs. No, or very low, expression was found in normal pancreatic tissue.

Conclusions: Our results suggest that HMGA1 and HMGA2 are implicated in pancreatic carcinogenesis and may play a role in tumour progression towards a more malignant phenotype.

Keywords: HMGA1, HMGA2, immunoreactivity, pancreatic ductal adenocarcinoma, pancreatic intraepithelial neoplasia

Abbreviations: CI, confidence interval; HMGA, high mobility group A; NF-κB, nuclear factor-κB; PanIN, pancreatic intraepithelial neoplasia; ROC, receiver operating characteristic; SD, standard deviation; TMA, tissue microarray

Address for correspondence: A Fusco, Istituto di Endocrinologia ed Oncologia Sperimentale, del Consiglio Nazionale delle Ricerche, via Pansini 5, 80131 Naples, Italy. e-mail: alfusco@unina.it
L Terracciano, Institute of Pathology, University of Basel, Schönbeinstrasse 40, 4031 Basel. e-mail: lterracciano@uhbs.ch

Introduction

Pancreatic ductal adenocarcinoma is a common cause of death from cancer, and has a dismal prognosis with currently no effective treatment.[1] Despite important advances in our understanding of the molecular biology of the early stages of neoplastic development, late molecular events that lead to tumour progression are largely unknown. Clinicopathological parameters such as tumour size, lymph node metastases and evidence of blood vessel or lymphatic invasion have been proven to be reliable prognostic determinants in pancreatic cancer.[1] The identification of reliable and reproducible biomarkers would enable better stratification of patients, and eventually provide a guide for individualized therapy. Pancreatic cancer follows a multistep model of progression through non-invasive precursor lesions. Pancreatic intraductal lesions have been classified into four groups of pancreatic intraepithelial neoplasias (PanINs): PanIN-1A, PanIN-1B, PanIN-2, and PanIN–3.[2] PanIN-3 shows severe epithelial dysplasia, and is most likely to progress to invasive carcinoma.[2]

The high mobility group A (HMGA) genes encode a family of non-histone chromatin-binding proteins, named for their rapid electrophoretic mobility in polyacrylamide gels.[3] HMGA1a and HMGA1b isoforms result from alternative splicing of *HMGA1* mRNA, whereas HMGA2 is encoded by the related gene *HMGA2*.[3] HMGA proteins bind the minor groove of AT-rich DNA sequences. Their DNA-binding domain is located in the N-terminal region of the protein, and contains three short basic repeats, the so-called AT-hooks.[4] Once bound to DNA, the HMGA proteins alter chromatin structure and thereby regulate the transcriptional activity of several genes.[5] HMGA proteins are normally expressed at high levels during embryonic development, and at very low levels in adult, differentiated tissues.[6] HMGA proteins participate, as transcriptional regulators, in many cellular functions, including regulation of the cell cycle, cell differentiation, senescence, and neoplastic transformation.[7] Both *HMGA1* and *HMGA2* have been reported to function as oncogenes and to be overexpressed in almost all human malignancies so far analysed, including ductal pancreatic adenocarcinoma.[8–20] Moreover, HMGA protein overexpression has been regarded as a poor prognostic feature, as it has often been found to correlate with the presence of metastasis and with reduced survival.[21]

The objective of the present study was to investigate the role of HMGA1 and HMGA2 expression in pancreatic carcinogenesis and to evaluate its prognostic significance. Using immunohistochemistry we analysed expression in different stages of pancreatic carcinogenesis, including invasive adenocarcinomas, PanINs, and normal pancreatic tissue, in a tissue microarray (TMA) combining 210 ductal adenocarcinomas of the pancreas from resection specimens, 40 cases of PanIN-3, and 40 normal controls.

Materials and methods

PATIENTS AND SPECIMENS

Formalin-fixed and paraffin-embedded tumours and control specimens were retrieved from the archives of the Institute of Pathology, University of Bern. All tumours and controls were reviewed by an experienced pathologist (E.K.). Histological subtypes other than ductal carcinoma were excluded. Tumours were re-staged according to the American Joint Committee on Cancer Staging Manual (seventh edition). Representative tumour areas were selected for the construction of the TMA. The TMA consisted of 210 surgically-resected ductal adenocarcinomas of the pancreas, and included 40 examples of PanIN-3 and 40 normal controls (normal pancreatic tissue and PanINs were selected from areas distant from the carcinomas). The 210 patients comprised 110 males and 100 females, with a mean age of 66.5 years (range: 20–92 years). The study was approved by the ethics committee of the University of Bern.

ASSESSMENT OF BEHAVIOUR

Medical charts were available for 77 of the 210 patients. Of these 77 patients, 60 (78%) died from the disease, and 7 (9%) were alive with recurrent/metastatic disease. The other 10 patients (13%) were alive without disease. The median follow-up time was 16 months. The clinicopathological features of these cases with survival information are given in Table 1.

CONSTRUCTION OF THE TMA

One core tissue biopsy with a diameter of 0.6 mm was taken from a representative region of individual paraffin-embedded pancreatic carcinomas (donor blocks), and placed into a new recipient paraffin block with a semi-automated tissue-arraying device. The presence of tumour tissue on the TMA was verified on a haematoxylin and eosin-stained slide. Two to three tissue cores of each tumour were available for biomarker analysis. Five-micrometre sections were cut with an adhesive-coated slide system (Instrumedics, Hackensack, NJ,

Table 1. Clinicopathological characteristics of cases with survival information (*N* = 77)

Clinicopathological features	Frequency, *N* (%)
Diagnosis	
Ductal carcinoma	77 (100.0)
Sex	
Female	33 (42.9)
Male	44 (57.1)
Tumour grade	
G1	16 (20.8)
G2	42 (54.6)
G3	19 (24.7)
pT stage	
pT1	3 (4.1)
pT2	12 (16.2)
pT3	52 (70.3)
pT4	7 (9.5)
pN stage	
pN0	27 (38.0)
pN1	44 (62.0)
Metastasis	
Absent	72 (93.5)
Present	5 (6.5)
Tumour diameter (mm), mean ± SD	31.4 ± 14.0
Survival time (months), median (range)	12.0 (0.5–48.0)

SD, Standard deviation.

USA) and examined by immunohistochemistry. The number of samples differed slightly between the individual markers, because of variability in the number of interpretable specimens on TMA sections.

IMMUNOHISTOCHEMISTRY

Freshly cut sections of TMA blocks were used for immunohistochemical staining with anti-HMGA1 and anti-HMGA2 antibodies. Briefly, punches were dewaxed and rehydrated in distilled water. Endogenous peroxidase activity was blocked with 0.5% H_2O_2. The sections were incubated with 10% normal goat serum (Dako Cytomation, Carpinteria, CA, USA) for 20 min, and then with the primary antibody at room temperature. Optimal staining was achieved after pretreatment in a microwave oven (98°C for 30 min, pH 6, dilution 1:250). Subsequently, sections were incubated with peroxidase-labelled secondary antibody (Dako Cytomation) for 30 min at room temperature. 3,3′-Diaminobenzidine was used as chromogen. Sections were then counterstained with Gill's haematoxylin. As a positive control, a TMA with various normal tissue samples was stained in parallel.

The antibodies used for HMGA1 immunostaining were raised against the synthetic peptide SSSKQQPLASKQ, which is specific for HMGA1. They were affinity purified against the synthetic peptide.[9] For HMGA2 immunohistochemistry, antibodies raised against a synthetic peptide located in the N-terminal region were used.[22]

The specificity of immunolabelling was validated by the absence of tumour staining when using antibodies preincubated with the peptide against which the antibodies were raised (data not shown). Similarly, no positivity was observed when tumour samples were incubated with a preimmune serum (data not shown).

IMMUNOHISTOCHEMICAL EVALUATION

Nuclear HMGA1 and HMGA2 staining was scored by two independent observers (S.P. and L.T.) blinded for clinical parameters. Slides were screened semiquantitatively for the percentage of positive cells and the intensity of the signal. At least 100 cells were counted for each punch. The percentage of positive cells per number of cells counted was scored in 10 groups from 0 (0–9%) to 9 (91–100%). The intensity of the signal was graded semiquantitatively into four groups from 0 (no positivity) to 3 (strong positivity). A case was considered to be positive if belonging at least to group 1 for the percentage (i.e. ≥10%), irrespective of intensity. In PanINs and normal controls, the epithelial cells of ductal structures were evaluated.

STATISTICAL METHODS

The selection of clinically important cut-off scores was based on receiver operating characteristic (ROC) curve analysis.[23,24] At each percentage score, the sensitivity and specificity for each outcome under study were plotted, generating an ROC curve. The score having the closest distance to the point with both maximum sensitivity and specificity, i.e. point (0.0, 1.0) on the curve, was selected as the cut-off score leading to the greatest number of tumours that were correctly classified as having or not having the outcome. In order to

enable the use of ROC curve analysis, the following clinicopathological features were dichotomized: T stage (early, T1 + T2; late, T3 + T4), N stage (N0, no lymph node involvement; N1, any lymph node involvement), tumour grade (low, G1 + G2; high, G3), and survival (death from pancreatic carcinoma or alive).

Chi-square tests were used to study the relationship between HMGA1 and HMGA2 expression and histological subgroups. Differences in HMGA1 and HMGA2 expression between normal tissue, PanIN and carcinoma were investigated with the non-parametric Wilcoxon rank sum test. Univariate survival analysis was carried out with the Kaplan–Meier log-rank test, and multivariate analysis with Cox proportional hazards regression. Hazard ratios and 95% confidence intervals (CIs) were used to determine the effect of each variable on survival time. In addition, logistic regression was performed in univariate and multivariate settings to determine the associations of protein expression and its independent effect on binary outcomes. The odds ratios and 95% CIs were evaluated. A Bonferroni correction for multiple comparisons was performed. A *P*-value ≤0.01 (two-sided) was required for the association to be statistically significant. All analyses were carried out with SAS (V9; SAS Institute, Cary, NC, USA).

Results

ANALYSIS OF HMGA1 AND HMGA2 EXPRESSION BY IMMUNOHISTOCHEMISTRY

Table 2 shows the differences in protein expression between normal pancreas, PanIN, and cancer, and Table 3 the correlation of HMGA1 and HMGA2 expression with pT stage, pN stage, and tumour grade. Survival related to protein marker expression is analysed in Table 4. Some representative images of immunohistochemical staining are illustrated in Figures 1 and 2.

PANCREATIC CARCINOMAS VERSUS NORMAL CONTROLS

Pancreatic carcinoma cases generally displayed strong nuclear HMGA1 and HMGA2 immunoreactivity, whereas absent or very low immunoreactivity was observed in normal pancreatic tissue. The mean ± standard deviation (SD) for the percentage of cells showing HMGA1 and HMGA2 protein expression were found to be 0 ± 0 and 0.2 ± 0.9, respectively, in normal tissue, as compared with 26.6 ± 30.5 and 16.3 ± 28.4, respectively, in carcinomas ($P < 0.001$; Table 2).

PANCREATIC CARCINOMA VERSUS PANIN

Percentages of cells showing HMGA1 and HMGA2 protein expression were significantly higher in ductal pancreatic adenocarcinomas (mean ± SD: 26.6 ± 30.5 and 16.3 ± 28.4, respectively) than in PanIN cases (11.1 ± 15.0 and 2.7 ± 13.5, respectively) ($P < 0.001$; Table 2).

PANIN VERSUS NORMAL CONTROLS

Means for the percentages of cells showing HMGA1 and HMGA2 protein expression were significantly higher in PanIN cases (11.1 ± 15.0 and 2.7 ± 13.5, respectively) than in normal tissue (0 ± 0 and 0.2 ± 0.9, respectively) ($P < 0.001$; Table 2).

Table 2. Differences in marker expression between normal pancreas, pancreatic intraepithelial neoplasia (PanIN) and cancer

	Normal	PanIN	Cancer	*P*-value
HMGA1				
n	31	31	183	<0.001
Mean ± SD	0 ± 0	11.1 ± 15.0	26.6 ± 30.5	
Median (min–max)	0 (0–0)	5.0 (0–50)	10.0 (0–100)	
HMGA2				
n	29	37	191	<0.001
Mean ± SD	0.2 ± 0.9	2.7 ± 13.5	16.3 ± 28.4	
Median (min–max)	0 (0–5)	0 (0–80)	0 (0–100)	

HMGA, High mobility group A; SD, standard deviation.
Expression is given as percentage of immunoreactive cells. Wilcoxon rank sum test.

Table 3. Protein marker expression related to stage (pT, pN), and tumour grade

	HMGA1	HMGA2
pT stage		
pT1–2	25.7 ± 28.7; 15.0	16.0 ± 28.4; 0.0
pT3–4	27.1 ± 31.3; 10.0	16.9 ± 28.9; 0.0
P-value	0.83	0.952
pN stage		
pN0	18.3 ± 22.8; 5.0	8.4 ± 19.0; 0.0
pN1	32.7 ± 33.6; 20.0	21.5 ± 32.4; 0.0
P-value	0.012	0.039
Tumour grade		
G1–2	22.2 ± 27.3; 10.0	12.0 ± 23.3; 0.0
G3	37.3 ± 35.1; 30.0	26.8 ± 36.0; 5.0
P-value	0.009	0.008

HMGA, High mobility group A.
Expression is given as the percentage of immunoreactive tumour cells. Mean ± standard deviation; median values. Wilcoxon rank sum test.

Table 4. Survival analysis related to protein markers using cut-off scores [median values, namely 10% for HMGA1 (nuclear), and 0% for HMGA2 (nuclear)]*

	Total no. of patients	No. of deaths	Median survival time (months) (95% CI)	*P*-value
HMGA1				
Negative	40	30	14 (10–17)	0.816
Positive	24	20	12.5 (10–22)	
HMGA2				
Negative	37	27	15 (10–24)	0.196
Positive	26	21	14 (12–18)	

CI, Confidence interval; HMGA, high mobility group A.
Log-rank test.
*Similar results were obtained when expression was analysed as a continuous variable by Cox regression analysis.

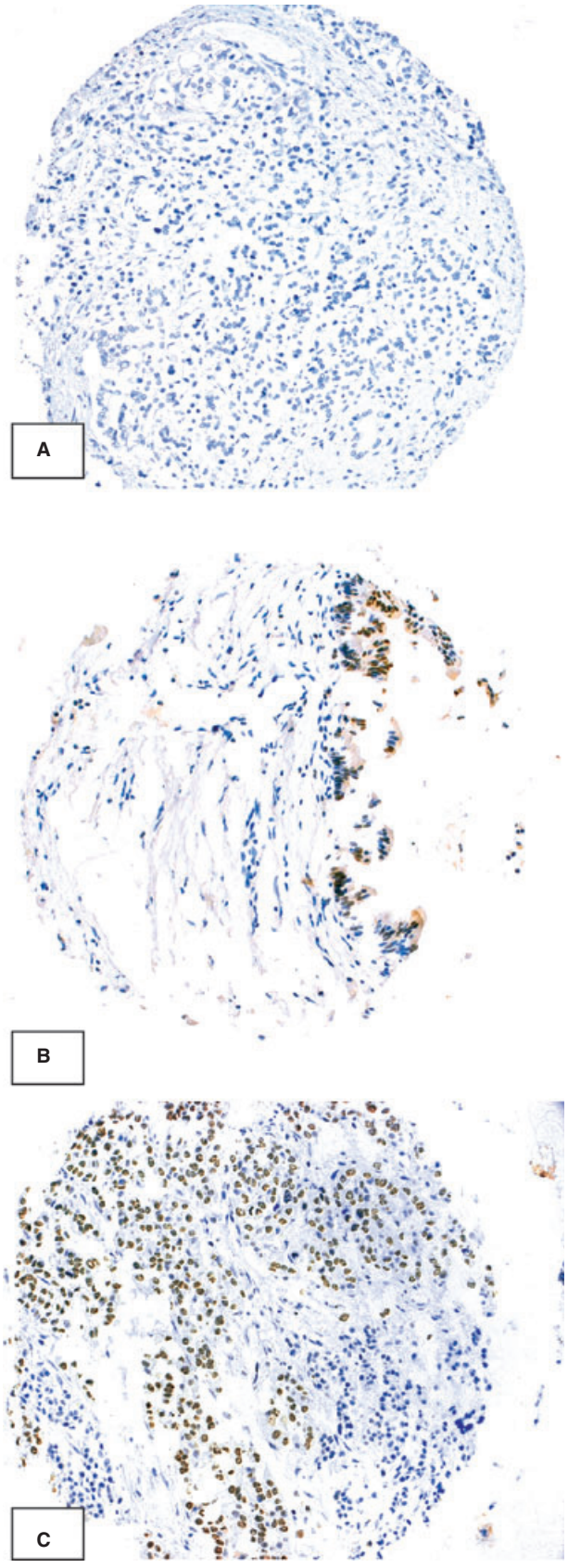

Figure 1. Examples of nuclear immunohistochemical detection of high mobility group A1 (HMGA1). Absent expression in normal pancreatic tissue (**A**) and moderate expression in pancreatic intraepithelial neoplasia (PanIN) (**B**), compared with strong, diffuse expression in pancreatic carcinoma (**C**).

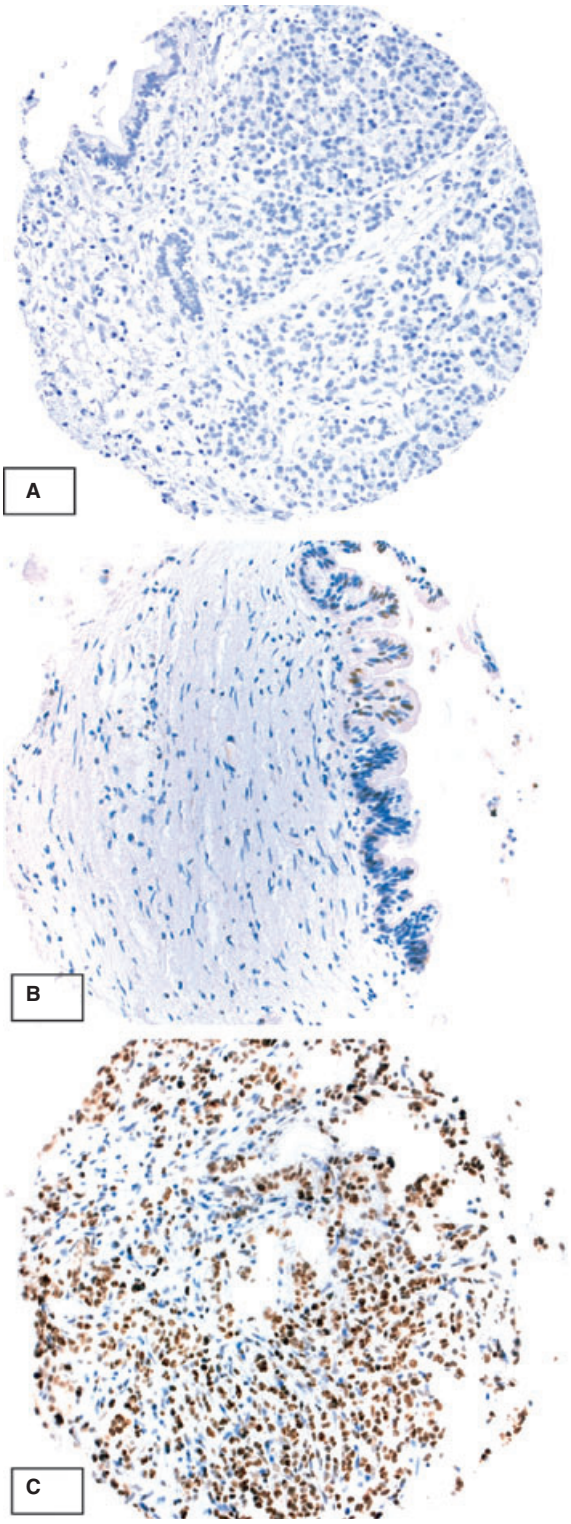

Figure 2. Examples of nuclear immunohistochemical detection of high mobility group A2 (HMGA2). **A**, Normal pancreatic tissue without HMGA2 expression. **B**, Pancreatic intraepithelial neoplasia (PanIN) with moderate HMGA2 expression. **C**, An example of ductal adenocarcinoma with strong nuclear HMGA2 expression.

PROTEIN EXPRESSION AND TUMOUR GRADING

Extent of nuclear HMGA1 and HMGA2 expression showed a positive correlation with higher tumour grade. Cells within poorly differentiated tumours (grade 3) more frequently expressed HMGA1 and HMGA2 (mean percentage expression ± SD: 37.3 ± 35.1 and 26.8 ± 36.0, respectively) than those in better-differentiated (grade 1 and 2) tumours (22.2 ± 27.3 and 12.0 ± 23.3, respectively) ($P = 0.009$ and $P = 0.008$, respectively; Table 3).

PROTEIN EXPRESSION AND TNM CLASSIFICATION OF THE TUMOURS

HMGA1 and HMGA2 expression showed a significant association with the pN stage of the tumours. Mean ± SD percentage expression levels for HMGA1 and HMGA2 were 18.3 ± 22.8 and 8.4 ± 19.0, respectively, for nodal negative (pN0) carcinomas, as compared with 32.7 ± 33.6 and 21.5 ± 32.4, respectively, for nodal positive (pN1) carcinomas ($P = 0.012$ and $P = 0.039$, respectively; Table 3). No association was noted between protein expression and pT stage of the tumours ($P = 0.83$ and $P = 0.952$, respectively; Table 3).

PROGNOSTIC SIGNIFICANCE

Median survival times were 12.5 and 14 months for HMGA1-positive and HMGA2-positive tumours, respectively, as compared with 14 and 15 months for HMGA1-negative and HMGA2-negative tumours, respectively. These differences were not statistically significant ($P = 0.816$ and $P = 0.196$, respectively; Table 4).

Discussion

Although most patients with pancreatic cancer present with advanced disease, the molecular events involved in tumour progression, invasion and metastasis are poorly understood.

In the present study, we investigated the immunohistochemical expression of HMGA1 and HMGA2 in 210 cases of ductal adenocarcinoma of the pancreas combined on a TMA including in addition 40 examples of PanIN-3 and 40 normal controls.

A major finding was the increasing mean protein expression of HMGA1 and HMGA2 between normal pancreatic tissue, PanIN cases, and invasive adenocarcinoma (Table 2). Mean HMGA1 and HMGA2 expression appeared to progressively increase through the

transition from normal tissue to pancreatic cancer. Moreover, HMGA1 and HMGA2 expression showed a positive correlation with malignancy grade and neoplastic progression, becoming higher with the dedifferentiation of the neoplasms and with the presence of lymph node metastasis. Therefore, our data suggest that HMGA1 and HMGA2 expression correlates with a more aggressive phenotype in pancreatic adenocarcinoma. These findings are in keeping with the recent studies of Hristov *et al.*,[19,20] who also noted an association between HMGA1 and HMGA2 expression and a more malignant phenotype in pancreatic cancer. HMGA1 was found to correlate with advanced tumour grade and decreased survival of their patients, whereas HMGA2 correlated with increasing tumour grade and lymph node metastasis. However, in our study, both HMGA1 and HMGA2 showed a positive correlation with lymph node metastasis. Although we found that patients with HMGA1 and HMGA2 negative tumours tended to survive longer, the association with patient outcome was not statistically significant. This may be because of the short survival time of most patients with pancreatic cancer. In addition, Hristov *et al.*[19] reported that HMGA1 expression correlated with a more advanced PanIN grade, whereas possible differences in protein expression between PanIN and adenocarcinoma were not discussed. In our study, only PanIN-3 lesions were included. Moreover, we demonstrated that mean protein expression was significantly higher in pancreatic ductal adenocarcinomas than in PanIN lesions.

A number of other groups have reported involvement of HMGA genes and proteins in the pathogenesis of pancreatic cancer. In one study, HMGA1 was found to be overexpressed in a small number of pancreatic adenocarcinomas and metastatic lesions, but without association with tumour grade.[25] More recently, Liau *et al.*[26] reported HMGA1 protein positivity in a high proportion of ductal pancreatic adenocarcinomas, also without correlation with tumour differentiation. However, in this study, in contrast to ours, only staining intensity was analysed, and the number of carcinomas was smaller. HMGA1 expression was also found to be increased in other pancreatic tumours, such as intraductal papillary mucinous neoplasms.[26] Studies in pancreatic ductal adenocarcinoma cell lines have shown that *HMGA1* knockdown decreases cellular invasion, anchorage-independent cell growth, and resistance to chemotherapeutic agents.[26,27] In addition, high-level expression of HMGA1 has been reported in almost all neoplastic tissues, including colon, breast, lung, ovarian, uterine, prostatic, gastric and head and neck carcinomas.[8–15] *HMGA2* has also been implicated in the development and progression of human malignancies, including lung adenocarcinomas, breast cancer, and squamous cell carcinomas of the oral cavity.[16–18] Additionally, *HMGA2* has been reported to play a role in the epithelial–mesenchymal transition that takes place during invasion and metastasis.[28] A previous study found increased *HMGA2* expression by reverse transcription polymerase chain reaction in ductal pancreatic adenocarcinomas, and HMGA2 expression by immunohistochemistry.[29] However, associations with grade and outcome were not included in the analysis, and HMGA2 expression was also found in pancreatic islet cells and, focally, in non-neoplastic ductal epithelial cells. In our study, focal HMGA2 immunoreactivity was also observed in a very small number of non-malignant ductal epithelial cells.

Regarding the processes underlying the involvement of HMGA genes in neoplastic transformation, it has been hypothesized that this probably occurs through oncofetal transcriptional mechanisms that have not yet been characterized.[21] It has been suggested that the elevated expression of HMGA1 in tumour cells requires a complex cooperation between SP1 family members and AP1 factors, induced by the activation of Ras GTPase signalling.[30] Moreover, the main function of the HMGA proteins, the regulation of gene transcription, is probably based on the ability of HMGA proteins to down-regulate or up-regulate the expression of genes that have a crucial role in the control of cell proliferation and invasion.[21] In particular, emerging evidence suggests that HMGA1 modulates gene expression, including pathways involved in inflammation, proliferation, transformation, metastatic progression, angiogenesis, and DNA repair. Most transcriptional targets include regulatory elements of nuclear factor-κB (NF-κB), a mediator of inflammatory pathways, suggesting that HMGA1 and NF-kB may cooperate to induce inflammatory signals and drive transformation.[31]

One of the advantages of this study is the use of TMAs, which have provided us with an efficient and cost-effective way of testing a large number of tumour specimens. Concerns could be raised about the TMA technique with regard to the possible limitations in sampling large, heterogeneous tumours. However, previous studies have shown comparable results between whole tissue sections and TMA cores, and have been able to reproduce numerous clinicopathological associations previously found with whole tissue sections.[32]

In conclusion, we found increasing mean HMGA1 and HMGA2 expression during neoplastic progression in ductal pancreatic adenocarcinoma, accompanied by

a positive correlation of protein expression with both increasing malignancy grade and the presence of lymph node metastasis. Our results support the idea that HMGA1 and HMGA2 may play a significant role in the late stages of pancreatic carcinogenesis and in the progression towards a more aggressive tumour phenotype.

References

1. Hidalgo M. Pancreatic cancer. *N. Engl. J. Med.* 2010; **362;** 1605–1617.
2. Hruban RH, Adsay NV, Albores-Saavedra J *et al.* Pancreatic intraepithelial neoplasia: a new nomenclature and classification system for pancreatic duct lesions. *Am. J. Surg. Pathol.* 2001; **25;** 579–586.
3. Johnson KR, Cook SA, Davisson MT. Chromosomal localization of the murine gene and two related sequences encoding high-mobility-group I and Y proteins. *Genomics* 1992; **12;** 503–509.
4. Reeves R, Nissen MS. The AT DNA-binding domain of mammalian high mobility group I chromosomal proteins. A novel peptide motif for recognizing DNA structure. *J. Biol. Chem.* 1990; **265;** 8573–8582.
5. Thanos D, Maniatis T. The high mobility group protein HMG I(Y) is required for NF-kB-depentent virus induction of the human IFN-β gene. *Cell* 1992; **27;** 777–789.
6. Chiappetta G, Avantaggiato V, Visconti R *et al.* High level expression of the HMGI(Y) gene during embryonic development. *Oncogene* 1996; **13;** 2439–2446.
7. Wood LJ, Maher JF, Bunton TE, Resar LM. The oncogenic properties of the HMG-1 gene family. *Cancer Res.* 2000; **60;** 4256–4261.
8. Fedele M, Bandiera A, Chiappetta G *et al.* Human colorectal carcinomas express high levels of high mobility group HMGI(Y) proteins. *Cancer Res.* 1996; **56;** 1896–1901.
9. Chiappetta G, Botti G, Monaco M *et al.* HMGA1 protein overexpression in human breast carcinomas: correlation with ErbB2 expression. *Clin. Cancer Res.* 2004; **10;** 7637–7644.
10. Sarhadi VK, Wikman H, Salmenkivi K *et al.* Increased expression of high mobility group A proteins in lung cancer. *J. Pathol.* 2006; **209;** 206–212.
11. Masciullo V, Baldassare G, Pentimalli F *et al.* HMGA1 protein over-expression is a frequent feature of epithelial ovarian carcinomas. *Carcinogenesis* 2003; **24;** 1191–1198.
12. Bandiera A, Bonifacio D, Manfioletti G *et al.* Expression of high mobility group I (HMGI) proteins in squamous intraepithelial lesions (SILs) of uterine cervix. *Cancer Res.* 1998; **58;** 426–431.
13. Tamimi Y, van der Poel HG, Denyn MM *et al.* Increased expression of high mobility group protein I (Y) in high grade prostate cancer determined by in situ hybridization. *Cancer Res.* 1993; **53;** 5512–5516.
14. Nam ES, Kim DH, Cho SJ *et al.* Expression of HMGI(Y) associated with malignant phenotype of human gastric tissue. *Histopathology* 2003; **42;** 466–471.
15. Rho YS, Lim YC, Park IS *et al.* High mobility group HMGI(Y) protein expression in head and neck squamous cell carcinoma. *Acta Otolaryngol.* 2007; **127;** 76–81.
16. Meyer B, Loeschke S, Schultze A *et al.* HMGA2 overexpression in non-small cell lung cancer. *Mol. Carcinog.* 2007; **46;** 503–511.
17. Rogalla P, Drechsler K, Kazmierczak B, Rippe V, Bonk U, Bullerdiek J. Expression of HMGI-C, a member of the high mobility group protein family, in a subset of breast cancers: relationship to histologic grade. *Mol. Carcinog.* 1997; **19;** 153–156.
18. Miyazawa J, Mitoro A, Kawashiri S, Chada KK, Imai K. Expression of mesenchyme-specific gene HMGA2 in squamous cell carcinomas of the oral cavity. *Cancer Res.* 2004; **64;** 2024–2029.
19. Hristov AC, Cope L, Delos Reyes M *et al.* HMGA2 protein expression correlates with lymph node metastasis and increased tumor grade in pancreatic ductal adenocarcinoma. *Mod. Pathol.* 2009; **22;** 43–49.
20. Hristov AC, Cope L, Di Cello F *et al.* HMGA1 correlates with advanced tumor grade and decreased survival in pancreatic ductal adenocarcinoma. *Mod. Pathol.* 2010; **23;** 98–104.
21. Fusco A, Fedele M. Roles of HMGA proteins in cancer. *Nat. Rev. Cancer* 2007; **7;** 899–910.
22. Fedele M, Visone R, De Martino I *et al.* HMGA2 induces pituitary tumorigenesis by enhancing E2F1 activity. *Cancer Cell* 2006; **9;** 459–471.
23. Hanley J. Receiver operating characteristic (ROC) methodology: the state of the art. *Crit. Rev. Diagn. Imaging* 1989; **29;** 307–337.
24. Zlobec I, Steele R, Terracciano L, Jass JR, Lugli A. Selecting immunohistochemical cut-off scores for novel biomarkers of progression and survival in colorectal cancer. *J. Clin. Pathol.* 2007; **60;** 1112–1116.
25. Abe N, Watanabe T, Masaki T *et al.* Pancreatic duct cell carcinomas express high levels of high mobility group I(Y) proteins. *Cancer Res.* 2000; **60;** 3117–3122.
26. Liau SS, Rocha F, Matros E, Redston M, Whang E. High mobility group AT-hook 1 (HMGA1) is an independent prognostic factor and novel therapeutic target in pancreatic adenocarcinoma. *Cancer* 2008; **113;** 302–314.
27. Liau SS, Wang EE. HMGA1 is a molecular determinant of chemoresistance to gemcitabine in pancreatic adenocarcinoma. *Clin. Cancer Res.* 2008; **14;** 1470–1477.
28. Thuault S, Valcourt U, Petersen M, Manfioletti G, Heldin CH, Moustakas A. Transforming growth factor-beta employs HMGA2 to elicit epithelial–mesenchymal transition. *J. Cell Biol.* 2006; **174;** 175–183.
29. Abe N, Watanabe T, Suzuki Y *et al.* An increased high-mobility group A2 expression level is associated with malignant phenotype in pancreatic exocrine tissue. *Br. J. Cancer* 2003; **89;** 2104–2109.
30. Cleynen I, Huysmans C, Sasazuki T, Shirasawa S, Van de Ven W, Peeters K. Transcriptional control of the human high mobility group A1 gene: basal and oncogenic Ras-regulated expression. *Cancer Res.* 2007; **15;** 4620–4629.
31. Resar LM. The high mobility group A1 gene: transforming inflammatory signals into cancer? *Cancer Res.* 2010; **70;** 436–439.
32. Kallionemi OP, Wagner U, Kononen J, Sauter G. Tissue microarray technology for high-throughput molecular profiling of cancer. *Hum. Mol. Genet.* 2001; **10;** 657–666.

European Journal of Cancer (2012) **xxx**, xxx–xxx

Available at www.sciencedirect.com

SciVerse ScienceDirect

journal homepage: www.ejcancer.info

UbcH10 overexpression in human lung carcinomas and its correlation with *EGFR* and *p53* mutational status

Pierlorenzo Pallante [a], Umberto Malapelle [b], Maria Teresa Berlingieri [a], Claudio Bellevicine [b], Romina Sepe [a], Antonella Federico [a], Danilo Rocco [c], Mario Galgani [a], Lorenzo Chiariotti [a], Montserrat Sanchez-Cespedes [d], Alfredo Fusco [a,*], Giancarlo Troncone [b]

[a] *Istituto di Endocrinologia ed Oncologia Sperimentale del CNR c/o Dipartimento di Biologia e Patologia Cellulare e Molecolare, Facoltà di Medicina e Chirurgia di Napoli, Università degli Studi di Napoli "Federico II", via Pansini 5, 80131 Naples, Italy*

[b] *Dipartimento di Scienze Biomorfologiche e Funzionali, Sezione di Anatomia Patologica, Facoltà di Medicina e Chirurgia di Napoli, Università degli Studi di Napoli "Federico II", via Pansini 5, 80131 Naples, Italy*

[c] *Azienda Ospedaliera di Rilievo Nazionale "V. Monaldi", via Bianchi, 80131 Naples, Italy*

[d] *Genes and Cancer Group, Cancer Epigenetics and Biology Program-PEBC, Bellvitge Biomedical Research Institute-IDIBELL, Hospitalet de Llobregat, Barcelona, Spain*

KEYWORDS
UbcH10
Non-small cell lung cancer
Immunohistochemistry
Diagnosis

Abstract ***Introduction:*** UbcH10 codes for the cancer related E2 Ubiquitin Conjugating Enzyme, an enzymatic molecule with a key role in the ubiquitin–proteasome pathway. Current studies have suggested a critical role of UbcH10 in a variety of malignancies, including human thyroid, breast, ovarian and colorectal carcinomas. The aim of this study has been to extend the analysis of UbcH10 expression to lung cancer. This neoplasia represents one of the leading cause of cancer mortality worldwide, and new tools for an accurate diagnosis/prognosis are needed.

Methods: The expression levels of UbcH10 were analysed in human non-small cell lung carcinoma (NSCLC) by quantitative RT-PCR and tissue microarray immunohistochemistry, and these values were correlated with the clinicopathological features of the patients affected by NSCLC.

Results: Our results demonstrate that UbcH10 is overexpressed in NSCLC compared to the normal lung tissue. Moreover, UbcH10 expression is significantly higher in squamous cell and large cell carcinomas than in adenocarcinomas, and directly and inversely correlated with the mutational status of

* *Corresponding author*: Tel.: +39 081 7463602/7463749; fax: +39 081 2296674.
E-mail address: alfusco@unina.it (A. Fusco).

0959-8049/$ - see front matter
http://dx.doi.org/10.1016/j.ejca.2012.09.033

Please cite this article in press as: Pallante P. et al., UbcH10 overexpression in human lung carcinomas and its correlation with *EGFR* and *p53* mutational status, *Eur J Cancer* (2012), http://dx.doi.org/10.1016/j.ejca.2012.09.033

p53 and *EGFR*, respectively. The suppression of UbcH10 expression by RNAi resulted in a drastic reduction of proliferation and migration abilities of lung carcinoma cell lines.

Conclusion: These results, taken together, indicate that UbcH10 overexpression has a critical role in lung carcinogenesis, and the evaluation of UbcH10 expression levels may be a new tool for the characterisation of NSCLC.

1. Introduction

Lung cancer represents the leading cause of cancer mortality with an increasing incidence worldwide.[1,2] The overall 5-year survival rate of the patients affected by this disease is only 15%.[3] Therefore, the high mortality rate requires the development of a more accurate early diagnostic tools and new targeted treatments.

Lung cancer is generally divided into two histopathological groups: non-small cell lung cancer (NSCLC) and small cell lung cancer (SCLC).[4] NSCLC, that represents 80% of lung cancer, is further subdivided into adenocarcinoma (AD), squamous cell carcinoma (SCC) and large cell carcinoma (LCC). This classification is also based on genetic variations, since NSCLC carries mutations of *EGFR* (10%), K-ras (20–30%) and $p16^{ink4}$ (50%), whereas SCLC shows mutations of Rb (90%) and $p14^{arf}$ (65%).[5–7]

Therefore, for patients' treatment it is primarily important to distinguish between SCLC and various subtypes of NSCLC. A small, but not exhaustive, panel of antibodies including cytokeratin 7, TTF-1 and p63, represent a valid support for a better definition of the NSCLC subtypes,[8] but the need of highly sensitive and specific markers to integrate this small panel is a very important issue.

We retain that one candidate for this role is the UbcH10 protein, the cancer-related E2 Ubiquitin conjugating enzyme,[9] an ubiquitin-binding enzyme involved in the process of ubiquitin-dependent proteolysis of key regulator molecules of the cell cycle.[10–12] Due to its role played in cell cycle regulation, UbcH10 can be considered a critical element in cancer progression. In fact, recent data have shown that the UbcH10 overexpression is associated with the late stages of neoplastic thyroid transformation.[13] In human breast carcinomas, the overexpression of UbcH10 closely correlates with a more aggressive phenotype.[14] Similar findings have been reported for ovarian[15] and colorectal carcinomas,[16] brain cancer[17] and various Hodgkin's (HL) and non-Hodgkin's lymphomas (NHL).[18] Moreover, it has been demonstrated that UbcH10 overexpression leads to the deregulation of cell growth in several carcinoma cell lines, since the suppression of the UbcH10 synthesis significantly reduces cell proliferation.[13–15]

Therefore, in this study we have analysed UbcH10 expression by reverse transcription polymerase chain reaction (RT-PCR) and immunohistochemistry in a panel of NSCLC samples. Our results demonstrate that UbcH10 was overexpressed in NSCLC compared to normal lung tissue and its overexpression was significantly higher in SCC and LCC than in AD. Moreover, UbcH10 overexpression was directly correlated with the loss of differentiation grade of NSCLC. A direct correlation was found between the UbcH10 expression levels and the mutational status of *p53*, whereas an inverse one was found with *EGFR*. Finally, we demonstrate that the suppression of UbcH10 expression by RNAi resulted in a drastic reduction of proliferation and migration abilities of two lung carcinoma cell lines.

2. Materials and methods

2.1. NSCLC tissue microarray analysis

To evaluate the expression pattern of UbcH10 in lung cancer, a tissue microarray (TMA), built at the Spanish National Cancer Research Center (CNIO, Madrid, Spain) was used. Tissues were provided by the CNIO Tumour Bank Network (2001–2004), in collaboration with Spanish Hospitals.[19] The study was approved by the institutional review boards and ethics committees, and informed consent was obtained from each patient. Tumours were reviewed by two pathologists and histologically classified according to the 2004 criteria.[20] Clinically relevant data were included (Supplementary Table S1). *p53* and *EGFR* mutations were detected using PCR and direct automatic sequencing following standard protocols.[19] Formalin-fixed, paraffin-embedded tissue blocks from lung primary tumours were used for TMA construction, following a previously described protocol.[19] Slides were reviewed by two pathologists, who selected areas containing tumour cells, avoiding those with necrosis, inflammation and keratinisation. The TMA comprised forty AD samples, thirty SCC samples, four LCC samples and one carcinoid cancer sample, with two cores sampled for each case.

Ten cases of normal lung tissue were also supplied as whole sections and included in the staining to assess UbcH10 expression in non-neoplastic lung.

TMA staining and analysis are reported in detail in Supplementary Materials and methods.

2.2. Cell cultures and RNA interference

A detailed list of the lung carcinoma cell lines and the growth conditions are reported in Supplementary Materials and methods.

Please cite this article in press as: Pallante P. et al., UbcH10 overexpression in human lung carcinomas and its correlation with *EGFR* and *p53* mutational status, *Eur J Cancer* (2012), http://dx.doi.org/10.1016/j.ejca.2012.09.033

For RNAi experiments, we used double-strand RNA oligonucleotides specific for UbcH10 coding region as previously reported.[13] As negative control, fluorescent non-silencing controls were used (Catalogue Number 1022563). All siRNA duplexes were purchased from Qiagen (Qiagen, Valencia, CA) and were transfected using Lipofectamine 2000 (Invitrogen, Carlsbad, CA) according to the manufacturer's recommendations. SiRNAs were used at a final concentration of 120 nM and 0.5×10^6 cells were seeded in a 100 mm plate.

2.3. Quantitative reverse transcription polymerase chain reaction (qRT-PCR)

One microgram of total RNA extracted from each lung carcinoma cell line (Supplementary Materials and methods) was reverse-transcribed with QuantiTect® Reverse Transcription Kit (Qiagen) according to the manufacturer's instructions. Real-Time Quantitative PCR was carried out with the CFX 96 thermocycler (Bio-Rad, Hercules, CA) in 96-well plates using a final volume of 20 µl. For PCR we used 10 µl of 2× Sybr Green (Applied Biosystems, Carlsbad, CA), 200 nM of each primer and cDNA generated from 20 ng of total RNA. The conditions used for PCR were 10 min at 95 °C and then 45 cycles of 15 s at 95 °C and 30 s at 60 °C. Each reaction was carried out in triplicate. We used the $2^{-\Delta\Delta CT}$ method to calculate relative expression levels. Primers used for qRT-PCR were UbcH10-fw 5′-GCCCGTAAAGGAGCTGAG-3′, UbcH10-rev 5′-GGGAAGGCAGAAATCCCT-3′, G6PD-fw 5′-ACAGAGTGAGCCCTTCTTCAA-3′ and G6PD-rev 5′-ATAGGAGTTGCGGGCAAAG-3′. qRT-PCR was also carried out using "TissueScan™ Real-Time Lung Cancer Disease Panel II" of cDNAs purchased from Origene (Origene Technologies Inc., Rockville, MD). This lung cancer cDNA panel (Product Code: HLRT102) contained five normal lung specimens and forty-three lung cancer specimens of different histotypes, whose clinicopathological features are freely available on the web (www.origene.com).

2.4. Protein extraction, Western blotting and antibodies

Protein extraction and Western blotting procedures were carried out as reported elsewhere.[21] Briefly, cells were washed twice in ice-cold PBS, and lysed in JS buffer (50 mM HEPES pH 7.5 containing 150 mM NaCl, 1% glycerol, 1% Triton X-100, 1.5 mM $MgCl_2$, 5 mM ethylene glycol tetraacetic acid (EGTA), 1 mM sodium orthovanadate (Na_3VO_4) and 1× protease inhibitor cocktail). Protein concentration was determined by the Bradford assay (Bio-Rad) using bovine serum albumin as standard, and equal amounts of proteins were analysed by sodium dodecyl sulphate–polyacrylamide gel electrophoresis (SDS–PAGE). After blotting, membranes were incubated with primary antibodies for UbcH10 (A-650, Boston Biochem Inc., Cambridge, MA) and β-actin (Clone AC-15 A5441, Sigma–Aldrich Co., St. Louis, MO). Membranes were then incubated with the horseradish peroxidase-conjugated secondary antibody (1:3.000) for 60 min (at room temperature) and the reaction was detected with a Western blotting detection system (Thermo Scientific, Rockville, IL).

2.5. Growth curve analysis

To construct the growth curves we used the Cell Proliferation Kit I (3-(4,5-Dimethylthiazol-2-yl)-2,5-diphenyltetrazolium bromide, MTT) from Roche (Mannhein, Germany) optimised for spectrophotometric quantisation of cell proliferation and viability in cell populations, using the of 96-well plates format. After siRNA transfection, 5×10^3 cells were plated in each well. The absorbance (550–690 nm) was measured by using a universal Absorbance Microplate Reader ELx800 (BioTek Instruments Inc., Winooski, VT) at the following time intervals: 0–24–48–72 h. The data obtained in this way were normalised with respect to the control and used to construct growth curves. Duplicates of the same 96-well plates were stained with 0.1% crystal violet dye for 30 minutes, then, after removing the solution containing the dye, the colour included into the cells was eluted with 1% SDS and its concentration was read in a spectrophotometer (570 nm).[21,22] The measurements were performed according to the time intervals of 0–24–48–72 h. For growth curve analysis, three independent experiments were performed and data were shown as means ± standard deviation (SD).

Fluorescence-activated cell sorting (FACS) analysis of NSCLC proliferation is fully described in Supplementary Materials and methods.

2.6. Migration assay

To evaluate the migration rate, we used Transwell culture chambers (Corning Incorporated, Corning, NY) adapted to 24-well plates containing special inserts made of a polycarbonate filter with 6.5 mm diameter and 8.0 µm pore size. 10^5 cells were washed three times with PBS and then resuspended in 1% foetal bovine serum (FBS) Dulbecco's modified Eagle medium (DMEM) culture medium and seeded in the upper chamber. The lower chamber was filled with 600 µl 10% FBS DMEM. The cells were then incubated at 37 °C for 24 h. After incubation, to block the migration, transwells were removed from wells and stained with 0.1% crystal violet in 25% methanol. The cells not migrated were removed from the top of the transwell with a cotton swab, while the cells successfully migrated into the lower chamber remained adherent to the bottom of the membrane. The percentage of migrated cells was assessed by the dye elution with 1% SDS and reading absorbance at

Please cite this article in press as: Pallante P. et al., UbcH10 overexpression in human lung carcinomas and its correlation with *EGFR* and *p53* mutational status, *Eur J Cancer* (2012), http://dx.doi.org/10.1016/j.ejca.2012.09.033

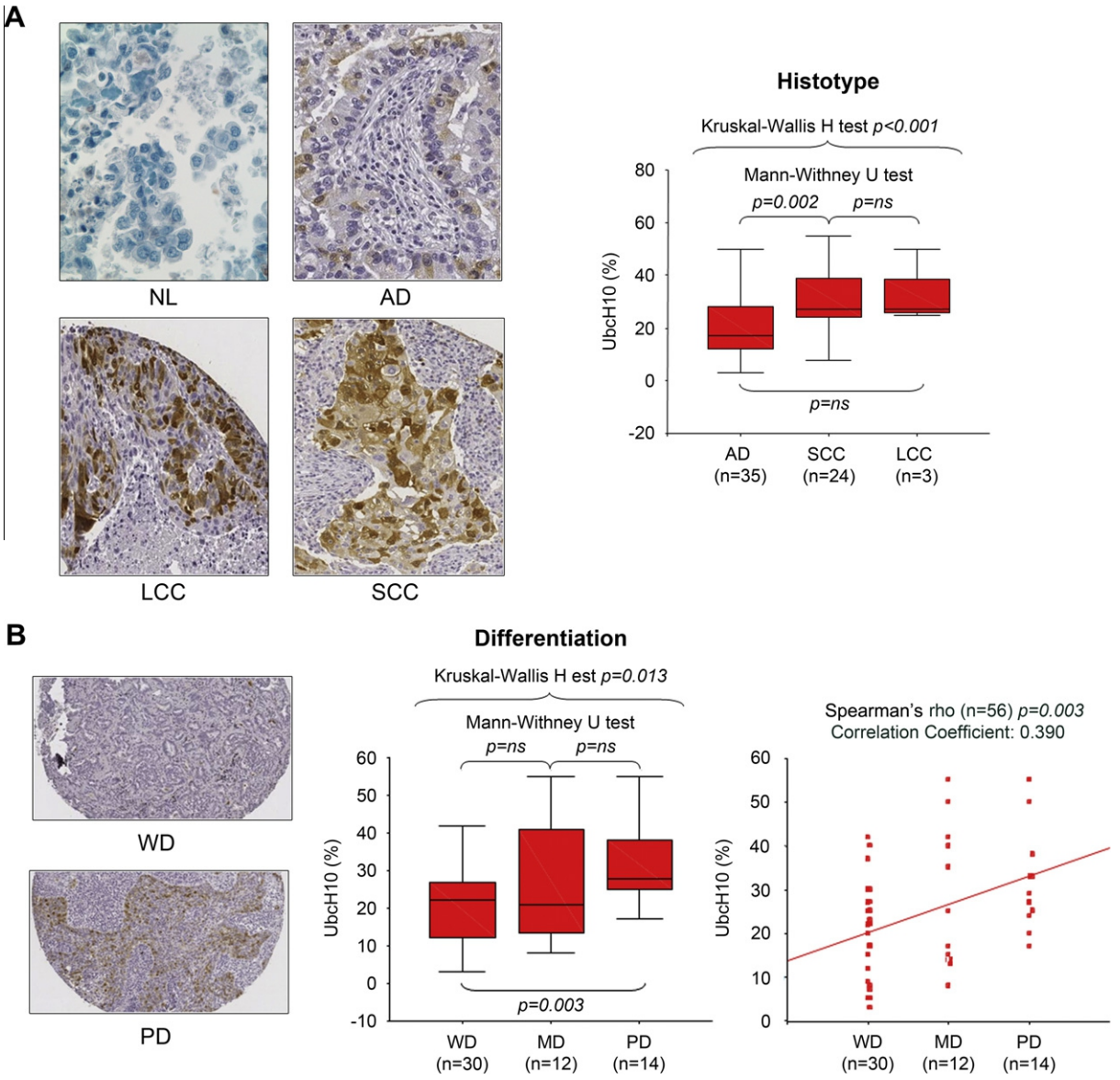

Fig. 1. Immunohistochemical detection of the UbcH10 protein in a lung cancer tissue microarray (TMA). The expression pattern of UbcH10 was analysed to find possible association with clinicopathological data of lung carcinoma samples TMA. (A) *Left panel*. Normal lung tissue shows no positivity for the UbcH10 expression. The immunostaining pattern shows the progressive increase of UbcH10 expression in representative non-small cell lung carcinoma (NSCLC) samples of different histotypes. It is of note the total absence of UbcH10 staining in the stroma cells. *Right panel*. Kruskal–Wallis H test and Mann–Whitney U test were used to correlate UbcH10 expression with NSCLC histotypes. The expression of the UbcH10 protein (% of stained cells) is higher in the three different histological types of NSCLC compared to normal lung parenchyma. While AD shows a slight increase of UbcH10, a marked overexpression of UbcH10 can be observed in SCC and LCC ($p < 0.001$). Box and whiskers: Tukey. NL, normal lung; AD, adenocarcinoma; SCC, squamous cell carcinoma; LCC, large cell carcinoma. (B) *Left panel*. The staining pattern of representative well and poorly differentiated lung carcinoma samples shows the absence of UbcH10 expression in the first case and, conversely, an intense UbcH10 staining in the latter case. *Right panel*. Statistical analyses were conducted to evaluate association between UbcH10 expression and NSCLC grade: the Spearman's rho correlation coefficient was calculated (0.390, $p = 0.003$). The expression of the UbcH10 protein (% of positive cells) increases with the progressive loss of NSCLC differentiation degree, going from well- to poorly-differentiated ($p = 0.013$). Box and whiskers: Tukey. WD, well differentiated; MD: moderately differentiated; PD: poorly differentiated.

570 nm. Three independent experiments were performed and data were shown as means ± SD.

2.7. Statistical methods

The statistical analysis on immunohistochemical and qRT-PCR data was performed employing as appropriate, the Kruskal–Wallis H test, the Mann–Whitney U test and the T test. The Spearman's rho correlation coefficient was calculated where necessary. A p-value < 0.05 was considered statistically significant for each analysis.

2.8. Ethics

All the analyses were performed according to the ethical standards of the local ethic committee.

Please cite this article in press as: Pallante P. et al., UbcH10 overexpression in human lung carcinomas and its correlation with *EGFR* and *p53* mutational status, *Eur J Cancer* (2012), http://dx.doi.org/10.1016/j.ejca.2012.09.033

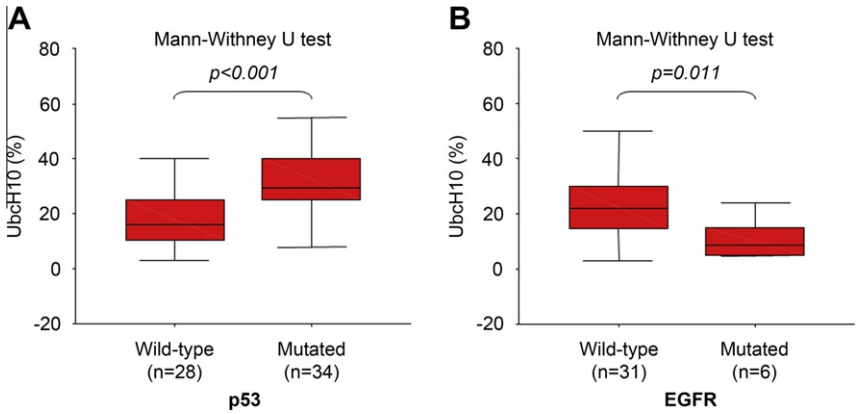

Fig. 2. Association of UbcH10 expression with *p53* and *EGFR* mutations. Mann–Whitney U test analysis was performed to evaluate the association between UbcH10 expression and *p53* and *EGFR* mutation status. The expression of the UbcH10 protein (% of positive cells) is directly correlated with *p53* mutation status (A) and inversely correlated with mutation status of *EGFR* (B) in non-small cell lung carcinoma (NSCLC) samples ($p < 0.001$ and $p = 0.011$, respectively). Box and whiskers: Tukey.

3. Results

3.1. Immunohistochemical analysis of UbcH10 expression in human NSCLC tissues

We analysed a lung carcinoma TMA comprising seventy-five cases of different histological types (Supplementary Fig. S1) by immunohistochemistry using antibodies raised against the UbcH10 protein. However, five AD samples, six SCC samples, one LCC sample and one carcinoid sample were excluded from this analysis because they were not technically suitable. Any normal lung tissue specimens analysed ($n = 10$) was negative for the expression of UbcH10, with only rare single cells in mitosis showing a weak positive signal for UbcH10 (Fig. 1A). In contrast, a strong UbcH10 expression with variable degree of intensity was evident in malignant lesions corresponding to the different histological types of NSCLC ($p < 0.001$, Kruskal–Wallis H test) (Fig. 1A).

The lung AD samples showed high UbcH10 expression levels with a median value of 17% (ranging from 3% to 75%) of positive cells (% of positive cells on total spots per sample, $p < 0.001$). Overexpression of UbcH10 was even more pronounced in SCC and LCC cases ($p = 0.002$, Mann–Whitney U test). In the SCC cases UbcH10 expression levels had a median value of 27% (ranging from 8% to 55%, $p < 0.001$). The same median value (27%) was also found in the LCC cases, but with a different range of expression (ranging from 25% to 50%, $p < 0.001$) (Fig. 1A).

The correlation between UbcH10 expression and tumour grade was possible in 56 cases, as 19 cases, either lacked the information on grade or missed the tissue cores (Supplementary Table S1). As a result of specific statistical analysis, we found that the expression of UbcH10 significantly correlated with different tumour grades ($p = 0.013$, Kruskal–Wallis H test; $p = 0.003$, Spearman's rho-correlation coefficient: 0.390) (Fig. 1B). Indeed, lower UbcH10 expression levels were found in the well differentiated carcinoma samples with a median value of 22% (ranging from 3% to 42%; $p = 0.013$) (Fig. 1B). Conversely, higher levels of UbcH10 expression were observed in the poorly differentiated carcinomas with a median value of 28% (ranging from 17% to 55%, $p = 0.013$).

Subsequently, we compared the expression of UbcH10 with that of Ki-67, a marker of proliferation commonly used in clinical diagnostics, in order to evaluate a possible association of UbcH10 expression with the carcinoma cell proliferation rate. By using the statistical Spearman's rho test, we found a significant association between the expression of the UbcH10 and Ki-67, since the coefficient of correlation (Spearman's rho) was 0.414 ($p = 0.004$) (Supplementary Fig. S2).

3.2. UbcH10 overexpression is directly and inversely correlated with p53 and EGFR mutational status, respectively, in NSCLC

Since mutations in the *p53* and *EGFR* genes are a frequent event in lung carcinomas[23,24] we analysed the correlation of UbcH10 expression with these mutations. As shown in Fig. 2A the expression of UbcH10 positively correlates with the presence of mutations in the *p53* gene ($p < 0.001$, Mann–Whitney U test). Indeed, the median value of UbcH10 expression was 16% (ranging from 3% to 55%, $p < 0.001$) in the carcinoma samples not carrying mutations in the *p53* gene, whereas it was 30% (ranging from 8% to 75%, $p < 0.001$) in the *p53*-mutated lung carcinomas. Conversely, the overexpression of UbcH10 appeared to be inversely correlated with the presence of mutations in the *EGFR* gene ($p = 0.011$, Mann–Whitney U test) (Fig. 2B). The median value of UbcH10 expression was 22% (ranging from 3% to 75%, $p = 0.011$) in the carcinoma samples not carrying *EGFR* mutations, while the median value was 9%

Please cite this article in press as: Pallante P. et al., UbcH10 overexpression in human lung carcinomas and its correlation with *EGFR* and *p53* mutational status, *Eur J Cancer* (2012), http://dx.doi.org/10.1016/j.ejca.2012.09.033

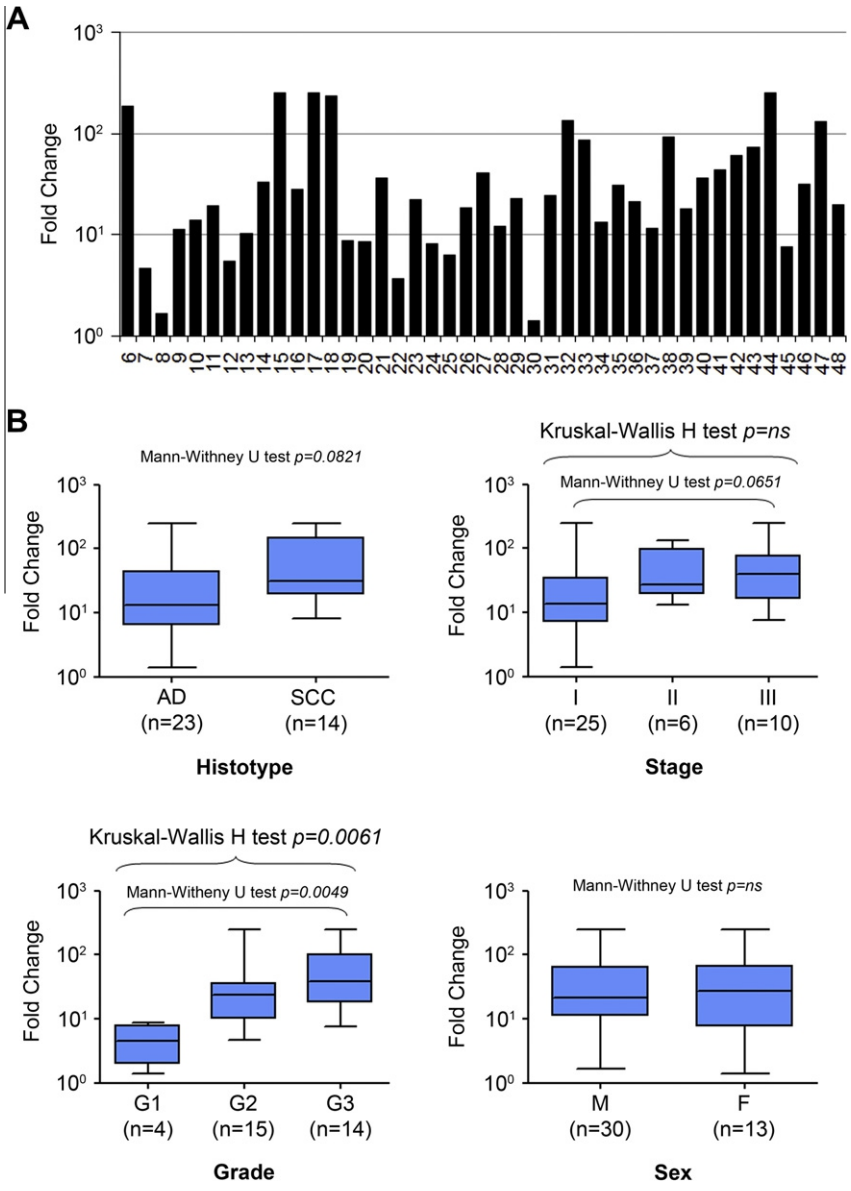

Fig. 3. Expression of UbcH10 specific mRNA in human non-small cell lung carcinoma (NSCLC) specimens. (A) A quantitative reverse transcription polymerase chain reaction (qRT-PCR) analysis was performed on a cDNA array comprising five normal lung control tissues and forty-three NSCLC tissues of different histotypes. The Fold Change values indicate the relative change in expression levels between the pool of normal samples (set equal to 1) and carcinoma samples. The range of variability of UbcH10 expression in normal lung tissues is less than 10%. UbcH10 is overexpressed in all the carcinomas analysed with a maximum Fold Change of 250. (B) Statistical analyses were conducted to evaluate the association between UbcH10 and clinicopathological parameters such as histology, stage, grade and sex (Kruskal–Wallis H test and Mann–Whitney U test). High UbcH10 Fold Change values are significantly associated with the progressive loss of cell differentiation ($p = 0.0061$). A particularly significant p-value ($p = 0.0049$) was obtained comparing the G3 versus G1 cases. A general correlation is found with stage and histotype although the test did not reach the statistical significance. No significant association was observed when UbcH10 expression was correlated with the sex of the patients. Box and whiskers: Min to Max.

(ranging from 5% to 24%, $p = 0.011$) in the samples carrying *EGFR* mutations (Fig. 2B).

3.3. qRT-PCR analysis of UbcH10 mRNA expression in a panel of human lung carcinoma tissues

UbcH10 mRNA expression was evaluated in a panel of lung carcinoma samples by qRT-PCR analysis. The UbcH10 overexpression levels showed a Fold Change between 10 and more than 100 in all the samples analysed. The median value of the UbcH10 Fold Change was 53.87 (ranging from 1.4 to 250) (Fig. 3A).

Statistical analyses showed that UbcH10 mRNA overexpression was significantly correlated with the progressive loss of cellular differentiation (tumour grade, $p = 0.0061$ Kruskal–Wallis H test; G3 versus G1, $p = 0.0049$, Mann–Whitney U test). However, no significant statistical correlation was found between UbcH10

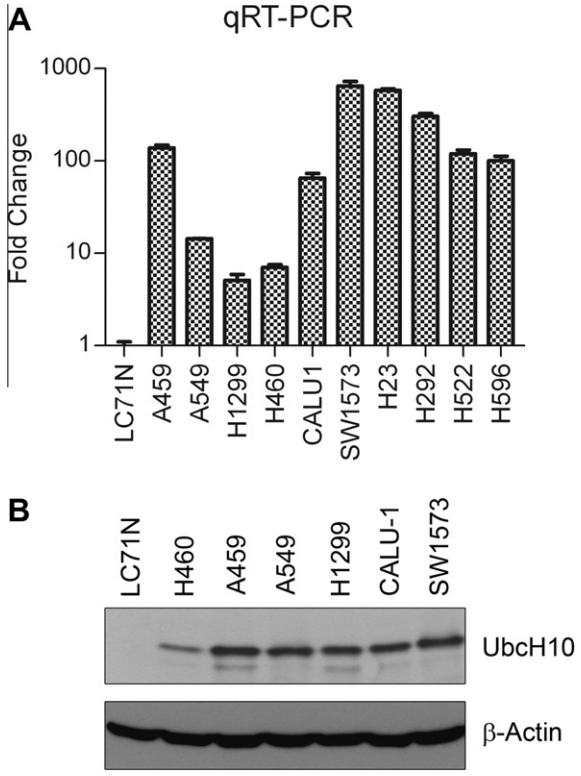

Fig. 4. UbcH10 expression in human lung carcinoma cell lines. (A) Human lung carcinoma cell lines were analysed for the expression of UbcH10 by quantitative reverse transcription polymerase chain reaction (qRT-PCR). The expression of β-actin gene was evaluated as a control to normalise the amount of RNA used. The Fold Change values indicate the relative change in expression levels between tumour cell lines and the normal lung tissue sample (LC71 N). (B) Thirty micrograms of lung carcinoma cell lysates were immunoblotted for UbcH10 levels. Blot against β-actin was used as protein loading control.

expression levels and tumour histotype and stage ($p = 0.0821$ and $p = 0.0651$, respectively, Mann–Whitney U test) (Fig. 3B) although a general association was evident. No correlation was found between UbcH10 expression and the sex and age of the patients (Fig. 3B and data not shown, respectively).

3.4. UbcH10 gene silencing in human lung carcinoma cells inhibits proliferation and migration

In order to define the role of UbcH10 overexpression in lung carcinogenesis, we first analysed the expression of UbcH10 in several lung carcinoma cell lines. As shown in Fig. 4A, all of them showed UbcH10-specific mRNA overexpression with respect to the normal lung tissue (Fig. 4A). In particular, UbcH10 overexpression was extremely high (10^2 Fold Change induction) in the A459, CALU1, SW1573, H23, H292, H522 and H596 cell lines, while it was less pronounced in A549, H1299 and H460 cell lines (10^1 Fold Change induction (Fig. 4A). These data were further confirmed by Western blot. Indeed, an intense band of 19.6 kDa, corresponding to the UbcH10 protein, was present in the A459, A549, H1299, CALU1 and SW1573 cells (Fig. 4B), whereas this band was less intense in the H460 cell line (Fig. 4B).

Subsequently, we silenced the expression of UbcH10 protein in A459 and A549 lung carcinoma cell lines. An efficient reduction of the UbcH10 protein levels (from 24 to 72 h) was achieved after siRNA transfection (Fig. 5A). Then, we analysed the growth properties of the UbcH10-silenced cells. As shown in Fig. 5B, a significant reduction in cell growth rate was observed in the A459 and A549 cells transfected with UbcH10 siRNA in comparison to the non-silencing control transfected and untransfected cells, as evaluated by MTT assay (Fig. 5B).

Then, to better characterise the effects of UbcH10 on cell cycle progression, a flow cytometric analysis was performed on the UbcH10 silenced lung carcinoma cells. As shown in Fig. 5C, the A459 and A549 cells transfected with siRNA against UbcH10 (siRNA UbcH10) were retained in G1 phase (64.36% and 65.25%, respectively) compared with the untransfected and control siRNA transfected cells (siRNA C) (54.21% and 58.27%, respectively).

Finally, we investigated the role of UbcH10 in cell migration by performing a migration assay. The silencing of UbcH10 expression resulted in a reduction of cell motility compared to control cells (Fig. 5D). As we can see in Fig. 5D, the crystal violet staining of wells (absorbance plotted in the histogram) carrying A459 and A549 cells transfected with UbcH10 siRNA was less intense (meaning that fewer cells had crossed the membrane) compared to the staining of wells carrying untransfected or non-silencing control transfected cells (Fig. 5D).

Therefore, these results clearly demonstrate that the block of UbcH10 expression markedly reduces the proliferation and migration of lung cancer cells.

4. Discussion

Today management of the patients affected by lung carcinomas requires a complex integration of clinical, histological and molecular factors. The markers currently available are still far from yielding complete informations; recently, gene expression profiling has fostered further investigation on novel biological markers of potential future clinical use.[25–30] Among those the UbcH10 protein deserves investigation. Indeed, our previous studies have shown a significant correlation between UbcH10 overexpression and aggressive carcinoma behaviour of ovarian, thyroid, breast and lymphoid neoplasms.[13–15,18] A close relationship between UbcH10 overexpression and poor tumour differentiation has also been described in bladder, liver, colorectal and brain tumours.[9,16,17,31] Therefore, the aim of this study was to evaluate whether UbcH10 also adds further

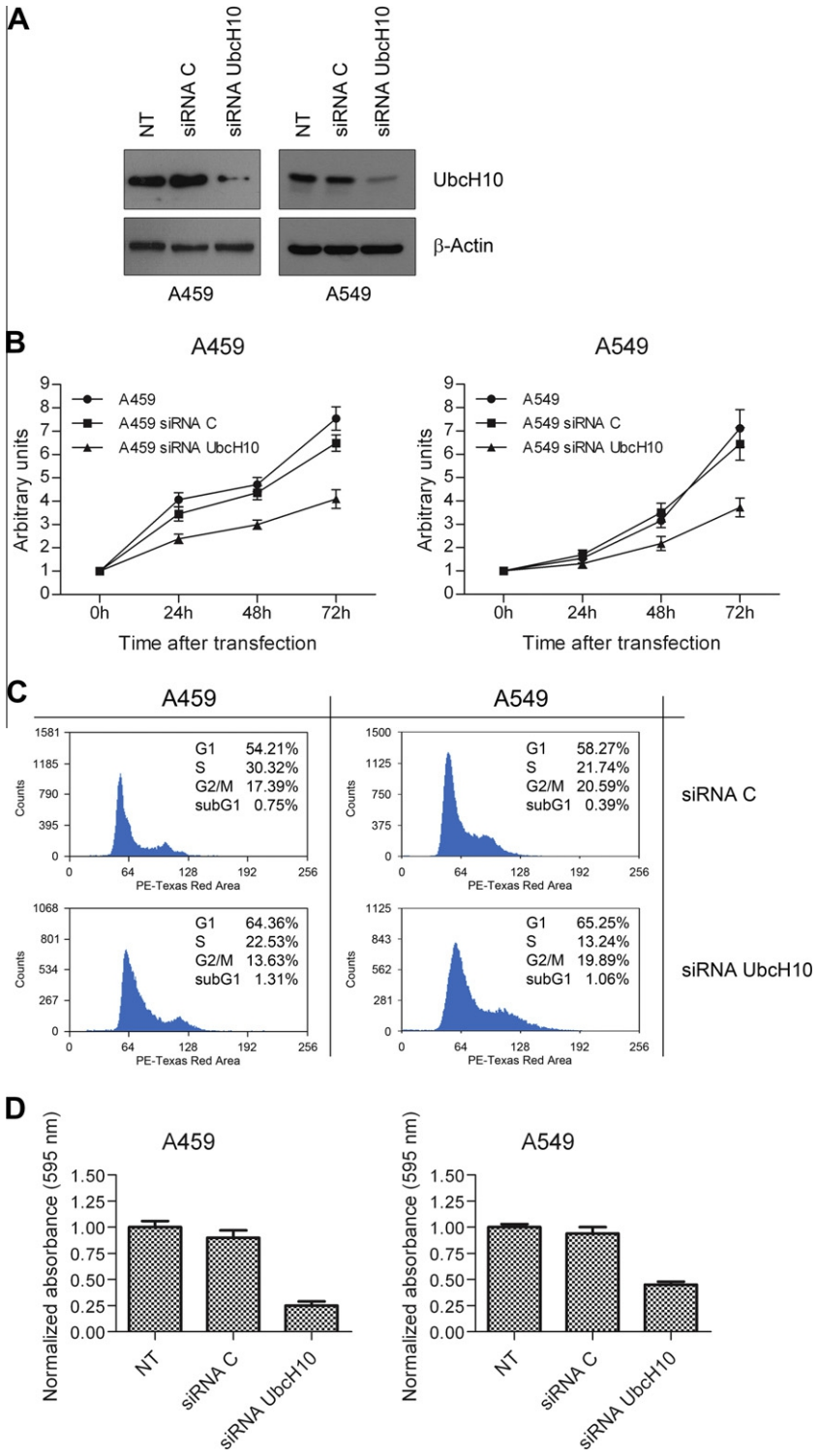

Fig. 5. Definition of the role of UbcH10 in lung carcinoma cell proliferation and migration. (A) A459 and A549 cells were transfected with 120 nM siRNA against UbcH10 and the relative control. Western blot was performed with lysate obtained from 24 h to 72 h after siRNA UbcH10 transfection. Total cell lysates were prepared and their concentration was measured using the Bradford assay. The expression of β-actin was used as loading control protein. (B) A459 and A549 cells proliferation was determined by 3-(4,5-Dimethylthiazol-2-yl)-2,5-diphenyltetrazolium bromide, MTT assay and absorbances were measured at 490 nm at different times after transfection (0 h, 24 h, 48 h and 72 h). After transfection in 100 mm plates, $5x10^3$ cells were seeded in each well of the 96-well plate. Data were shown as means ± standard deviation (SD) of triplicate experiments. (C) The distribution of cells in the different phases of the cell cycle was evaluated by Fluorescence-activated cell sorting (FACS) analysis at 48 h after transfection. $2x10^5$ cells were stained with a solution containing 50 μg/ml propidium iodide and analysed for DNA content. (D) The migration of A459 and A549 lung carcinoma cells was assessed 24 h after the silencing of UbcH10 compared to control cells. For migration assays, transwell polycarbonate filters with 6.5 mm diameter and 8.0 μm pore size were used. 10^5 cells were seeded in the upper chamber and after 24 h incubation, transwells were stained with crystal violet and absorbance was read at 595 nm.

Please cite this article in press as: Pallante P. et al., UbcH10 overexpression in human lung carcinomas and its correlation with *EGFR* and *p53* mutational status, *Eur J Cancer* (2012), http://dx.doi.org/10.1016/j.ejca.2012.09.033

useful information to the clinical work-up of patients affected by NSCLC.

For this study we took advantage of a TMA including seventy-five lung carcinoma samples: this allowed to simultaneously analyse a large number of samples correlating the UbcH10 expression levels with a set of clinicopathological and molecular parameters relative to each patient. The evaluation of the UbcH10 mRNA levels by qRT-PCR yielded similar results. Although each technique was applied to a distinct set of samples, our data suggest that there is a good correlation between IHC and qRT-PCR. By the immunohistochemical analysis of this TMA we found that UbcH10 was overexpressed in all of the NSCLC analysed in comparison with normal lung. UbcH10 levels were higher in SCC and LCC compared to AD. Statistical analyses also showed that the expression of UbcH10 in NSCLC was moderately associated with proliferation index and, consistently with the results previously reported in other cancer types,[13–16,32–34] was directly correlated with the loss of tumour differentiation, since poor differentiated carcinomas showed higher levels of UbcH10 with respect to the well-differentiated ones. In agreement with this result, higher levels of UbcH10 were found in the NSCLC tumour samples expressing a mutated p53 protein that is well known to contribute to lung carcinoma progression towards a less differentiated phenotype.[23,24,35] Conversely, a lower UbcH10 expression was observed in the presence of mutations in the *EGFR* gene. This finding could have an important impact on the therapy of NSCLC patients, since only patients carrying *EGFR* mutations undergo treatment with small-molecules inhibiting the *EGFR* tyrosine kinase. Therefore, UbcH10 levels could represent, in a clinical perspective, an additional indicator for the presence of *EGFR* mutations, enforcing the criteria for choosing the eligible patients undergoing anti-cancer treatments.

Functional studies demonstrated that the suppression of UbcH10 expression reduced the proliferation rate of two lung carcinoma cells, confirming the important role played by UbcH10 in lung carcinogenesis, likely due to its ability to modulate the degradation of proteins such as mitotic cyclins[36] involved in cell cycle control. Consistently, FACS analysis showed an accumulation of the UbcH10-silenced lung carcinoma cells in the G1 phase of the cell cycle.

Finally, we report that UbcH10 was also able to positively regulate the migration of lung carcinoma cells, suggesting that UbcH10 might be involved, acting on the ubiquitin–proteasome pathway, in the regulation of the expression levels of proteins that modulate the migration and invasiveness of cancer cells.

In conclusion, our results indicate a critical role of UbcH10 in lung carcinogenesis. Further investigation is required to evaluate the clinical role of UbcH10 detection as a tool to identify subset of NSCLC featuring specific biological characteristics.

Conflict of interest statement

None declared.

Acknowledgements

This work was supported by grants from: AIRC (IG 5346), Ministero dell'Università e della Ricerca Scientifica e Tecnologica – MIUR (PRIN 2008), "Progetto di Interesse strategico Invecchiamento (PNR-CNR Aging Program) PNR-CNR 2012–2014" and Progetto PON01-02782: "Nuove strategie nanotecnologiche per la messa a punto di farmaci e presidi diagnostici diretti verso cellule cancerose circolanti".

We thank Mr. Mario Berardone for artwork.

Appendix A. Supplementary data

Supplementary data associated with this article can be found, in the online version, at http://dx.doi.org/10.1016/j.ejca.2012.09.033.

References

1. Walker S. Updates in non-small cell lung cancer. *Clin J Oncol Nurs* 2008;**12**:587–96.
2. Christiani DC. Genetic susceptibility to lung cancer. *J Clin Oncol* 2006;**24**:1651–2.
3. Sun S, Schiller JH, Gazdar AF. Lung cancer in never smokers – a different disease. *Nat Rev Cancer* 2007;**7**:778–90.
4. Spira A, Ettinger DS. Multidisciplinary management of lung cancer. *N Engl J Med* 2004;**350**:379–92.
5. Meuwissen R, Berns A. Mouse models for human lung cancer. *Genes Dev* 2005;**19**:643–64.
6. Lowe SW, Sherr CJ. Tumor suppression by Ink4a–Arf: progress and puzzles. *Curr Opin Genet Dev* 2003;**13**:77–83.
7. Sher YP, Chou CC, Chou RH, et al. Human kallikrein 8 protease confers a favorable clinical outcome in non-small cell lung cancer by suppressing tumor cell invasiveness. *Cancer Res* 2006;**66**: 11763–70.
8. Rossi G, Pelosi G, Graziano P, Barbareschi M, Papotti M. A reevaluation of the clinical significance of histological subtyping of non–small-cell lung carcinoma: diagnostic algorithms in the era of personalized treatments. *Int J Surg Pathol* 2009;**17**:206–18.
9. Okamoto Y, Ozaki T, Miyazaki K, Aoyama M, Miyazaki M, Nakagawara A. UbcH10 is the cancer-related E2 ubiquitin-conjugating enzyme. *Cancer Res* 2003;**63**:4167–73.
10. Lin Y, Hwang WC, Basavappa R. Structural and functional analysis of the human mitotic-specific ubiquitin-conjugating enzyme, UbcH10. *J Biol Chem* 2002;**277**:21913–21.
11. Rape M, Kirschner MW. Autonomous regulation of the anaphase-promoting complex couples mitosis to S-phase entry. *Nature* 2004;**432**:588–95.
12. de Gramont A, Ganier O, Cohen-Fix O. Before and after the spindle assembly checkpoint – an APC/C point of view. *Cell Cycle* 2006;**5**:2168–71.
13. Pallante P, Berlingieri MT, Troncone G, et al. UbcH10 overexpression may represent a marker of anaplastic thyroid carcinomas. *Br J Cancer* 2005;**93**:464–71.

14. Berlingieri MT, Pallante P, Sboner A, et al. UbcH10 is overexpressed in malignant breast carcinomas. *Eur J Cancer* 2007;**43**:2729–35.
15. Berlingieri MT, Pallante P, Guida M, et al. UbcH10 expression may be a useful tool in the prognosis of ovarian carcinomas. *Oncogene* 2007;**26**:2136–40.
16. Chen SM, Jiang CY, Wu JY, et al. RNA interference-mediated silencing of UBCH10 gene inhibits colorectal cancer cell growth in vitro and in vivo. *Clin Exp Pharmacol Physiol* 2010;**37**:525–9.
17. Donato G, Iofrida G, Lavano A, et al. Analysis of UbcH10 expression represents a useful tool for the diagnosis and therapy of astrocytic tumors. *Clin Neuropathol* 2008;**27**:219–23.
18. Troncone G, Guerriero E, Pallante P, et al. UbcH10 expression in human lymphomas. *Histopathology* 2009;**54**:731–40.
19. Angulo B, Suarez-Gauthier A, Lopez-Rios F, et al. Expression signatures in lung cancer reveal a profile for EGFR-mutant tumours and identify selective PIK3CA overexpression by gene amplification. *J Pathol* 2008;**214**:347–56.
20. Travis WD, Brambilla E, Müller-Hermelink HK, Harris CC. Pathology and genetics of tumours of lung, pleura, thymus and heart. In: Travis WD, editor. *World Health Organization Classification of Tumours*. Lyon: IARC Press; 2004. p. 9–122.
21. Quintavalle C, Incoronato M, Puca L, et al. C-FLIPL enhances anti-apoptotic Akt functions by modulation of Gsk3beta activity. *Cell Death Differ* 2010;**17**:1908–16.
22. Quintavalle C, Garofalo M, Zanca C, et al. MiR-221/222 overexpression in human glioblastoma increases invasiveness by targeting the protein phosphate PTPmu. *Oncogene* 2011;**31**:858–68.
23. Toyooka S, Tsuda T, Gazdar AF. The TP53 gene, tobacco exposure, and lung cancer. *Hum Mutat* 2003;**21**:229–39.
24. Sekido Y, Fong KM, Minna JD. Molecular genetics of lung cancer. *Annu Rev Med* 2003;**54**:73–87.
25. Beer DG, Kardia SL, Huang CC, et al. Gene-expression profiles predict survival of patients with lung adenocarcinoma. *Nat Med* 2002;**8**:816–24.
26. Granville CA, Dennis PA. An overview of lung cancer genomics and proteomics. *Am J Respir Cell Mol Biol* 2005;**32**:169–76.
27. Tsao MS, Sakurada A, Cutz JC, et al. Erlotinib in lung cancer – molecular and clinical predictors of outcome. *N Engl J Med* 2005;**353**:133–44.
28. Wigle DA, Jurisica I, Radulovich N, et al. Molecular profiling of non-small cell lung cancer and correlation with disease-free survival. *Cancer Res* 2002;**62**:3005–8.
29. Endoh H, Tomida S, Yatabe Y, et al. Prognostic model of pulmonary adenocarcinoma by expression profiling of eight genes as determined by quantitative real-time reverse transcriptase polymerase chain reaction. *J Clin Oncol* 2004;**22**:811–9.
30. Hoheisel JD. Microarray technology: beyond transcript profiling and genotype analysis. *Nat Rev Genet* 2006;**7**:200–10.
31. Han SS, Liu QG, Yao YM, et al. UbcH10 expression in hepatocellular carcinoma and its clinicopathological significance. *Nan Fang Yi Ke Da Xue Xue Bao* 2011;**31**:280–4.
32. Fujita T, Ikeda H, Kawasaki K, et al. Clinicopathological relevance of UbcH10 in breast cancer. *Cancer Sci* 2009;**100**:238–48.
33. Fujita T, Ikeda H, Taira N, Hatoh S, Naito M, Doihara H. Overexpression of UbcH10 alternates the cell cycle profile and accelerate the tumor proliferation in colon cancer. *BMC Cancer* 2009;**9**:87.
34. Troncone G, Volante M, Iaccarino A, et al. Cyclin D1 and D3 overexpression predicts malignant behavior in thyroid fine-needle aspirates suspicious for Hurthle cell neoplasms. *Cancer Cytopathol* 2009;**117**:522–9.
35. Feldser DM, Kostova KK, Winslow MM, et al. Stage-specific sensitivity to p53 restoration during lung cancer progression. *Nature* 2010;**468**:572–5.
36. Lukas J, Bartek J. Cell division: the heart of the cycle. *Nature* 2004;**432**:564–7.

Please cite this article in press as: Pallante P. et al., UbcH10 overexpression in human lung carcinomas and its correlation with *EGFR* and *p53* mutational status, *Eur J Cancer* (2012), http://dx.doi.org/10.1016/j.ejca.2012.09.033